CIVIL ENGINEERING STUDIES

STRUCTURAL RESEARCH SERIES NO. 104

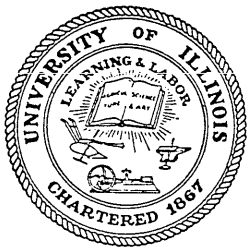

FATIGUE OF DUCTILE METALS AT RANGES OF STRESS EXTENDED TO COMPRESSION

By
J. L. MERRITT
R. J. MOSBORG
and
W. H. MUNSE

Approved by
N. M. NEWMARK

Technical Report
to
OFFICE OF NAVAL RESEARCH
Contract N6ori-071(05), Task Order V
Project NR-031-182

UNIVERSITY OF ILLINOIS
URBANA, ILLINOIS

FATIGUE OF DUCTILE METALS AT RANGES OF STRESS EXTENDED TO COMPRESSION

Technical Report to the
Office of Naval Research
Contract N6-ori-71, Task Order V
Project NR-031-182

by

J. L. Merritt, R. J. Mosborg,

and

W. H. Munse

Approved by

N. M. Newmark

University of Illinois
Urbana, Illinois
1 July 1955

TABLE OF CONTENTS

LIST OF TABLES

LIST OF FIGURES

LIST OF FIGURES (Cont'd)

FATIGUE OF DUCTILE METALS AT RANGES OF STRESS EXTENDED TO COMPRESSION

I. INTRODUCTION

1. Historical

Fatigue of engineering materials has been recognized as an elusive but very definite problem for approximately a century. During this period, hundreds of thousands of tests have been conducted which have resulted in the presentation of a relatively large number of both quantitative and qualitative theories. The qualitative theories remain somewhat controversial, but the use of the microscope and of X-ray diffraction has brought engineers and other scientists into closer accord on the subject. On the other hand, the quantitative picture of the problem has remained obscure.

Qualitatively, it is generally agreed that fatigue failures are not unique but are merely the result of a stressing action. Failure by means of any stressing action, at our present state of knowledge, is considered basically a consequence of slip. The slip within crystals and eventual failure is explained by the dislocation theory of which there are many slightly differing versions. The dislocation theory has been developed and has been explained rationally, and yet the actual proof of the theory has been obliterated by what may be considered our present macroscopic view of the particles involved in the theory. Furthermore, our macroscopic concept completely precludes a quantitative application of the dislocation theory.

As a consequence, numerous statistical studies have been initiated to develop criteria which are readily applicable to design. These studies have yielded a satisfactory result in the realm of static properties of materials. Generally, static properties may be determined accurately by either the von Mises-Hencky maximum distortion energy theory or the Tresca maximum shear stress theory. The maximum normal stress theory for some conditions yields satisfactory results, but this theory has been experimentally invalidated by the observation that the superposition of a moderate hydrostatic stress on an existing stress state has no effect on the yield or flow conditions.

The three theories mentioned above have also been applied to the problem of fatigue. Moore and Morkovin (36, 37, 38)* analyzed their extensive tests which involved full stress reversal on varying sizes of specimen for three materials by means of the three theories. They concluded that of the three theories, the maximum distortion energy theory gave the best results. However, for small specimens this theory gave inconsistent results. In their conclusions, Moore and Morkovin give two possible alternatives which may be briefly summarized as:

1) The maximum distortion energy theory could be correct if the inconsistencies were attributed to poor assumptions in the analysis or slight inaccuracies in the experimental results.

2) None of the theories is correct and fatigue failure is a result of factors not accounted for in their derivation.

---

* Numbers in parentheses throughout this report refer to items in the List of References.

Either of these alternatives will explain the possible inconsistencies noted by Moore and Morkovin but the first alternative has been invalidated by results obtained by Hoffman (28) and Elling (20, 41). These investigators found that in tests of materials on which the repeated stress range was predominantly compression or pure compression, the failure would occur at maximum stresses far exceeding those necessary to cause failure under a similar stress range of predominantly tension. This would invalidate all of the popular theories as they are generally presented since they predict that failure will occur at the same stress for either tension or compression.

Elling (20) reports that failure of unnotched specimens of killed, annealed, strain-hardened, structural steel occurs at a constant stress range when the stresses are predominantly compression. This observation is qualitatively in agreement with Smith's (46) conclusion but quantitatively the agreement is in error. Both conclude that failure under such conditions occurs at a constant range of stress. However, Elling's constant range of stress appears to be greater than the endurance limit range for full reversal while Smith concludes this constant range should be equal to this endurance limit. The fact that Elling tested strain-hardened material may explain this difference. However, it appears that Elling's results are directly comparable with Hoffman's results from the same material which had not been strain hardened.

Peterson in a discussion of Hoffman and Elling's (41) test results suggests a seemingly logical revision to the maximum distortion energy theory which could theoretically define conditions for failure

where compressive ranges of stress are employed. This suggestion is presented only pictorially with no attempt at actual analysis.

Almen (1, 2, 3, 41) maintains that fatigue failures are tension failures. It is not disputed that tension microstresses may result from repeated loading in pure compression. As a matter of fact, such stresses doubtlessly are produced. However, even considering the stress concentration resulting from the discontinuity at the surface of an unnotched specimen, it is somewhat questionable that residual tensile stresses of magnitude sufficient to initiate a crack are produced unless an additional stress raiser is introduced. Furthermore, even if such tensile stresses are produced, we arrive at the stalemate that with our present state of knowledge microstresses cannot be evaluated. Consequently, at this time, only a statistical theory involving parameters which may be readily measured or computed would be of practical value.

Yen (52) presents a hypothesis which essentially states that repeated full reversal loading of a notched specimen will result in a true stress range equal to the theoretical value. His conclusion is based on the supposition that a material will work harden a sufficient amount to develop the theoretical stress at the root of the notch after a number of load repetitions.

Smith (44) presents a hypothesis which considers strain concentrations rather than stress concentrations. He assumes that the strains developed at the root of a notch are the theoretical values, a supposition which generally agrees with experiment. Using these theoretical strains and a stress-strain diagram for the material, he finds a stress corresponding to the strain developed in a notched fatigue

specimen which he calls the "true stress". In a very few applications of his hypothesis, Smith illustrates that this true stress correlates with the stress at failure for a comparable number of cycles of load on an unnotched specimen. The few applications of his hypothesis included only one series of tests on one aluminum alloy tested from zero to tension. Consequently, Smith's results cannot be considered conclusive nor are they applicable to a perfectly plastic material since in this case the "true stress" would be a constant value over a wide variation of fatigue strain ranges.

2. Object and Scope of Investigation

The object of the study reported herein was to extend the results of fatigue tests into a field which was previously almost entirely neglected; that is, the field of compression fatigue. Naturally, it was hoped that at least a partial answer to this century old problem of fatigue could be found, and a rather lengthy analysis of the current data as well as prior related data was employed in an attempt to obtain this answer. As stated above, our present state of knowledge precludes the proof of a dislocation theory so that the answer sought was one of a statistical nature which would be applicable to design.

The results obtained by Hoffman (28), Elling (20), and Smith (44) seemed to indicate that it was possible that the true range of stress was the cause of fatigue failure of ductile metals. Furthermore, it seemed that Yen's hypothesis revised to consider an apparent change in mean stress was tenable. The unpredictable work hardening characteristics of a material subjected to load reversals or relatively high stresses in a single sense rendered an analysis using experimental

results necessary. A simple consideration of residual stress patterns to be expected in a notched specimen subjected to a fatigue cycle involving a predominance of tension illustrated that the true range of stress to be expected under such conditions could be predominantly compression. Consequently, if a correlation between the true range of stress in notched and unnotched specimens of a material was to be investigated, a number of test results involving stress ranges predominantly in compression would be desired.

A review of the literature led to the surprising realization that an extremely limited number of these tests had been run. In fact, the only such results found were those summarized by Smith (46). This relative absence of data rendered it necessary to undertake a rather comprehensive axial fatigue test program involving ranges of stress varying from pure compression to tensile stresses approaching the static ultimate strength. The material selected for study was a fully killed, annealed, structural grade steel. The selection of this material was based on its uniform mechanical and chemical properties and its use in engineering design. An unnotched axial load specimen and a notched axial load specimen with a theoretical stress concentration factor of 2.0 were studied. The net cross-section for both specimen types was 0.100 sq. in. (dia. = 0.357 in.). Choice of specimen size was dictated by the 10,000-lb capacity Sonntag machine used in the tests and the expected maximum stresses required. The notch geometry was chosen to be similar to that used by Moore and Morkovin (36) so that a similar procedure in preparing specimens could be used.

A total of 127 tests were run in the current series, 94 unnotched specimens and 33 notched specimens. The results of both series of tests were plotted on modified Goodman diagrams on which constant life contours were established by interpolation from the individual S-N diagrams for 1×10^5, 5×10^5, and 2×10^6 cycles. Comparison of the two resulting diagrams led to the conclusion that the true range of stress hypothesis was invalid for this series of tests.

Peterson's (41) suggested revision to the maximum distortion energy theory was then studied. Qualitatively, his revised theory gives constant life contours similar in shape to those determined experimentally. However, no numerical correlation between the experimental curves and the theory was apparent.

Next, a purely empirical study was tried. This consisted of expressing the constant life contours for the unnotched and notched specimens by algebraic equations. It was found that straight lines and arcs of circles could be fitted to the interpolated cycle contours, and the results exhibited relatively small errors for the current tests. However, modified Goodman diagrams drawn for the results of 984 tests reported by Grover, Bishop, and Jackson (23-26) quickly illustrated the fallacy of the purely empirical equations. These tests involved axial loading of sheet specimens of 24S-T3 and 75S-T6 aluminum alloys and normalized 4130 steel. Five theoretical stress concentrations were also included. These were 1.0 (unnotched), 1.5, 2.0, 4.0, and 5.0.

Returning to a study of the current test results it appeared that a variation of fatigue reduction factor (defined on page 9) with fatigue stress range was a possible explanation. The fatigue reduction

factor was computed for each constant life contour for a number of ranges of stress. This computed fatigue reduction factor ranged from the theoretical stress concentration for a range of pure compression to no stress concentration for high tension stresses. The fatigue reduction factor as a function of fatigue stress range was readily established. The resulting empirical equation modified for a stress concentration factor of 1.0 was applied to the tests of unnotched specimens in order to compute a hypothetical static stress necessary to predict the test results of the unnotched specimens when the empirical modified fatigue reduction factor was applied to it. The results thus derived were compared to Grover, Bishop, and Jackson's tests but no correlation was obtained.

At this point in the analysis, it seemed that statistically the fatigue problem could not be answered. Further study of the current tests and those by Grover, Bishop, and Jackson indicated, however, that a possible answer to the problem might exist because the slopes of the straight lines representing all constant life contours for the notched specimens of the four materials were constant, within reasonable limits. Furthermore, the cycle contours for unnotched specimens, except for the current results, could be approximated by straight lines with a constant slope differing from that found for the notched specimens.

This trend in the constant life contours was most encouraging but in order to define failure conditions a determination of the zero to tension intercept of the life cycle contours was necessary. This determination posed a difficult problem. However, approximate values of these intercepts were obtained by an algebraic correlation of the

fatigue intercept with the static tensile properties. This correlation seems to give results which appear to be reasonable, but they may be fortuitous since they cannot be justified by any theoretical considerations. Thus, the analysis presented herein gives reasonable results with the exception of the unnotched tests of the current series. However, it should not be applied until it has been more thoroughly investigated.

3. Definitions and Notation

The terms, fatigue and repeated loading, are used interchangeably throughout this report. Their meaning defines the entire problem of the action of materials including failure when they are subjected to numerous repetitions of stress.

Stress Range -- the algebraic difference of the maximum and minimum stress imposed on a specimen with tensile stress defined as positive and compressive stress as negative.

Mean Stress -- the algebraic average of the maximum and minimum stresses.

Alternating Stress -- that range of stress which is superposed on the mean stress in a fatigue cycle.

Full Stress Reversal -- a stress range where the maximum and minimum stresses are of equal magnitude but opposite sign.

Average Applied Nominal Stress -- the applied load divided by the original net area.

Average Applied True Stress -- the applied load divided by either the measured net area or the estimated net area corresponding to the applied load.

Theoretical Maximum Stress -- the maximum stress developed at the root of a notch as predicted by the theory of elasticity. That is the product of either the average applied nominal stress or the average applied true stress and the theoretical stress concentration factor.

Theoretical Stress Concentration Factor -- the theoretical maximum nominal or true stress divided by the average applied nominal stress or the average applied true stress, respectively.

Range Ratio -- the quotient of the arithmetic minimum stress and the arithmetic maximum stress.

Fatigue Reduction Factor -- the quotient of the average stress at failure in an unnotched specimen and the stress at failure in a notched specimen for the same range ratio and the same life.

The Common Fatigue Intercept Stress -- numerically equal to the product of the theoretical stress concentration factor and the corresponding interpolated test stress at the zero to tension axis of a modified Goodman diagram.

Constant Life Contour -- a curve established on modified Goodman coordinates defining the fatigue stress range necessary to cause failure at a specific life denoted by the number of cycles of stress repetition.

Notation:

σ_1 = average algebraic minimum stress in a fatigue cycle, ksi

σ_2 = average algebraic maximum stress in a fatigue cycle, ksi

σ_F = common fatigue intercept stress for the 2×10^6 cycle life contour on the zero to tension axis, ksi

σ_U = nominal static ultimate tensile strength, ksi

σ_Y = yield strength by 0.2 per cent offset method or lower yield point for an elasto-plastic material, ksi

r = per cent reduction of area obtained in a standard tensile coupon test

e = per cent elongation in 2 in. obtained in a standard tensile coupon test

K_T = theoretical stress concentration factor

K_T' = stress concentration factor for unnotched specimens

N = number of cycles to failure in a fatigue test

σ_N = common fatigue intercept stress at N cycles, ksi

m = the slope of the constant life contours

4. Acknowledgments

The work reported herein was conducted as part of a cooperative agreement between the University of Illinois, Department of Civil Engineering, and the Office of Naval Research under Contract N6-ori-71, Task Order V, Project Designation NR-031-182. All work was performed under the general direction of Dr. N. M. Newmark, Research Professor of Structural Engineering. The tests were planned and conducted by Research Assistants R. E. Elling and J. L. Merritt. The test program was under the general supervision of W. H. Munse, Research Associate Professor of Civil Engineering, and direct supervision of R. J. Mosborg, Research Assistant Professor of Civil Engineering.

Sincere gratitude is hereby expressed to H. F. Moore, Research Professor of Theoretical and Applied Mechanics Emeritus, and J. E. Stallmeyer, Research Assistant Professor of Civil Engineering for their helpful suggestions. Further suggestions, which were equally appreciated, were made by several of the machinists employed in the departmental

machine shop. E. E. Kirby, one of the machinists, did an excellent job of preparing the majority of the specimens.

V. J. McDonald, Research Assistant Professor of Civil Engineering, who is in charge of instrumentation in the laboratory, developed the procedure and equipment necessary for the calibration of the fatigue machine. Finally, sincere appreciation is acknowledged C. M. Fuller for his assistance in analyzing the data and his work in tracing the figures.

II. DESCRIPTION OF TESTS

1. Specimen Preparation

The stock from which all specimens were prepared was a 3/4 in. thick x 72 in. wide plate of structural grade fully killed steel shown in Fig. 1. For all practical purposes, this parent plate met the requirements for ASTM designation A7-52T. Its ladle analysis and average tensile properties are summarized in Tables 1a and 1b, respectively.

The initial step in the specimen preparation consisted of flame cutting a 12-3/4 in. or 13-1/2 in. length from the full width of the plate. This strip was then marked and sawed as shown in Fig. 1. The outer edges were discarded since it was felt that the variation in physical properties could be reduced by doing so (43). Blanks from one entire 6-ft strip were annealed in one heat in an electric furnace at 1650°F. for approximately one hour and then were slowly cooled in the furnace. Following this heat treatment, the pieces were sawed into bars 7/8 in. wide. Each of these bars was then machined to 3/4 in. square and its ends turned parallel.

Some bars were turned into specimens immediately after they had been machined to 3/4 in. square while others were statically prestressed. The static prestressing was introduced in order to reduce the large amount of yielding which occurred during the fatigue tests at the high fatigue stresses in both tension and compression. Large amounts of plastic deformation complicated the test procedure for in some instances the limit switch of the fatigue machine was reached before actual failure occurred. Of greater importance, however, is the fact

that many of the failures were more characteristic of general yielding than of fatigue; i.e., the failure appeared as a necking down of the specimen rather than the usual horizontal fatigue crack of brittle nature. Since general yielding of a notched specimen is hardly conceivable, this yielding characteristic of the unnotched specimens could have nullified the intended purpose of this investigation. In addition, for relatively high compressive fatigue stresses plastic buckling occurred in the specimens without prestress. This phenomenon could not be eliminated by changing the specimen geometry due to the limitations of the test apparatus. Thus, another method of eliminating the buckling had to be employed. This was accomplished to a large extent by the static compressive prestress.

This prestressing procedure seemed to be justified in that the static cycle of stress would correspond to the first cycle or perhaps the first few cycles of fatigue stress. Comparison of the results reported herein and Hoffman's (28, 41) results for the same material tends to indicate that this assumption is correct.

In this study, the values of static prestress were chosen, in most instances, by the limits of the equipment used in the process. However, the values were selected at increments of stress which were roughly equal over the entire range. The values of prestress were computed as the quotient of the load and the area corresponding to this load, the true stress by conventional definition. It was not always possible to attain exactly a chosen prestress but nominally the studied static prestresses included 50,000, 69,000, 86,000 and 97,000 psi compression, and 60,000 and 74,000 psi tension. A tabulation of the average values

and the maximum deviations from these averages obtained in the static prestressing operation is given in Table 2. A stress-strain diagram illustrating the entire compression prestress process is given in Fig. 2.

The abnormally high value of Poisson's ratio recorded for the 97,000 psi prestress completely escapes explanation. It was computed using small deformation theory, but large deformation theory would give even greater values. Transverse strain was determined by micrometering the bar to thousandths of an inch at 5 equally spaced points in each direction. The initial and final widths and breadths were then averaged from these ten measurements. Two values for the transverse strain were then computed, one value for the width and the other for the breadth of the bar. These two values were again averaged giving a single average value for transverse strain. Longitudinal strain was obtained by measuring the initial and final lengths of the bar to hundredths of an inch.

Incidentally, a very brief study was made of the distribution of strain over the length of the bar. It was found that the greatest transverse and longitudinal strains occurred near the outer eighth points of the bar and the smallest values occurred at the midpoint of the bar. The magnitude of this variation was small and could hardly be considered significant.

The static compressive prestress was accomplished in increments of approximately 1 in. total strain with the 3/4 in. square bar supported along its length by 1/2 in. thick steel guide plates held in position by a 6 in. square block of wood which was notched longitudinally through its

center to accommodate the guide plates. It was clamped transversely in both directions by bolted steel clamps. These 1 in. increments of total strain were repeated until the desired prestress was reached. A detailed illustrated explanation of this compression prestressing process is given by Elling (20) who developed the equipment used in this process.

Only one change was made in Elling's procedure. This change consisted of not planing the bars to the original 3/4 in. square cross-section after each completed cycle of prestress. As may be seen in Fig. 2 and Table 2, the elimination of the intermediate planing apparently did not affect the process for the first four cycles of loading. It should be noted that the stress-strain diagram for the last two cycles of compressive prestress without intermediate machining are not shown in the figure. They are not shown since the plot of the first four cycles with and without intermediate machining showed no significant difference in the final values of stress and strain attained. It became apparent, however, on the last cycle of compressive prestress where the bars had not been machined, that the final stress attained was not the same as that obtained by Elling for the same strain. It appears that the stress is not the significant quantity so that this inconsistency is of little consequence and the values of strain were thus held constant.

The inconsistencies in the stress attained became apparent when an attempt was made to replace a bar in its supporting blocks to attain a slightly higher stress. Actually, the stress attained during this added cycle was found to be less than at the end of the previous cycle. The significance of this observation would appear to be that the stress attained is a function of the lateral clamping force exerted by

the supporting blocks, and thus stress should be given less weight than longitudinal strain. However, it is more convenient to state stresses rather than strains and thus approximate prestresses are used in reporting the fatigue data.

All material that was prestressed for use in the Sonntag machine was strained at a constant rate of 0.042 in. per min. which corresponds to the rate of operation of the static preload mechanism of this machine as described below. The rate of strain should not affect the fatigue results; nevertheless, it was eliminated as a variable by maintaining a constant strain rate.

Since Elling was primarily interested in the phenomenon of compression fatigue, he considered only material prestressed in compression. In this investigation however, static tension prestresses also seemed desirable. The latter was accomplished by merely placing the 3/4 in. square bars in standard tension V-notch grips of a 120,000 lb capacity universal testing machine and tensioning them the desired amount. Each bar was gripped so that approximately 5 in. remained clear between the grips, and the fatigue specimen was cut from the middle of this 5 in. length with the minimum section of the prestressed bar placed at the center of the test section. The strain rate during prestressing was again maintained at a constant rate of 0.042 in. per min.

For the 60,000 psi tensile prestress the 3/4 in. square bars were not reduced in section; they were merely gripped in the machine and the load was applied continuously until the desired stress was obtained. Before installing them in the machine, a 4 in. gage length was laid out on two of the machined longitudinal surfaces. These initial gage

lengths were measured with a pair of dividers. Similarly, the same gage lengths were measured at the end of the load cycle. For the 74,000 psi tensile prestress it became necessary to reduce the transverse dimension in one direction by removing 1/16 in. from either side, because the transverse yielding would render it impossible to fabricate the required 3/4 in. threads at the end of the fatigue specimen. The length of this 5/8 x 3/4 in. reduced section was 2-1/4 in. on which a 2 in. gage length was laid out. The initial and final gage lengths were again measured with a pair of dividers. The transverse dimension for both prestresses were measured initially and finally with a 0.001 in. micrometer. These measurments were taken at each end of the gage length as well as at the center and then were averaged in the case of the 60,000 psi prestress specimens while for the 74,000 psi prestress specimens the minimum cross section was used to compute the stresses. The reason for the different method of computation was the fact that the 60,000 psi material showed no necked area while the 74,000 psi material exhibited significant necking at approximately the center of the gage length.

The static tensile properties determined from standard 0.505 in. diameter tensile coupon tests of the prestressed material are summarized in Table 3 and shown graphically in Fig. 3.

The physical dimensions of the unnotched specimens are shown in Fig. 4. These unnotched specimens were prepared from material both with and without prestress. In either case, the actual specimen preparation was the same. The bars were first turned to 3/4 in. diameter in a lathe. Next the specimens were cut to their approximate desired length and the centers were established on their ends. The length of

the bar after prestressing determined whether one or two specimens were prepared from each bar.

The threads were turned and the ends were faced between centers in a lathe. A template was used to form the contour on all specimens and heavy spring tension applied against the template assured uniformity of all specimens. The contour was formed by a roller follower which followed the template while the lathe compound fed automatically. During the cutting operation, oil flowed continuously over the specimen to reduce the heating so that the specimen never felt excessively warm. Therefore, the temperature attained during the specimen preparation should not have exceeded 110-120°F. It is quite doubtful that even this temperature was reached since no noticeable heating was observed. A cutting tool was used to form the specimen to within 0.001 in. of the desired minimum diameter and polishing was used to reduce the specimen to the desired diameter.

The polishing was accomplished by leaving the specimen between the centers of the template equipped lathe. The standard tool holder was replaced by one adapted to support vertically a 1/16 HP 6000 rpm electric motor. A special abrasive cloth holder was made for this motor in which folded abrasive cloth was clamped through the center of this holder which projected about 1/4 in. on either side of it. Thus, the abrasive cloth contacted the specimen only during a very small proportion of each revolution of the motor, greatly reducing the possibility of heating during the polishing operation. During polishing, the lathe was run at less than 200 rpm while the motor which rotated at right angles to the axis of the specimen, was run at slightly less than

its no load speed of approximately 6000 rpm. Because of the differential in speed of rotation, the scratches introduced during the operation were essentially longitudinal.

The polish was accomplished in four stages using successively No. 80, No. 120, and No. 240 aluminum oxide cloth and then Crocus Cloth.

The notched specimens were prepared only from material without prestress. In their preparation the same procedure as that used for the unnotched specimens was followed except that the template was used to turn the bar to the outer reduced diameter as specified in Fig. 4. When this outer diameter was reached, a tool ground to the proper notch dimensions was used to cut the notch to within about 0.001 in. of its proper width and depth. A length of piano wire with a diameter one standard size smaller than the width of the notch was then installed in the chuck on the polishing motor used in polishing the unnotched specimens. The lathe and motor were run at the same speed as used in the polishing of unnotched specimens in order to polish the notch. The latter was accomplished in two stages. The abrasives used were a mixture of oil and Nos. 240 and FFF. aluminum oxide dust which were fed down the piece of piano wire to accomplish the polish in the same manner as described for the unnotched specimens except, of course, that the lathe compound was held stationary. This method of polishing the notched specimens is similar to that used by Moore and Morkovin in which they obtained a consistent circular contour in the notches.

The static tensile coupon specimens conformed to the ASTM standard 0.505 in. dia. tensile specimen.

The specimen number gives the position of the specimen in the parent plate and are typical of those shown in Fig. 1. The final two letters "A" and "B" are used only to differentiate between two specimens from one bar and they do not give the position of the specimen in the individual bar.

2. Testing Equipment

In a direct extension of Elling's tests, twenty additional tests were completed in the Wilson lever-type machine. However, the results of these tests are not included herein for in these tests an attempt was being made to further develop Elling's conclusion that failure by fatigue would not occur for stress ranges of less than 90 per cent of the static prestress. As a consequence of this endeavor, the stress ranges employed were such that the static prestress probably would not correspond to the first few cycles of fatigue stress and the results are not comparable with those reported below.

The original data reported herein was obtained in a 10,000 lb capacity Sonntag universal fatigue testing machine, Model SF-10-U. A general view of this machine and the attached tension-compression apparatus used in testing is shown in Fig. 5. This is a constant load type machine in which the alternating load is obtained from the vertical component of centrifugal force produced by an adjustable weight turning at a constant speed of 1800 rpm. A friction clutch allows the main motor to reach synchronous speed almost instantaneously while the adjustable weight reaches the same speed within 8-12 seconds to prevent momentary overload of the specimen. The position of the adjustable weight

naturally determines the amount of applied alternating load from 0 to ±5000 lb. The horizontal component of centrifugal force caused by the rotating mass is absorbed by four flexplates attached to the oscillator of the machine. To clarify the above description, Figs. 7 and 8, taken inside the cabinet of the machine, are included.

The load is maintained at a constant value by an electronic load maintainer which is coupled into the mechanism for applying the mean load in a fatigue cycle. This electronic load maintainer consists essentially of an inductance bridge of which the balance of one arm may be controlled manually or automatically by an adjustable iron core moving in an activated coil of the electronic circuit. Manually, the inductance balance is affected or the desired mean load in a fatigue cycle is set by the counter located on the base plate of the machine as shown in Fig. 7. This counter actually measures the deflection of four heavy springs located at the base of the oscillator in thousandths of an inch. These springs are calibrated so that it is more convenient to state the calibration constant in terms of the load applied per division of the counter. The determination of and the value of this calibration constant will be discussed below.

The counter is connected by a flexible shaft to the electronic coil, the housing of which is rigidly fastened to the base plate to which the four heavy springs are attached. Turning the crank located to the right of the counter adjusts the position of the coil. The iron core for this coil is rigidly fastened to the base of the oscillator where the opposite ends of the heavy springs are also rigidly attached. Thus, from a balanced zero load position, the counter may be set to any desired load

between zero and 5000 lb in either tension or compression, the capacity of the mean load mechanism.

The no load inductance balance of the electronic circuit is initially set by removing entirely the core from the coil and adjusting a separate induction coil located in the power supply cabinet until balance is indicated. The indication of balance in all cases is determined by a Weston Sensitrol located on the control panel of the machine. This control panel is shown in Fig. 6 with the Sensitrol located in the lower left hand corner. This meter serves two purposes other than indicating balance of the preload mechanism. The first of these is that it automatically stops the loading device when the set load is reached if the load is being controlled manually. Its second purpose is to automatically start the loading device whenever the mean load falls below the set value if the load is being controlled automatically. Incidentally, the automatic load control only operates when the main motor is running; the manual control may be operated separately.

The mean load or preload is applied by a separate induction motor which is connected to a gear reduction box. This gear reduction box drives a continuous chain which in turn rotates two sprockets located beneath the lower base plate of the machine, one on either side of the oscillator. These sprockets are connected to two specially designed screws which possess little or no backlash. These screws then either raise or lower the plate which supports the four heavy springs under the oscillator, thereby applying the load to the specimen.

The cycle counter shown in the lower right corner of Fig. 6 counts the cycles in 1000's and is driven by a separate synchronous

motor. This motor is activated through the main motor circuit so that it starts when the main motor starts and stops accordingly. Since it is also a synchronous motor, it runs at a constant speed equal to that of the main motor.

When a specimen fails, the displacement increases to approximately $\pm 1/2$ in. and two limit switches located at the base of the oscillator break the main motor circuit. However, the use of these switches as limit switches resulted in the fracture surfaces being pounded until they were greatly distorted before the machine actually stopped. Since valuable information may often be gained from the appearance of the fracture surface, a means was devised to stop the machine before total fracture occurred. This consisted of installing an additional limit switch to the upper plate of the machine and an adjustable actuator to the oscillator. This actuator could then be adjusted so that only a small additional displacement occurring during a test would completely shut off the machine. This additional assembly is shown in the foreground in Fig. 8. To prevent excessive displacement of the mean load apparatus from the action of the automatic load maintainer, two other limit switches were installed as standard equipment which limit the total displacement to approximately $\pm 7/16$ in.

The cabinet of the Sonntag machine is only a shell which supports the test mechanism on twelve springs, three located at each corner. Being entirely spring supported, the test mechanism neither receives nor emits external vibrations which might cause overload of the specimen. This cabinet also houses the electronic equipment and controls which are rigidly attached to it.

The Sonntag machine is designed to perform various types of fatigue tests. However, for this study only axial tension and compression loads were used. The tension-compression apparatus used is standard for the machine except for the tension spherical specimen holders which were fabricated and hand lapped into their respective seats for these tests. This modification was necessary since the maximum thread diameter of the specimens was 3/4 in. while the standard holders can accommodate only a 1 in. diameter. Figures 9, 10, and 11 show the tension-compression apparatus, and are self explanatory. Naturally, the spherical compression seats and tension holders greatly facilitate the attainment of an axial load on the specimen while it is being tightened in the tension-compression apparatus.

A standard universal testing machine of 120,000 lb total capacity was used to prestress all material and to test the standard 0.505 tensile coupon specimens. A platen pacer was used to maintain a constant total strain rate of 0.042 in. per min.for both the prestressing process and the testing of the coupons.

3. Test Procedure

Unless a new specimen was set up immediately following the failure of the previous one, the main motor of the fatigue machine was run for at least a half hour to allow the machine to warm up. While the machine was warming up, the spherical tension specimen holders and half round compression bearings were removed and thoroughly wiped clean. The seats for these parts were similarly cleaned. Each part was then coated with a thin film of SAE 20 oil which was followed by evenly spreading a coat of

a dry molybdenum-sulfur lubricant on the oiled part. The parts removed from the tension-compression apparatus were reassembled and the specimen was placed in test position.

The machine was then stopped, the preload zero was recorded, and the specimen was tightened. The twelve shoulder bolts shown in Fig. 11 were tightened cyclically in an attempt to eliminate as far as possible any bending which might be introduced as the specimen was drawn down. Each cycle consisted of tightening diagonally opposite bolts in alternate pull-heads until an entire cycle was completed. Each succeeding cycle reversed the previous one. At the completion of each cycle of tightening, the clamping force introduced in the specimen was removed by controlling the preload motor manually. The estimated maximum clamping force introduced on any specimen was 500 lb.

At the completion of the tightening operation, the desired mean load was set on the preload counter, and the desired alternating load was set by adjusting the rotating mass. The mean load was then applied manually until the desired value of preload was reached. When yielding occurred with just the mean load on the specimen, the load was maintained manually until no drift was recorded on the sensitrol over a period of five minutes. This five minute interval was arbitrarily chosen as the point at which the load could be considered stable.

When the mean load had stabilized, the main motor was started and the automatic load maintainer was turned on simultaneously. In tests where yielding occurred, the frequency of operation of the load maintainer was timed until its period of operation reached five minutes. Again this interval was arbitrarily chosen as the point at which stability

had been reached. In many of the statically prestressed specimens, it is interesting to note that yielding apparently did not begin immediately but occurred after a significant number of cycles in the tests. Almost without exception, this yielding would first occur in a sense opposite to that set on the load maintainer. After yielding progressed for a short time in this sense, it reversed itself and often yielding also progressed in the reversed sense. The yielding in a sense opposite to that set on the load maintainer can doubtlessly be attributed to the Bauschinger effect and was found to have a relatively short duration during the cyclic straining. Since the load maintainer is only operative in the sense originally set, the Sensitrol had to be watched quite closely during this type of test to insure that the desired stress range was maintained.

Once stability had been attained, the added limit switch was set so that it would stop the machine when a crack occurred in the specimen. This switch worked quite well in tests where the range was predominantly tension provided that it was reset periodically to compensate for the small amount of yielding which usually occurred. However, when the stress range was predominantly compression the added switch was not particularly effective since the yielding which occurred just prior to failure, with very few exceptions, rendered it inoperative since the trip under such conditions moved away from the switch as yielding progressed. Consequently, it appears advisable to provide a second similar limit switch which will remain operative when compression yielding occurs.

After the main motor was started, it was not stopped until failure occurred or until it became apparent that no failure would occur. As intimated above, the tests were very closely observed until the load had essentially stabilized after which it was checked periodically with the interval between checks seldom being greater than eight hours. Checking the machine consisted of visual inspection of the specimen and its holders as well as the entire machine, especially the direction of drift of the Sensitrol. Also, the number of accumulated cycles, the gross diameter of the specimen, and the room temperature were recorded.

All static tests were conducted at a constant strain rate of 0.042 in. per min. Before each test, the minimum diameter of each specimen was determined by a 0.001 in. micrometer. An autographic load-strain recording was obtained with a 2 in. gage length microformer extensometer for strains up to four per cent. Until the microformer was removed, no diameter measurements were possible but the reduction in diameter was on the order of 0.001 in. at 4 per cent strain.

The microformer was removed while no load was being applied and a calibrated clip gage was inserted in the gage holes which had been formed by the microformer. The strains indicated by the bonded electrical strain gages on the clip gage were measured with a portable strain indicator. These clip gage strains were readily reduced to specimen strains with the calibration constant. Load on the specimen and the specimen diameter were recorded at intervals of 200 micro in. per in. strain indicated by the clip gage or a specimen strain of 1.2 per cent. After the clip gage was removed, the specimen was fractured and the fracture load was noted. Following failure, the final gage length and the diameter of the fractured specimen were measured.

III. TEST RESULTS AND ANALYSIS

1. Current Test Results

The results of the ninety-four tests of unnctched specimens conducted in this investigation are summarized in Table 4 and in Fig. 12. The true stress range in Table 4 was computed using a number of definitions of the area "corresponding to the applied load". Obviously, when yielding occurred throughout the test the area corresponding to the applied load could not be uniquely defined. The definition adopted depended upon the experimental conditions which prevailed. These conditions may be briefly summarized as:

1) When total fracture occurred and the test was so short that only the diameter at the start of the dynamic test was known, the true stress range was computed using the one measured diameter.

2) Early in the program only initial and final specimen diameters were measured. Eight tests were run before diameter measurements were made each time the machine was checked. When yielding obviously ceased during the test and no failure occurred, the final area defined the true stresses if no other areas were available. Otherwise the average of the initial and final areas defined the true stresses.

3) If yielding occurred throughout the test at roughly a constant rate, as indicated by constant frequency of operation of the Sensitrol, the average of the initial and final areas during the dynamic test seemed to be the most reasonable value of area.

4) When yielding occurred throughout the test but at a varying rate with essential stability occurring rather early, the most

reasonable area seemed to be defined as the average of the area where the preload essentially stabilized and at failure.

5) When yielding, as indicated by the load maintainer, began after the test was underway, the true range of stress is defined by the average of the areas when yielding began and at failure. In a majority of tests, yielding began immediately for which case the column in Table 4 containing the number of cycles at which yielding started is left blank.

6) When yielding stopped rather early in the test so that for most of the test a constant area existed, the area at which yielding ceased was used to compute the true stresses. The cessation of yielding was determined by the approximate number of cycles at which changes in specimen diameter were no longer noted.

7) In one test the preload limit switch was reached at approximately the point where stability of yielding was reached. Consequently, the test was allowed to continue even though the load maintainer was no longer operative. For this case, the true range of stress was computed using the area existing at the time that the limit switch was tripped.

The error in the stresses computed by the above means decreases in the order of definition of area from 1 to 6. No accurate estimation of the error can be made. However, it is believed that the error ranges from about 10 per cent for definition 1 to about 2 per cent for definition 6.

The general yielding type of failure reported in the column for remarks is defined as those failures where the specimen contained no crack at failure. Failure in these cases occurred by constant yielding

throughout the test or by rapid yielding during the last few thousand cycles of the test. In either case, this yielding resulted in a considerably necked region where the area was so greatly reduced that the specimen could not sustain the load. In this regard it is interesting to note that in all tests of greater than 20,000 cycle duration, three distinct periods of relative flow were apparent. The first period was characterized by a decreasing rate of yielding for about ten to fifteen thousand cycles. The second period, that which encompassed the major portion of the test, was one in which practically no yielding occurred. The third period occurred during the last twenty to fifty thousand cycles and was characterized by an increased rate of yielding. This observation agrees with the qualitative pictures drawn by other authors in the field of fatigue.

In Fig. 12 the results of all valid tests of unnotched specimens in the current series are plotted on modified Goodman coordinates. These tests are those in which no apparent buckling of the specimen occurred. Each test is represented by two points in the plot, one point denotes the average nominal stresses and the other the average true stresses. In some regions these two points obviously coincide. In the final analysis the true stresses were not considered; however, they are included on the plots for completeness. At each plotted point the number of cycles to failure in thousands is reported so that the plot summarizes the data as completely as possible. Also included on these diagrams are the empirical average nominal stress contours for specified constant lives; the derivation of which is given later in this chapter.

In addition to the plot of the actual test values, the points defining the average nominal stress ranges for 1×10^5, 5×10^5, and 2×10^6 cycles to failure obtained by interpolation of the data are given. These interpolated values are shown for comparison with the empirically derived contours. The S-N curves utilized in this interpolation are of the usual shape and are not included herein because their inclusion would add greatly to the length of the report without materially adding to its clarity. A tabulation of the results of these interpolations is given in Table 6.

In the tabulated data, it is apparent that all failures for stresses of tension to greater tension were characterized by general yielding. In only one test at these stress ranges was a crack actually apparent at the surface of the specimen at failure and that was in specimen I-1-A. All other failures for a zero to tension range and tension to greater tension ranges exhibited serious necking but no crack appeared. This general yielding phenomena may account for the constantly decreasing slope of the constant life contours obtained from the test results.

The tabulated data also illustrates that buckling of the unnotched specimens occurred for all tests of virgin material in which the compression stress exceeded the tension stress. Consequently, only the results of tests of statically prestressed material are shown in the region of tension to greater compression ranges. Since buckling of the virgin material occurred at such a low stress, the absence of buckling at higher stresses on the prestressed material may be open somewhat to question. In the test results reported, no buckling was noted.

Projecting the contours obtained from the test results to the pure compression axis gives results in very good agreement with those obtained by Hoffman and Elling (28 and 41) whose specimen geometry was such that buckling was unlikely.

A rather large extrapolation of the S-N curves was necessary in the region approaching pure compression, but it is felt that the errors introduced by this extrapolation are not serious. The extrapolation was accomplished by using the results of the buckled specimens as well as those of the specimens which did not apparently buckle. Despite the presence of the observed buckling, the test results obtained from buckled specimens are not far from correct in terms of the usual S-N curve.

To complete this discussion, the stress ranges employed on the prestressed material will be described. As noted previously the static prestressing cycle was considered to be equivalent to the first few cycles of fatigue stress. For this to be true the maximum stress of the range employed had to approach the static prestress as closely as possible. This maximum stress was determined by a trial and error procedure consisting of varying the stresses applied to each specimen until no apparent buckling occurred for a specimen tested in the compression range and no serious yielding occurred for a specimen tested in the tension range. The first specimen tested under these conditions was subjected to a maximum stress approximately equal to the static prestress and a minimum stress defined by an extrapolation of the experimental curves. Succeeding specimens were tested at successively smaller values of maximum stress until the desired conditions were met. The fact that

an extrapolation of the constant life contours to the pure compression axis gives results in good agreement with Hoffman and Elling's seems to justify the hypothesis that the static prestress is equivalent to the first few cycles of fatigue stress.

The wide difference between the results of tests of virgin material and material statically prestressed in tension should be noted. If an experimental 2×10^6 constant life contour is drawn on Fig. 12 and is extended to pass through the results of the tension prestressed material, it is found that this contour remains approximately a straight line in the tension region. Such a straight line would be in agreement with constant strain results reported by Smith (46) and suggests that the results obtained under conditions of constant load are not comparable to those obtained under conditions of constant strain. Usually under conditions of constant strain an attempt is made to maintain constant load conditions by periodically adjusting the machine to compensate for changes in load range resulting from yielding. This periodic adjustment results in successive stages of work hardening which would ultimately lead to a condition similar to that employed in the present study in the tension range. The apparent agreement in the compression range of the present series where strain hardened material was exclusively used with constant strain tests by Hoffman and Elling may also be a manifestation of this observation.

Finally it should be noted that a definite stress condition separating failure from no failure seems to exist in the current tests of material strain hardened in tension. This condition as may be seen in Fig. 12 seems to be a maximum stress of 61,000 psi with a minimum

stress of 30,000 psi for 60,000 psi tensile prestress. The corresponding point for the 74,000 psi tensile stress appears to be a maximum stress of 70,000 psi with a minimum stress of 45,000 psi. However, this result should not be considered conclusive since only one value of minimum stress was considered in each case.

The results of the tests of the ~~thirty~~-three notched specimens with a theoretical stress concentration factor of 2.0 are summarized in Table 5 and in Fig. 13. The true stresses reported in the table were computed in a manner similar to that used for the unnotched tests. However, the change in notch depth could not be measured during the test because the notch depth micrometer would not fit into the apparatus. Therefore, only measurements of the gross diameter were made and these measurements were used as a basis for selection of the reasonable area for computing true stresses. If no yielding occurred or if yielding did not appear to occur until failure, the initial net area was used to define true stresses. When the majority of yielding occurred very early in the test with no significant change in gross diameter occurring subsequently, the final area was used to compute the true stresses. With yielding apparently occurring throughout a test the average of the initial and final net areas during the dynamic tests were used in the computation. The errors in true stress computed in this manner should be approximately the same as those stated for the unnotched series. The number of cycles appled until yielding appeared to stop was considered the point at which the gross and net area reached stable values.

One should notice that in the tests involving rather high compressive stresses cracks formed but apparently did not propagate

significantly even after a large number of subsequent cycles of stress. This observation may indicate that a tension residual stress was introduced at the root of the notch while the majority of the cross-section carried a compressive stress. In fact, it would seem that this would be the case, but, unfortunately, no correlation exists between the stress range of a notched specimen subjected to rather high compression and that of an unnotched specimen subjected to predominantly tension stresses.

For high tension or compression ranges the notched specimens yielded considerably but the magnitude of the total deformation was much less than that for the unnotched specimens. Also, the notched specimens generally work hardened sufficiently to withstand the applied forces much more rapidly than the unnotched specimens. In all failures of notched specimens, a definite crack was detected despite the amount of yielding which occurred in the test.

In Fig. 13 the results of the tests of notched specimens are plotted on modified Goodman coordinates. In the notched series, buckling did not seem to occur until a maximum compressive stress of 70,000 psi was attained. Consequently, only two specimens of the thirty-three tested showed evidence of buckling.

A summary of the modified Goodman diagrams for the notched and unnotched specimens is shown in Fig. 14. This figure will be described in detail in Section 3.

2. Tests by Grover, Bishop, and Jackson (23, 24, 25, 26, 27)

The results of 984 tests of 24S-T3 and 75S-T6 aluminum alloy and normalized 4130 steel are summarized by these investigators in tabular form as well as on numerous S-N curves. Their tests include

unnotched specimens and notched specimens with theoretical stress concentration factors of 1.5, 2.0, 4.0, and 5.0. The included stress ranges vary from full reversal to high tension to greater tension. These tests were conducted on electrolytically polished sheet specimens in Krouse constant strain type axial load fatigue machines. By frequently adjusting their machines, the authors state that constant load conditions were essentially maintained. In their analysis, Messrs. Grover, Bishop, and Jackson conclude that the indicated fatigue reduction factor is always equal to or less than the theoretical stress concentration factor. Also they found that the difference between the fatigue reduction factor and the theoretical stress concentration factor increases with increasing notch severity but not in proportional amounts.

For all values of theoretical stress concentrations studied for each material, points corresponding to 1×10^5, 5×10^5, and 2×10^6 cycles to failure were selected from the S-N curves given by these three investigators. These points were then plotted on modified Goodman diagrams of the same type used in summarizing the current series of tests. The resulting plots are shown in Figs. 15 through 23. Also included in these figures are the empirical constant life contours whose derivation is given in section 4 of this chapter.

The trend of the results of the notched tests of the aluminum alloys and high alloy steel as shown on the modified Goodman diagrams is similar to those of the current study. However, the trends of the results for the unnotched specimens are generally different than those for the current series. Yet, the test results for unnotched specimens of normalized 4130 steel appear to be in better agreement with the results for

the killed structural steel in that the experimental constant life contours appear to have a steadily decreasing slope as the range approaches the static ultimate tensile strength. It is unfortunate though that these earlier investigators did not extend their tests further into the tension region so that this trend could be more definitely established. This semblance of a trend may nullify the previously described possibility that fatigue tests run under conditions of constant load are not comparable to those run under conditions of constant strain. Therefore, this question certainly warrants further study.

3. Summary of Attempted Analysis

The analyses which were pursued and which failed to yield consistent or reliable results are briefly summarized in Chapter I. Their failure seems to render a more detailed description of little or no apparent value. Consequently, further discussion will not be included here except for the case of the hypothesis concerning true range of stress which at the outset was a primary consideration in the study.

The primary disproof of the true range of stress hypothesis is illustrated in Fig. 14. This figure portrays the interpolated constant life contours resulting from the actual test results on modified Goodman coordinates. Six groups of contours are shown in the figure.

The lowest group of contours, consisting of three individual solid lines and two individual short dashed lines which intersect at the diagonal full reversal line, are the constant life contours for average stress on the net section of notched specimens. The solid lines portray the average applied nominal stress while the short dashed lines

portray the average applied true stress. For the 2×10^6 cycle contour the nominal stress is the same as the true stress since no change in area was observed in these tests.

The intermediate group of six curves which intersect the above described group portray the constant life contours for unnotched specimens. The contours made up of long dashes describe the average applied nominal stress while the contours made up of an alternation of long dashes and short dashes describe the average applied true stress.

The highest group of contours is related to the lowest group by the theoretical stress concentration factor of 2.0. Consequently, the same symbol is used for the contours of each group. This highest group of contours represents the theoretical stress at the root of the notch for the notched specimen tests based on a stress concentration of 2.0.

The wide variation in the shapes of the contours for the unnotched and notched specimens in itself disproves the premise which led to this study. A better illustration of the fallacy of the hypothesis is a consideration of the range of stress to cause failure under full reversal in a notched specimen. For failure of a notched specimen in 2×10^6 cycles of full reversal of stress, a range of 76,400 psi (theoretical maximum) was required. For failure of an unnotched specimen in 2×10^6 cycles at a range of stress of 76,400 psi the required stress ranged from 70,000 psi compression to 6,400 psi tension as also seen in Fig. 14. This range would require a mean stress of 31,800 psi compression to be developed in the notched specimen if the true range of stress hypothesis were valid. The attainment of such an extreme mean

stress in a notched specimen subjected nominally to full stress reversal is not at all tenable.

4. Derivation of Empirical Constant Life Contours

Early in the analysis, it became apparent that all of the constant life contours on the modified Goodman diagrams could be reasonably well represented by straight lines with the exception of the current series of unnotched tests. As a result, average straight lines were fitted to the results by eye. The slopes and the intercepts on the zero to tension axis for these straight lines were then determined. It was noticed that the slopes for the notched specimens were relatively constant. Therefore, these slopes were tabulated and an average of the thirty-nine resulting values gave a value of 0.700. The slopes for the unnotched tests were not nearly as consistent; nevertheless, it seemed possible that reasonable results could be obtained by following the same procedure for this series. The resulting average of twelve slopes for the unnotched series was 0.500. The errors computed between these average values of slope and the values of the slopes used in computing the averages are tabulated completely in Table 7.

After the slopes of the straight line average contours were defined, it was necessary to also define the intercept in order to completely define the contour. At first, this appeared to be an impossible task, but eventually an empirical approach was selected which correlates the zero to tension intercept with the static tensile properties of the material. Before a description of this correlation is presented it is emphasized that the result is absolutely empirical and may well be fortuitous. The element of chance is expressly

illustrated in the fact that one of the parameters used was not given by Grover, Bishop, and Jackson so that average values from the literature had to be inserted. Nevertheless, the final result, as illustrated in Table 7, leads to a maximum error of 59.3 per cent for the intercept of the unnotched tests of the current series. However, this series obviously does not lend itself well to this straight line analysis. For the remainder of the materials tested, the maximum error is 25.1 per cent which, considering the usual nature of the scatter in fatigue tests, is good. Furthermore, a series of tests located after this analysis had been completed gave more opportunity to check the results. This series of tests was a group of zero to tension fatigue tests with notched specimens of 15 different steels reported by Baron and Larson (11). In this last series all of the parameters required in the empirical analysis were reported and the maximum error in the computed intercept for the various series is 38.4 per cent, as shown in Table 8. Again, considering the nature of fatigue results this error does not seem too severe. As may be seen in Table 8, the maximum error in computed intercept is recorded for material M with a stress range of 0-30,000 psi. At this stress range the average life was 477,000 cycles while at a stress range of 0-31,500 psi the average life was 515,000 cycles. The next highest error is 33.8 per cent for the Baron and Larson series.

Finally, it should also be emphasized that the following analysis is certainly not the only possible one. This analysis assumes that the theoretical stress concentration is developed in the notched specimens and disregards any additional stress concentration which might arise through inherent defects in the material. Since small stress

oncentrations undoubtedly exist in unnotched specimens of any material r virtue of inherent defects in the material structure, this assumption s not entirely realistic. A more realistic approach would be one in ich either a constant value or a function of the theoretical stress oncentration factor is assumed for the concentration due to inherent efects. Such an approach could be accomplished by assuming various alues or functions describing the concentration due to defects and itting them to the results to determine the best agreement. However, ssuming no added concentration from defects in the materials would esult in the greatest error between derived and experimental values for he unnotched specimens and lesser error as the severity of the imposed otch was increased. Yet, in the results of the subsequent analysis the aximum error in intercept was generally observed for the greatest notch everity so that refinement seems to be unnecessary.

Despite the numerous reservations discussed above the results f the analysis seem to warrant presentation and may suggest a basis for urther investigation.

The intercepts on the zero to tension axis of the modified oodman diagrams for only notched specimens at a constant life contour of x 10^6 cycles were reduced to a common value. This was accomplished by ultiplying the observed intercept by the corresponding theoretical stress oncentration factor for each material. This procedure gave one common ntercept stress for the ASTM-A7 steel, four for each of the aluminum lloys, and four for the 4130 steel. The values were averaged to provide ne value for each material as follows:

Material	Average Nominal Common Intercept Stress psi	Range of Values In Average psi
Annealed ASTM-A7	68,000	Only one value
24S-T3 Aluminum Alloy	48,000	43,100 - 54,800
75S-T6 Aluminum Alloy	50,000	43,800 - 56,800
Normalized 4130 Steel	107,000	96,000 - 120,000

It should be obvious that these average common intercept stresses correspond theoretically to the stress at failure in 2×10^6 cycles for a hypothetical unnotched specimen containing no stress raiser. The observed intercepts for the 2×10^6 cycle contour were used in the analysis because smaller amounts of yielding would be encountered at this life than at lesser lives, and, therefore, these data are possibly more reliable.

Except for the reduction of area of the three materials tested by Grover, Bishop, and Jackson, all static tensile properties of the four materials were known. Average values for the reduction of area for 24S-T3 aluminum alloy and normalized 4130 steel were found in Reference (21) while that for 75S-T6 aluminum alloy was found in Reference (10). The necessity for using average values rather than actual values for the specific material studied was most unfortunate and renders the analysis even more questionable. Following are the average static tensile properties used in the analysis.

Material	Yield Strength ksi	Ultimate Tensile Strength ksi	Per Cent Elongation in 2 in.	Per Cent Reduction of Area
Annealed ASTM - A7	33.65[a]	56.15	43.1	63.3
24S-T3 Aluminum Alloy	54.00[b]	73.00	18.2	26.0
75S-T6 Aluminum Alloy	76.00[b]	82.50	11.4	36.0
Normalized 4130 Steel	98.50[b]	117.00	14.3	66.0

[a] Lower yield point

[b] 0.2 per cent offset

Many functions of the above properties singly and in combination were investigated in an attempt to relate the common fatigue intercept stress to the static tensile properties. All such attempts failed except the following which reduced to four simultaneous equations:

$$33.65\ A + 56.15\ B + 43.1\ C + 63.3\ D - 68000 = 0 \quad \text{(ASTM-A7)}$$
$$54.00\ A + 73.00\ B + 18.2\ C + 26.0\ D - 48000 = 0 \quad \text{(24S-T3)} \qquad (1)$$
$$76.00\ A + 82.50\ B + 11.4\ C + 36.0\ D - 50000 = 0 \quad \text{(75S-T6)}$$
$$98.50\ A + 117.00\ B + 14.3\ C + 66.0\ D - 107000 = 0 \quad \text{(4130)}$$

The coefficients of A, B, C, and D are the yield strength, σ_Y, the ultimate tensile strength, σ_U, the per cent elongation, e, and the per cent reduction of area, r. The constant terms are similarly the common fatigue intercept stresses, σ_F. The solution of these equations yielded:

$$A = -1604;\ B = +1705;\ C = -1246;\ \text{and}\ D = +1263.$$

Thus, the general equation given below was found:

$$1705\ \sigma_U - 1604\ \sigma_Y + 1263\ r - 1246\ e = \sigma_F\ . \qquad (2)$$

One will notice in the above equation that the coefficients of the two static strength parameters and the coefficients of the two static ductility parameters are approximately equal, and "factoring" would give an equation of the following general form:

$$\sigma_F = R(\sigma_U - \sigma_Y) + S(r - e) \tag{3}$$

Adjusting the factors R and S to give the least error in σ_F for the notched specimens of the four materials, one obtains the expression:

$$\sigma_F = 1743\ (\sigma_U - \sigma_Y) + 1443\ (r - e) \text{ in ksi.} \tag{4}$$

The second constant in this expression obviously has stress units. Unfortunately, however, this inconsistency could not be resolved. This expression seems to give reasonable results for relatively ductile materials. As an illustration consider a material which has been work hardened to its static ultimate tensile strength where $\sigma_U - \sigma_Y = 0$ such as the material prestressed to 74,000 psi tension from the current tests. For this material substitution in equation (4) yields approximately $\sigma_F = 63{,}500$ psi which would seem to be entirely within reason.

We have also established that:

$$\sigma_2 = m\sigma_1 + \frac{\sigma_F}{K_T} \tag{5}$$

defines the 2×10^6 cycle constant life contour.

Failure at 2×10^6 cycles is of interest since this life corresponds to that frequently defined as the endurance limit for steel. However, it would be valuable to be able to define failure at any number of cycles, N. Consequently, an extrapolation procedure based on actual test results

Material	Yield Strength ksi	Ultimate Tensile Strength ksi	Per Cent Elongation in 2 in.	Per Cent Reduction of Area
Annealed ASTM - A7	33.65[a]	56.15	43.1	63.3
24S-T3 Aluminum Alloy	54.00[b]	73.00	18.2	26.0
75S-T6 Aluminum Alloy	76.00[b]	82.50	11.4	36.0
Normalized 4130 Steel	98.50[b]	117.00	14.3	66.0

[a] Lower yield point

[b] 0.2 per cent offset

Many functions of the above properties singly and in combination were investigated in an attempt to relate the common fatigue intercept stress to the static tensile properties. All such attempts failed except the following which reduced to four simultaneous equations:

$$\begin{aligned} 33.65\ A + 56.15\ B + 43.1\ C + 63.3\ D - 68000 &= 0 \quad \text{(ASTM-A7)} \\ 54.00\ A + 73.00\ B + 18.2\ C + 26.0\ D - 48000 &= 0 \quad \text{(24S-T3)} \\ 76.00\ A + 82.50\ B + 11.4\ C + 36.0\ D - 50000 &= 0 \quad \text{(75S-T6)} \\ 98.50\ A + 117.00\ B + 14.3\ C + 66.0\ D - 107000 &= 0 \quad \text{(4130)} \end{aligned} \tag{1}$$

The coefficients of A, B, C, and D are the yield strength, σ_Y, the ultimate tensile strength, σ_U, the per cent elongation, e, and the per cent reduction of area, r. The constant terms are similarly the common fatigue intercept stresses, σ_F. The solution of these equations yielded:

$$A = -1604;\ B = +1705;\ C = -1246;\ \text{and}\ D = +1263.$$

Thus, the general equation given below was found:

$$1705\ \sigma_U - 1604\ \sigma_Y + 1263\ r - 1246\ e = \sigma_F\ . \tag{2}$$

One will notice in the above equation that the coefficients of the two static strength parameters and the coefficients of the two static ductility parameters are approximately equal, and "factoring" would give an equation of the following general form:

$$\sigma_F = R(\sigma_U - \sigma_Y) + S(r - e) \qquad (3)$$

Adjusting the factors R and S to give the least error in σ_F for the notched specimens of the four materials, one obtains the expression:

$$\sigma_F = 1743\ (\sigma_U - \sigma_Y) + 1443\ (r - e) \text{ in ksi.} \qquad (4)$$

The second constant in this expression obviously has stress units. Unfortunately, however, this inconsistency could not be resolved. This expression seems to give reasonable results for relatively ductile materials. As an illustration consider a material which has been work hardened to its static ultimate tensile strength where $\sigma_U - \sigma_Y = 0$ such as the material prestressed to 74,000 psi tension from the current tests. For this material substitution in equation (4) yields approximately $\sigma_F = 63{,}500$ psi which would seem to be entirely within reason.

We have also established that:

$$\sigma_2 = m\sigma_1 + \frac{\sigma_F}{K_T} \qquad (5)$$

defines the 2×10^6 cycle constant life contour.

Failure at 2×10^6 cycles is of interest since this life corresponds to that frequently defined as the endurance limit for steel. However, it would be valuable to be able to define failure at any number of cycles, N. Consequently, an extrapolation procedure based on actual test results

averaged in the constant life contours of the Goodman Diagrams has been established. It is apparent from the test results that the slope of the constant life contours decreases slightly as the number of cycles defining the contour decreases. Yet, the many approximations and averages used in the derivation so far renders a consideration of this change in slope absurd. Therefore, only a correction to the common fatigue intercept stress, σ_F, was considered in adapting the analysis to various numbers of cycles to failure. This was accomplished by plotting the average intercepts of the constant life cycle contours fitted to the interpolated test data on an S-N log-log coordinate system. Straight lines fitted each of the three points plotted for each stress concentration in each material. The slopes of these straight lines were then computed and resulted in an average slope of 0.115 for notched specimens and 0.057 for unnotched specimens of all four materials. The total range in thirteen individual slopes averaged for the notched specimens was from 0.065 to 0.161 with all but these two values falling between 0.085 and 0.133. On the other hand, the range in slopes averaged for the unnotched specimens was from 0.020 to 0.100 for five individual slopes. Defining σ_N as the common fatigue intercept stress for N cycles to failure and using the average slopes described above, one obtains:

$$\begin{aligned} \sigma_N &= \sigma_F \left(\frac{2 \times 10^6}{N}\right)^{0.115} \quad \text{for notched specimens.} \\ \sigma_N &= \sigma_F \left(\frac{2 \times 10^6}{N}\right)^{0.057} \quad \text{for unnotched specimens.} \end{aligned} \tag{6}$$

Consequently, for any number of cycles, N, we obtain by substitution in equation (5):

$$\sigma_2 = m\sigma_1 + \frac{\sigma_N}{K_T} \tag{7}$$

For the tests analyzed herein we have, thus, established:

$$\sigma_2 = 0.700\ \sigma_1 + \frac{\sigma_F}{K_T}\left(\frac{2 \times 10^6}{N}\right)^{0.115} \quad \text{for notched specimens}$$

$$\sigma_2 = 0.500\ \sigma_1 + \frac{\sigma_F}{K'_T}\left(\frac{2 \times 10^6}{N}\right)^{0.057} \quad \text{for unnotched specimens.} \tag{8}$$

In the second equation (8) a stress concentration factor, K'_T, is included despite the fact that it deals only with unnotched test results. As explained above, a stress concentration in an unnotched specimen is entirely feasible by virtue of the inherent defects in a material. The determination of this unnotched stress concentration was the next step in the analysis. This determination was accomplished for each material by dividing the common fatigue intercept stress for the 2×10^6 cycle life contour, σ_F, for a material by the observed corresponding intercept value obtained from the unnotched test results. The following results were thus obtained:

Material	K'_T
Annealed ASTM-A7	1.548
24S-T3 Aluminum Alloy	1.168
75S-T6 Aluminum Alloy	1.133
Normalized 4130 Steel	1.333
Average	1.296

Using the above average value of K'_T led to gross errors for the unnotched specimens of all four materials. As a result, it seemed quite

possible that the inherent defects in the two different materials (aluminum and steel) could vary widely. Thus, the values of K_T' were averaged for the two aluminum alloys giving a value of 1.15 and a corresponding average of 1.44 for the two steels. Use of the latter averages gave good agreement for the two aluminum alloys but a large error still remained for the steels. Noting that the material properties of the aluminum alloys were quite similar while those of the steel were quite dissimilar, one might anticipate the last result obtained. The final analysis of the unnotched specimens consisted of using the average value of K_T' for the two aluminums and the computed value of K_T' to one decimal place for each of the steels. Thus, the resulting equations for the unnotched specimens are:

$$\sigma_2 = 0.500\,\sigma_1 + \frac{\sigma_F}{1.15}\left(\frac{2 \times 10^6}{N}\right)^{0.057} \quad \text{for the two aluminum alloys.}$$

$$\sigma_2 = 0.500\,\sigma_1 + \frac{\sigma_F}{1.5}\left(\frac{2 \times 10^6}{N}\right)^{0.057} \quad \text{for annealed ASTM-A7 steel.} \tag{9}$$

$$\sigma_2 = 0.500\,\sigma_1 + \frac{\sigma_F}{1.3}\left(\frac{2 \times 10^6}{N}\right)^{0.057} \quad \text{for normalized 4130 steel.}$$

These empirical equations in addition to equations (4) and (8) define the empirical nominal stress constant life contours shown on Figs. 12, 13, and 15 through 23 where the interpolated test values are also shown. Thus, a graphical comparison between the test and empirically derived results may be drawn readily and the maximum errors are tabulated in Table 7. With the exception of the unnotched tests of annealed ASTM-A7 steel, the results appear to be surprisingly good.

The discrepancy between the derived and experimental results is quite apparent in the unnotched series of the current program. By making the broad assumption that the empirical derivation given herein is valid, a possible explanation of the apparent gross error for this case may perhaps be due to a severe sensitivity of unnotched annealed ASTM-A7 steel to eccentricities of loading in fatigue. However, no theoretical or experimental evidence can be found to support this supposition. Furthermore, a material with a well defined yield point may possibly exhibit vastly altered fatigue properties when tested in the absence of stress raisers. Lastly, there remains the question raised earlier regarding the possible incomparability of constant strain and constant load fatigue testing.

In the notched test results of annealed ASTM-A7 steel where the agreement of the derived and experimental values appears to be good, the consistent positive error of the derived result in the compressive range may possibly be explained in the following manner. Plastic buckling was noted in the unnotched tests at the yield point of the material. Consequently, even though buckling was not apparent in any notched test except at the maximum compressive stress employed, a condition of plastic instability may have caused the experimental results in the compression range to fall consistently below the derived results.

For both the unnotched and notched tests of 24S-T3 aluminum alloy the experimental and derived results compare quite favorably. Similarly the comparison for all tests of 75S-T6 aluminum alloy is favorable but the errors are generally slightly greater than for the other aluminum alloy. The 4130 steel tests show the greatest deviation between

experimental and derived results, but even here the comparison seems to be quite favorable.

As stated previously after the analysis was complete a group of tests were found which provided additional means of checking the correlation between the static tensile properties and the zero to tension fatigue intercept. This group of tests was reported by Baron and Larson (11) and included the results of zero to tension constant strain fatigue tests for fifteen different steels. A complete tabulation of the static tensile properties of these steels was reported in the same reference. The theoretical stress concentration employed by Baron and Larson was 2.32. A complete tabulation of Baron and Larson's average experimental results, as compared to the derived results reported herein, is given in Table 8. From failure at as little as 111,000 cycles to no failure in 3,058,000 cycles, a range of maximum fatigue stress from 23,000 psi to 40,000 psi and a wide range of static tensile properties, the absolute error between the derived and experimental values ranged from 0.3 to 38.4 per cent for three basic types of steel. Admittedly this error is large, but the overall results seem to check sufficiently well to justify further study to determine the validity of the analysis developed herein.

5. Estimation of Variations in Test Results

The greatest possible source of error in the reported stresses is the amount of bending introduced in both unnotched and notched specimens from the eccentricities of applied axial loads. This bending would not affect the average stresses reported herein, but it would seriously affect the maximum and minimum stresses attained in a specimen. To

measure these maximum and minimum stresses is essentially impossible, but estimates of maximum and minimum stresses can easily be obtained from strain measurements. Measuring strains in each specimen tested would be both excessively time consuming and expensive. Therefore, the strain distribution was measured only in the calibration tests of the fatigue machine. Three calibration specimens or weigh bars were used in this calibration, and six SR-4 electrical resistance strain gages were mounted in pairs at intervals of 120 deg around the circumference on each of the weigh bars. One gage of each pair was the "active" gage measuring the longitudinal strain and the other was a "compensating" gage oriented 90 deg to the axis of the active gage and applied on the same longitudinal line. This gage afforded an automatic temperature strain compensation for each strain measurement. Each pair of gages formed two arms of the measuring bridge, the strain in which was recorded on a six channel recording oscillograph. The strain induced in each of the three circuits was recorded concurrently using three channels of the oscillograph while two of the other three channels recorded specimen temperature and machine speed.

Each of the weigh bars was designed for a maximum average strain of 500 micro-inches per inch so that no yielding would occur during any calibration. Also, this limitation on the strain practically assured that no strain gage would fail by fatigue during the dynamic calibrations. Obviously, only one weigh bar was required in order to calibrate the fatigue machine over its full range of load. However, it was felt desirable to have greater sensitivity than was afforded by merely using one weigh bar. Thus, three weigh bars, C1 with a capacity of $\pm$1,500 lbs, C2

with a capacity of ±5,000 lb, and C3 with a capacity of ±10,000 lb were made to operate at the limiting strain of 500 micro-inches per inch. Each of the three weigh bars was statically calibrated over its full range in a 120,000 lb universal testing machine. The strains were recorded at each increment of load using three channels of the oscillograph. A fourth channel was used to record the weigh bar temperature for the purpose of comparison in the event that serious temperature rises might be recorded during the dynamic calibration. The specimen temperature was measured by clamping an iron-constantan thermocouple directly to the specimen. Static calibrations were completed for each direction (tension and compression) of load for two orientations of the weigh bar. These orientations were obtained by merely rotating the weigh bar through 90° after the first calibration run and repeating the loading. By orienting the weigh bars in two different positions, an indication of the source of the recorded eccentricities could be roughly determined. If the eccentricity of load resulted in bending in the same relative direction for each orientation, the bending was probably caused by imperfect fabrication of the weigh bar while if the position of the applied load changed with weigh bar orientation, the bending was probably caused by the specimen holders, the machine, or the specimen alignment. In this manner it was found that the source of bending was inherent in the specimen in the case of weigh bars C1 and C3 while in C2 it was mainly due to the mis-alignment of the specimen or the machine.

The preload mechanism as well as the eccentric of the fatigue machine was calibrated before the current test program was begun. Except for the fact that only one orientation of the weigh bar was used, the

calibration technique was the same for the first preload calibration as for the static calibration. In the dynamic calibration of the eccentric the increments of load and the procedure were essentially the same as those used in the static calibration. However, in the dynamic calibration a fifth channel of the oscillograph was used to check the constancy of the speed of the eccentric. The latter measurement was necessary since the alternating load is applied by centrifugal force produced by the eccentric; the magnitude of the load is controlled solely by the speed of the eccentric. In all calibrations the speed was found to be in accordance with the specified value.

The initial calibration of the fatigue machine indicated that a serious amount of bending was being introduced by the tension-compression apparatus. As a consequence, a portable strain indicator was used to measure the individual strains on weigh bar C1 and thus align this apparatus more accurately in an attempt to reduce the bending as much as possible. The alignment was adjusted by trial and error until the strain readings for each gage in two different orientations of the weigh bar were essentially constant which would indicate that the recorded bending was due to the specimen and not the machine.

Following this alignment and approximately every two months during the test program, the preload mechanism was re-calibrated using the two smaller weigh bars and a portable strain indicator to measure the individual strains. Only the preload mechanism was re-calibrated since it seemed inconceivable that the eccentric could change its load characteristics which depended only on the mass of the eccentric and its rotating speed. During every calibration the three strains were measured

individually for each load increment so that the plane of strain distribution over the cross-section could be determined. From this plane of strain, the eccentricites were computed and these eccentricities are summarized in Fig. 24. It is interesting to note that differences in eccentricities were observed with the machine warm or cold for weigh bar C2. Since only this one weigh bar shows consistent variations between the machine being warm or cold, no logical explanation can be given for the observation.

As seen in Fig. 24, the eccentricities are rather high for small values of applied load but they rapidly decrease as the load increases. It is felt that the magnitude of eccentricity which might have been expected at the maximum load in each fatigue test was on the order of 0.015 in. as estimated from the calibration tests. Since the weigh bars used in calibration were prepared in the same manner and with the same amount of care as the test specimens, the eccentricity measured on the weigh bars should be essentially the same as that on the test specimens. An eccentricity of 0.015 in. on a specimen of 0.357 in. diameter may not appear serious but it can readily be shown that such an eccentricity would give a 33.6 per cent difference between average and maximum stress for unnotched specimens and a similar difference of 30.2 per cent for notched specimens. This variation was computed from a consideration of the theory of elasticity; therefore, the severity of the difference, when one considers stresses, may not be too serious since the majority of the tests were run at stresses in the plastic range. On the other hand, if one considers strains there will be no reduction in this difference. Yet statistically one is assured that eccentricities varied from specimen

to specimen so that the large amount of averaging of test data utilized herein may, at least to some extent, reduce the magnitude of the difference due to bending.

It should be noted here that Grover, Bishop, and Jackson as well as Baron and Larson, and apparently the majority of those who have studied axial load fatigue characteristics report no estimate of their eccentricities of applied loads. As has just been illustrated, relatively small eccentricities may lead to rather large variations in stress so that the conclusions reached as a result of axial fatigue tests may be misleading if no measure of the bending in the specimens is considered.

A rather minor source of error results from the fatigue machine. A summary of the results of the calibrations of the machine is given in Table 9. In the final analysis of the current series of tests, the average calibration constants given in this table were used. Consequently, it is felt that the reported data are as accurate as they can be. However, in this analysis the effects of drift in the preload and the backlash in the preload were not included since their application is not readily apparent. It is felt that the average error due to the machine is approximately 1.5 per cent of the average stresses reported. Thus, this source of error is negligible especially when it is compared to the possible variation due to bending.

IV. CONCLUSIONS AND RECOMMENDATIONS

1. Conclusions

The conclusions reached in this study are described in detail in the preceding chapter. For convenience, however, they are briefly summarized here:

a. Based on the theoretical maximum range of stress in a notched specimen, failure of ASTM-A7 steel in fatigue does not appear to be a function of the true range of stress developed in an unnotched specimen of the same material.

b. A rational revision to the maximum distortion energy theory to explain fatigue failures in compression is not apparent.

c. A variation of fatigue reduction factor with range ratio seems indicated but the variation is not consistent for different materials or perhaps for different test conditions.

d. Unnotched fatigue specimens of steel may behave differently than similar aluminum alloy specimens especially at fatigue ranges of high tension to greater tension.

e. Constant strain conditions approximating constant load conditions may not be comparable to constant load conditions of fatigue testing.

f. Static work hardening in compression appears to be comparable to the first few cycles of fatigue stress provided the maximum fatigue stress is approximately equal to the stress attained during the work hardening.

g. Under fatigue conditions of constant load in the tension

to greater tension range the failures resemble general yielding rather than the brittle fracture characteristic of fatigue.

h. Straight line constant life contours plotted on modified Goodman coordinates have a constant slope, within reasonable limits, of 0.700 for notched specimens of annealed ASTM-A7 steel, 24S-T3 and 75S-T6 aluminum alloys, and normalized 4130 steel. For the last three materials however, the stress ranges include no tests predominately in compression.

i. The corresponding slope for unnotched specimens of the same materials is 0.500, but the error for annealed ASTM-A7 steel is large since the experimental contours for this material deviate considerably from a straight line.

j. The S-N curves for notched specimens of the four materials reported have a constant slope, within reasonable limits, of 0.115 between 1×10^5 and 2×10^6 cycles.

k. With the same reservations as in j the slope is 0.057 for unnotched specimens.

l. A fatigue reduction or stress concentration factor whose magnitude is a function of the material seems indicated for unnotched specimens.

2. Correlation of Zero to Tension Fatigue Intercept with Static Tensile Properties, Its Uncertainties and Limitations

The following purely empirical equations derived in Chapter III give reasonable results except for unnotched ASTM-A7 steel:

$$\sigma_2 = 0.700\,\sigma_1 + \frac{\sigma_F}{K_T}\left(\frac{2 \times 10^6}{N}\right)^{0.115} \qquad \text{for all notched specimens} \qquad (8)$$

$$\sigma_2 = 0.500\,\sigma_1 + \frac{\sigma_F}{1.15}\left(\frac{2 \times 10^6}{N}\right)^{0.057} \qquad \text{for unnotched 24S-T3 and 75S-T6 aluminum alloys}$$

$$\sigma_2 = 0.500\,\sigma_1 + \frac{\sigma_F}{1.5}\left(\frac{2 \times 10^6}{N}\right)^{0.057} \qquad \text{for unnotched annealed ASTM-A7 steel} \qquad (9)$$

$$\sigma_2 = 0.500\,\sigma_1 + \frac{\sigma_F}{1.3}\left(\frac{2 \times 10^6}{N}\right)^{0.057} \qquad \text{for unnotched normalized 4130 steel}$$

where

$$\sigma_F = 1743\,(\sigma_U - \sigma_Y) + 1443\,(r - e) \qquad \text{for all reasonably ductile materials} \qquad (4)$$

Despite the seemingly good correlation, the analysis resulting in these equations is quite uncertain by virtue of the fact that the per cent reduction of area was not stated for the actual materials tested by Grover, Bishop, and Jackson. Average values of this property were taken from the literature and used in the analysis. This uncertainty is not alleviated by the favorable comparison with Baron and Larson's results since, for the series reported herein, the error at the intercept is averaged out by tests at different stress ranges while the overall fatigue results for the steels studied by Baron and Larson are not known. Therefore, further studies of these purely empirical relations would be desirable to determine whether these expressions are realistic.

Furthermore, the limitations of these equations must be realized even for the purpose of checking their validity. All of the materials analyzed herein are rather ductile so that the application of the analysis to brittle materials is not advocated. The analyses include

considerations of specimen lives ranging from 1×10^5 to 2×10^6 cycles so that correlation outside this range is questionable. Lastly, for only the current series of tests is the complete modified Goodman diagram known. Consequently, projection of the proposed analysis to compression ranges of fatigue stress for other materials would be a pure extrapolation.

3. Recommendations for Future Study

The analysis presented herein should be thoroughly investigated in order to determine whether or not it is valid. Not only should the possibly fortuitous expression for the zero to tension fatigue intercept be checked, but also the values of the slopes of the contours of constant life and the interpolation for different numbers of cycles. Should any or all of the findings reported herein prove valid their range of applicability should then be thoroughly investigated.

Failure of unnotched specimens is largely an academic problem since stress raisers are practically always present in engineering structures. Yet, as a measure of the strength which inherent defects usurp from a material, one might be interested in an unnotched fatigue reduction factor. Two general methods of computing such a quantity are presented herein and could be studied should the need arise. One which is more rational than the other would consist of running a series of notched fatigue tests with two or more values of theoretical stress concentration. Also, a series of unnotched tests would be required. The fatigue reduction factor as some function of the theoretical stress concentration could then be assumed and a hypothetical stress for failure in a specimen with no stress raiser computed. Assuming various functions

one could perhaps find a constant hypothetical stress for all theoretical stress concentrations considered. The final result would be the fatigue reduction factor for an unnotched specimen. The other method corresponds to the analysis used herein and consists of computing an average hypothetical stress as above by multiplying the theoretical stress concentration factor by the corresponding stress at failure and averaging the result for the stress concentrations considered.

An investigation to check the observed possible lack of comparability of unnotched fatigue tests of steel and aluminum alloys in the range of high tension to greater tension may be of value in explaining the fatigue phenomenon.

Lastly, the possible lack of correlation between results of constant load fatigue testing and constant strain fatigue testing, where constant load conditions are approximated, may be significant. Thus, work might also be directed along this line.

APPENDIX A

LIST OF REFERENCES

1. Almen, J. O., "Effects of Residual Stress on the Fatigue of Metals," Product Engineering, v. 14, No. 6, June 1943, pp. 348-352.

2. Almen, J. O., "Improving Fatigue Strength of Machine Parts," Machine Design, v. 15, No. 6, June 1943, pp. 124-129, 192, 194, 196, 198.

3. Almen, J. O., "Fatigue Failures are Tensile Failures," Product Engineering, v. 22, March 1951, pp. 101-124.

4. Anonymous, "Fatigue of Mild Steel," The Engineer, v. 153, No. 3973, March 4, 1932, pp. 255-257.

5. Anonymous, "The Fatigue Endurance of Killed and Rimmed Steels," Metallurgia, v. 21, March 1940, p. 153.

6. Anonymous, "Surface Finishing," Steel, v. 113, No. 1, July 5, 1943, pp. 102-104, 147.

7. Anonymous, "Fatigue Strength of Nitrided Surfaces," The Iron Age, v. 153, Jan. 27, 1944, p. 55.

8. Anonymous, "The Failure of Metals by Fatigue," Metallurgia, v. 35, April 1947, pp. 289-293.

9. Anonymous, "Fatigue of Ferrous Materials: Some Factors that Influence Resistance to the Damaging Effects of Fatigue Stressing," Metallurgia, v. 36, Sept. 1947, pp. 249-251.

10. Aul, E. L., Dana, A. W. and Sachs, G., "Tension Properties of Aluminum Alloys in the Presence of Stress Raisers II -- Comparison of Notch Strength Properties of 24S-T, 75S-T, and 24S-T86 Aluminum Alloys," NACA TN 1831, Washington, March 1949.

11. Baron, Frank and Larson, E. W. Jr., "Static and Fatigue Properties of High Strength Low-Alloy Steel Plates Related to Those of Carbon and Silicon Steel Plates," Proceedings ASTM, v. 53, 1953, pp. 805-824.

12. Barret, C. S., "Distortion of Metal Grains by Fatigue and Static Stressing," Metals and Alloys, v. 8, 1937, pp. 13-21.

13. Basquin, O. H., "The Exponential Law of Endurance Tests," Proceedings ASTM, v. 10, 1910, pp. 625-630.

14. Boresi, A. P. and Dolan, T. J., "An Appraisal of the Prot Method of Fatigue Testing (Part I)," Technical Report No. 34, ONR Project NR-031-005, Dept. of Theo. and App. Mechanics, University of Illinois, Urbana, Jan. 1953.

15. Bulleid, C. H., "Fatigue Tests of Cast Iron," Engineering (London), October 1, 1926, p. 429.

16. Donaldson, J. W., "The Fatigue of Cast Iron," Foundry Trade Journal, July 2, 1936, pp. 9-11.

17. Donaldson, J. W., "Further Investigation of Fatigue Strength of Cast Iron," Foundry Trade Journal, Dec. 3, 1936, pp. 432, 442.

18. Donaldson, J. W., "Strength and Other Mechanical Properties of Cast Iron," Metal Treatment, v. 10, No. 35, Autumn 1943, pp. 157-164.

19. Eagan, T. E. and James, J. D., "A Practical Evaluation of Ductile Cast Iron. Part II," The Iron Age, Dec. 15, 1949, p. 77.

20. Elling, R. E., "Tests of Metals in Repeated Axial Compression and Tension," Master's Thesis, University of Illinois, Urbana, 1952.

21. Everhart, J. L., Lindlief, W. E., Kanegis, J., Weissler, P. G., and Siegel, F., "Mechanical Properties of Metals and Alloys," NBS Circular No. C447, U. S. Gov't. Printing Office, Washington, 1943.

22. Feltham, Paul, "Fatigue in Metals: A Critical Survey of Recent Research and Theories," Iron and Steel, v. 21, No. 11, Oct. 1948, pp. 431-436.

23. Grover, H. J., Bishop, S. M., and Jackson, L. R., "Fatigue Strengths of Aircraft Materials: Axial-Load Fatigue Tests on Unnotched Sheet Specimens of 24S-T3 and 75S-T6 Aluminum Alloys and of SAE 4130 Steel," NACA TN 2324, Washington, March 1951.

24. Grover, H. J., Bishop, S. M., and Jackson, L. R., "Fatigue Strengths of Aircraft Materials: Axial-Load Fatigue Tests on Notched Sheet Specimens of 24S-T3 and 75S-T6 Aluminum Alloys and of SAE 4130 Steel with Stress-Concentration Factors of 2.0 and 4.0," NACA TN 2389, Washington, June 1951.

25. Grover, H. J., Bishop, S. M., and Jackson, L. R., "Fatigue Strengths of Aircraft Materials: Axial-Load Fatigue Tests on Notched Sheet Specimens of 24S-T3 and 75S-T6 Aluminum Alloys and of SAE 4130 Steel with Stress-Concentration Factor of 5.0," NACA TN 2390, Washington, June 1951.

26. Grover, H. J., Hyler, W. S., and Jackson, L. R., "Fatigue Strengths of Aircraft Materials: Axial-Load Fatigue Tests on Notched Sheet Specimens of 24S-T3 and 75S-T6 Aluminum Alloys and of SAE 4130 Steel with Stress-Concentration Factor of 1.5," NACA TN 2639, Washington, Feb. 1952.

27. Grover, H. J., Hyler, W. S., Kuhn, Paul, Landers, C. B., and Howell, F. M., "Axial-Load Fatigue Properties of 24S-T and 75S-T Aluminum Alloys as Determined in Several Laboratories," NACA TN 2928, Washington, May, 1953.

28. Hoffman, M. E., Jr., "Repeated Compression Tests of Various Metals," Master's Thesis, University of Illinois, Urbana, 1950.

29. Irwin, P. L., "Fatigue of Metals by Direct Stress," Proceedings ASTM, v. 25, Part II, 1925, pp. 53-67.

30. Love, W. J., "Structural Changes in Ingot Iron Caused by Plastic and Repeated Stressing," Technical Report to ONR, U.S.N., Contract N6-ori-71, T. O. IV, Project NR-031-005, Dept. of Theo. and App. Mechanics, University of Illinois, Urbana, Nov. 1952.

31. McDowell, J. F., "The Fatigue Endurance of Killed, Capped, and Rimmed Steels," Metals and Alloys, v. 11, No. 1, Jan. 1940, pp. 27-32.

32. Moore, H. F., "Fatigue of Metals - Developments in the United States," Metals and Alloys, v. 10, Nos. 5 and 6, May 1939, pp. 158-162 and June 1939, pp. 180-183.

33. Moore, H. F., and Kommers, J. B., "An Investigation of the Fatigue of Metals," Engineering Experiment Station, Bulletin 124, University of Illinois, Urbana, 1921.

34. Moore, H. F. and Konzo, Seichi, "A Study of the Ikeda Short-Time (Electrical Resistance) Test for Fatigue Strength of Metals," Engineering Experiment Station, Bulletin 205, University of Illinois, Urbana, 1930.

35. Moore, H. F., and Krouse, G. N., "Repeated Stress (Fatigue) Testing Machines Used in the Materials Testing Laboratory of the University of Illinois," Engineering Experiment Station, Circular 33, University of Illinois, Urbana, 1934.

36. Moore, H. F., and Morkovin, D., "Progress Report on the Effect of Size of Specimen on Fatigue Strength of Three Types of Steel," Proceedings ASTM, v. 42, 1942, pp. 145-153.

37. Moore, H. F., and Morkovin, D., "Second Progress Report on the Effect of Size of Specimen on Fatigue Strength of Three Types of Steel," Proceedings ASTM, v. 43, 1943, pp. 109-124.

38. Moore, H. F., and Morkovin, D., "Third Progress Report on the Effect of Size of Specimen on Fatigue Strength of Three Types of Steel," Proceedings ASTM, v. 44, 1944, pp. 137-160.

39. Moore, H. F., "A Study of Size Effects and Notch Sensitivity in Fatigue Tests of Steel," Proceedings ASTM, v. 45, 1945, pp. 507-530.

40. Neuber, N., Theory of Notch Stresses, Principles for Exact Stress Calculation, Translated from the German by F. A. Raven, J. W. Edwards Press, Ann Arbor, 1946.

41. Newmark, N. M., Mosborg, R. J., Munse, W. H., and Elling, R. E., "Fatigue Tests in Axial Compression," Proceedings ASTM, v. 51, 1951, pp. 792-810.

42. Roos, P. K., Lemmon, D. C., and Ransom, J. T., "Influence of Type of Machine, Range of Speed, and Specimen Shape on Fatigue Test Data," Authorized Reprint from ASTM Bulletin No. 158, May 1949.

43. Schutz, F. W., Jr., and Newmark, N. M., "The Efficiency of Riveted Structural Joints," Civil Engineering Studies, Structural Research Series, No. 30, University of Illinois, Urbana, Sept. 1952, p. 12.

44. Smith, C. R., "Prediction of Fatigue Failures in Aluminum Alloy Structures Subjected to Repeated Loads," Paper presented at Spring 1954 Meeting, SESA, Cincinnati, Ohio.

45. Smith, J. O., "The Effect of Range of Stress on the Torsional Fatigue Strength of Steel," Engineering Experiment Station, Bulletin 316, University of Illinois, Urbana, 1939.

46. Smith, J. O.,"Effects of Range of Stress on the Fatigue Strength of Metals," Engineering Experiment Station, Bulletin 334, University of Illinois, Urbana, 1942.

47. Sonntag Scientific Corporation, Description and Instructions for Sonntag Universal Fatigue Testing Machine Model SF-10-U, Greenwich, 1950.

48. Timoshenko, S., Strength of Materials, Part II, 2nd ed., D. Van Nostrand, New York, 1941, pp. 428-462.

49. Wilson, W. M., "Flexure Fatigue Strength of Steel Beams," Engineering Experiment Station, Bulletin 377, University of Illinois, Urbana, 1948.

50. Wilson, W. M., and Burke, J. L., "Rate of Propagation of Fatigue Cracks in 12-in. by 3/4-in. Steel Plates with Severe Geometrical Stress Raisers," Engineering Experiment Station, Bulletin 371, University of Illinois, Urbana, 1947.

51. Wilson, W. M., and Thomas, F. P., "Fatigue Tests of Riveted Joints," Engineering Experiment Station, Bulletin 302, University of Illinois, Urbana, 1938, pp. 98-103.

52. Yen, C. S., "Stress Distribution in a Metal Specimen by Plastic Deformation During Repeated Loading," Technical Report No. 14 on The Behavior of Metals Under Repeated Stress, Dept. of Theo. and App. Mechanics, University of Illinois, Urbana, Nov. 1949.

TABLE 1a

CHEMICAL ANALYSIS OF PARENT PLATE MATERIAL

	Chemical Composition Per Cent
C	0.23
Mn	0.47
P	0.008
S	0.029
Si	0.16
N	0.008

TABLE 1b*

STATIC TENSILE PROPERTIES OF THE PARENT PLATE AS ROLLED

Yield Strength	33400 psi
Ultimate Strength	59400 psi
Per Cent Elongation in 8 in.	32.6
Per Cent Reduction in Area	60.6

* Average of 2 tests conducted on the plate used in the current series by W. E. Boas and reported in "Development of Small Specimen Acceptance Tests for Ordinary Structural Steels," Master's Thesis, University of Illinois, Urbana, 1947.

TABLE 2

SUMMARY OF RESULTS OBTAINED DURING THE PRESTRESSING OF MATERIAL

		Stated Prestress psi	*True Prestress psi	Residual Longitudinal Strain in./in.	Residual Transverse Strain in./in.	Poisson's Ratio
Average for 6 Bars		-50,000	-50,200	0.0522	0.0242	0.464
Max. Deviation from Average in Per Cent	+	------	5.98	4.41	5.79	6.68
	-	------	7.97	4.98	6.20	4.31
Average for 25 Bars		-69,000	-68,600	0.1400	0.0738	0.527
Max. Deviation from Average in Per Cent	+	------	7.29	5.00	7.86	4.93
	-	------	5.83	3.79	7.59	6.07
Average for 12 bars		-86,000	-85,800	0.3065	0.1956	0.638
Max. Deviation from Average in Per Cent	+	------	1.52	2.25	4.50	2.82
	-	------	2.10	2.77	2.97	0.94
Average for 12 Bars		-97,000	-92,600	0.4990	0.4160	0.833
Max. Deviation from Average in Per Cent	+	------	1.08	0.80	0.97	1.32
	-	------	0.97	0.80	1.92	1.44
Average for 18 Bars		+60,000	+59,500	0.1198	0.0564	0.471
Max. Deviation from Average in Per Cent	+	------	4.03	22.45	21.8	4.46
	-	------	1.51	8.85	4.79	4.46
Average for 18 Bars		+74,000	+73,400	0.2583	0.1224	0.474
Max. Deviation from Average in Per Cent	+	------	2.04	4.53	7.19	6.54
	-	------	3.95	12.89	15,69	4.01

* Load divided by corresponding area: - = compression; + = tension

Strain rate = 0.042 in./min. for all bars.

TABULATION OF RESULTS FROM STATIC TENSILE TESTS OF ANNEALED AND PRESTRESSED MATERIAL

Specimen No.	Actual Prestress psi	Upper Yield Point psi	Lower Yield Point psi	Ultimate Nominal Stress psi	Strength True Stress psi	Fracture Nominal Stress psi	Strength True Stress psi	Per Cent Elong. in 2"	Per Cent Reduct. of Area	Modulus of Elasticity ksi
L-1-B	0	[illegible]	[illegible]	56750	69600	45000	111000	43.8	59.5	32800
M-2-B	0	[illegible]	[illegible]	[illegible]	69500	39800	105300	43.5	62.2	30700
N-2-B	0	[illegible]	[illegible]	[illegible]	69500	40000	112800	43.0	64.5	28300
O-3-B	0	[illegible]	[illegible]	56700	70900	40500	105200	41.3	61.5	29300
P-3-B	0	[illegible]	31700	56200	70300	39000	113000	45.0	65.5	28000
Q-4-B	0	40850	34900	56150	72100	40000	106700	41.8	62.5	28800
S-5-B	0	38750	35300	55400	68800	39000	116300	43.3	66.5	29800
W-4-B	0	39400	35250	55850	69000	39000	106900	45.5	63.5	30100
T-5-B	0	34850	33000	56100	70700	40000	105200	42.5	62.0	31400
Y-5-B	0	39000	36000	56000	69600	40000	105300	42.5	62.0	30600
Z-6-B	0	42400	36000	56250	70800	40000	111000	41.5	64.0	32800
AA-6-B	0	37700	31400	56000	69900	39600	115200	-	65.8	29200
Averages	0	39550	33650	56150	70050	40150	109500	43.1	63.3	30200
K-8-B	-50300	-	30150	55800	69500	40500	112500	41.0	64.0	-
Q-3-B	-50500	-	29950	55800	69700	40000	114000	41.5	65.0	-
T-8-B	-49800	-	29500	56600	70000	41000	102800	42.0	60.0	-
CC-3-B	-50100	-	33200	56700	69800	40500	107300	40.5	62.3	-
Z-5-B	-50200	-	32550	56800	69500	40500	107300	41.5	62.3	-
EE-8-B	-50500	-	32800	58200	72300	42000	109100	40.5	62.3	-
Averages	-50200	-	31360	56650	70130	40750	108800	41.2	62.7	-
P-2-A	-68900	-	36250	60700	64500	42500	108400	28.5	60.8	-
P-2-B	-68900	-	36250	61200	65000	41000	105700	28.0	61.2	-
Y-2-A	-68800	-	39150	60600	71400	40500	105100	28.0	61.5	-
Y-2-B	-68800	-	39500	61500	65500	41500	102000	26.0	59.2	-
DD-4-A	-68500	-	38600	59700	77000	40500	118000	27.0	65.6	-
DD-4-B	-68500	-	39650	61100	63600	42000	108700	25.0	61.3	-
Averages	-68750	-	38250	60800	67800	41300	108000	27.1	61.6	-

TABULATION OF RESULTS FROM STATIC TENSILE TESTS OF ANNEALED AND PRESTRESSED MATERIAL

Specimen No.	Actual Prestress psi	Upper Yield Point psi	Lower Yield Point psi	Ultimate Nominal Stress psi	Strength True Stress psi	Fracture Nominal Stress psi	Strength True Stress psi	Per Cent Elong. in 2"	Per Cent Reduct. of Area	Modulus of Elasticity ksi
L-4	-84000	-	44600	70800	88400	45000	112000	22.0	59.8	-
O-2	-84700	-	43750	70500	74500	45000	113300	22.0	60.3	-
Q-7	-87000	-	44250	70700	75100	44500	118000	21.0	62.1	-
W-3	-86600	-	45250	71100	74900	45000	119200	21.0	62.3	-
AA-1	-86600	-	45250	71400	75200	45000	114900	21.0	60.7	-
CC-7	-86100	-	45750	71100	75000	45000	125700	21.0	64.2	-
Averages	-85850	-	44800	70900	77200	44900	117200	21.3	61.6	-
L-6	-92200	-	49000	79500	84800	48500	119200	21.0	59.3	-
O-4	-92000	-	48700	79900	85600	49200	117700	19.5	58.1	-
S-2	-91800	-	50250	79500	83400	49000	118700	19.0	58.7	-
W-5	-93400	-	50750	80700	85400	52000	137800	20.5	61.1	-
AA-3	-93100	-	49750	80800	86000	50500	127300	17.5	60.3	-
DD-1	-93400	-	49900	79900	85000	49000	133300	20.5	63.1	-
Averages	-92650	-	49750	80100	85000	49700	125700	19.7	60.1	-
L-8	-61900	-	62600	65500	73300	46500	107500	28.5	56.8	-
O-6	+59700	-	60500	64300	71000	45000	104700	30.5	57.0	-
S-8	+59300	-	59500	63200	70000	44500	111700	31.5	55.1	-
AA-5	+59300	-	62200	64700	71500	45500	113200	31.0	59.8	-
CC-8	+59200	-	62200	64000	70100	45500	111800	30.0	59.3	-
DD-7	+59300	-	61750	64000	70100	45000	107800	29.0	58.2	-
Averages	+59800	-	61450	64300	71000	45300	109500	30.1	57.7	-
L-2*	+71800	-	68900	69900	75200	52300	103000	3.5	49.2	
O-8*	+74700	-	68800	70300	70400	51500	107800	8.5	52.2	-
T-6*	+74000	-	68800	70300	71400	52000	100000	6.0	48.0	
Z-7*	+74000	-	71200	69500	83000	52500	113000	4.0	53.5	-
CC-6*	+73500	-	72700	72400	72800	54100	107800	5.0	49.7	
DD-8	+73100	-	74100	73500	81800	53600	116200	14.0	54.0	-

*Broke outside gage length.

TABLE 4

SUMMARY OF FATIGUE TEST RESULTS -- UNNOTCHED SPECIMENS OF ANNEALED ASTM-A7 STEEL
ZERO PRESTRESS

Spec. No.	Nominal Stress Range max. + = tension - = compr.	min.	True Stress Range max. + = tension - = compr.	min.	Per Cent Change In Area For Computing True Range + = increase - = reduction	At Failure	No. of Cycles When Yielding Started 1000's	Stopped 1000's	No. of Cycles to Fail. 1000's	True Prestress psi	Remarks
E2A	+27250	-27250	+27250	-27250	0	0	-	0	135	-	
E2B	+27350	-27350	+27350	-27350	0	0	-	0	286	-	
F1A	+27680	-26820	+27680	-26820	0	0	-	0	95	-	
F1B	+24435	-24005	+24435	-24005	0	0	-	0	914	-	
G1A	+22765	-23635	+22765	-23635	0	0	-	0	4713[a]	-	
G1B	+23750	-23750	+23750	-23750	0	0	-	0	4439[a]	-	
H1A	+36300	-100	+36300	-100	0	0	-	0	3282[a]	-	
H1B	+40850	+450	+43000	+475	-5.1[c]	-5.1[a]	-	11	3887[a]	-	
I1A	+45550	+50	+55600	+60	-18.0[d]	-36.0	-	75	194	-	
I1B	+42450	+50	+44600	+50	-5.0[g]	------	-	15	3364	-	
J1A	+43900	0	+45200	0	-4.1[g]	------	-	15	3391	-	
J1B	+24465	-24035	+24465	-24035	0	0	-	0	4485[a]	-	
E4A	+25465	-25035	+25465	-25035	0	0	-	0	355	-	
E4B	+36070	-14130	+44000	-17250	-18.0[d]	-36.0	-	40[k]	40	-	General Yielding Type of Failure
E5A	+33550	-12050	+34950	-12570	-4.0[g]	-7.0	-	99	424	-	
E5B	+32500	-11900	+32500	-11900	0	-5.1	-	0	837	-	
F2A	+31530	-11970	+31530	-11970	------	------	-	0	1678	-	
F2B	+50150	+15150	+58000	+17400	-13.0	-13.0[a]	-	536	3103[a]	-	
F3A	+55750	+14250	+69700	+17800	-20.0[d]	-41.0	-	17[k]	17	-	General Yielding Type of Failure
F3B	+52400	+15000	+64300	+18420	-18.6[d]	-37.2	-	293[k]	293	-	General Yielding Type of Failure
G2A	+51100	+15300	+58900	+17600	-13.1[g]	-13.1[a]	-	682	4427[a]	-	

TABLE 4 (CONT'D)

SUMMARY OF FATIGUE TEST RESULTS -- UNNOTCHED SPECIMENS OF ANNEALED ASTM -A7 STEEL
ZERO PRESTRESS

Spec. No.	Nominal Stress Range max. + = tension - = compr.		True Stress Range max. + = tension - = compr.		Per Cent Change In Area For Computing True Range + = increase - = reduction	At Failure	No. of Cycles When Yielding Started 1000's	Stopped 1000's	No. of Cycles to Fail. 1000's	True Prestress psi	Remarks
G2B	+60770	+30430	+89100	+44600	-31.8[d]	-58.6	-	14[k]	14	-	General Yielding Type of Failure
G3A	+58630	+29970	+73100	+37350	-19.8[d]	-34.6	-	12[k]	12	-	General Yielding Type of Failure
G3B	+55900	+30700	+69400	+38170	-19.4[d]	-35.6	-	19[k]	19	-	General Yielding Type of Failure
H2A	+52510	+30290	+66200	+38200	-20.7[d]	-38.2	-	1322[k]	1322	-	General Yielding Type of Failure
H2B	+53600	+30400	+67400	+38200	-20.4[d]	-36.5	-	520[k]	520	-	General Yielding Type of Failure
H3A	+51880	+30220	+58950	+34400	-12.0[g]	-12.0[a]	-	983	4960[a]	-	
H3B	+57600	+45500	+77500	+61150	-25.6[d]	-37.3	-	7[k]	7	-	General Yielding Type of Failure
I3A	+55650	+45550	+67700	+55500	-17.8[d]	-25.2	-	8[k]	8	-	General Yielding Type of Failure
I3B	+53130	+45070	+65100	+55400	-18.4[d]	-28.6	-	544[k]	544	-	General Yielding Type of Failure
J2A	+54350	+45250	+64100	+53500	-15.3[g]	-15.3[a]	-	2808	4526[a]	-	
J2B	+54550	+45450	+67400	+55000	-17.3[d]	-26.5	-	2151[k]	2151	-	General Yielding Type of Failure
Z1A	+55050	+45950	+63800	+53200	-13.7[d]	-19.4	-	32[k]	32	-	General Yielding Type of Failure
I2A	+54650	+45550	+67400	+56300	-18.9[d]	-29.4	-	78[k]	78	-	General Yielding Type of Failure
Z1B	+43800	+200	+47550	+220	-8.0[g]	-16.6	-	352	2600	-	
I2B	+44550	+150	+50600	+170	-11.9[d]	-23.8	-	531[k]	531	-	

SUMMARY OF FATIGUE TEST RESULTS -- UNNOTCHED SPECIMENS OF ANNEALED ASTM -A7 STEEL
ZERO PRESTRESS

Spec. No.	Nominal Stress Range max. (+ = tension, - = compr.)	Nominal Stress Range min. (+ = tension, - = compr.)	True Stress Range max. (+ = tension, - = compr.)	True Stress Range min. (+ = tension, - = compr.)	Per Cent Change In Area For Computing True Range (+ = increase, - = reduction)	Per Cent Change In Area At Failure (+ = increase, - = reduction)	No. of Cycles When Yielding Started 1000's	No. of Cycles When Yielding Stopped 1000's	No. of Cycles to Fail. 1000's	True Prestress psi	Remarks
M1A	+24440	-35960	+23150	-33950	+ 5.7[d]	+11.4	-	36[k]	36	-	Specimen buckled
Q1A	+17860	-38140	+17200	-36400	+ 5.0[d]	+ 9.8	-	375[k]	375	-	Specimen buckled
Q1B	+52090	+44510	+63950	+54600	-18.5[g]	-18.5[a]	-	2178	1507[4][a]	-	
K1A	+52520	+44680	+60600	+51600	-13.3[d]	-19.1	-	2502	2502[a]	-	
K1B	+29500	-35500	+27850	-34600	+ 2.5[b]	+ 2.5	-	5[k]	5	-	Specimen buckled
O1A	+20620	-35380	+19600	-33650	+ 5.1[d]	+ 8.2	-	195[k]	195	-	Specimen buckled
O1B	+19020	-35480	+17830	-33250	+ 6.6[e]	+ 7.1	-	907[k]	907	-	Specimen buckled
M1B	+54500	+54500	+67200	+67200	-18.9[h]	-18.9	-	0	0	-	Preload limit switch reached before starting test
S1A	+52850	+44750	+64500	+54600	-17.8[h]	-17.8	-	40[k]	40[a]	-	Preload limit switch reached a 40,000 cycles
					50,000 psi COMPRESSIVE PRESTRESS						
K8A	+17300	-40700	+16320	-38400	+ 6.0[e]	+ 6.4	-	1033[k]	1033	-50300	
Q3A	+19500	-35600	+18870	-34400	+ 3.3[g]	+ 3.3	-	198	3246	-50500	
T8A	+19550	-35550	+18890	-34350	+ 3.4[g]	+ 3.4[a]	-	940	12827[a]	-49800	
Z5A	+21380	-35220	+21380	-35220	-	-	38	1842	1842	-50200	Specimen buckled
			+20870	-34450	+ 2.2[f]	+ 4.3					
CC3A	+25060	-35440	+25060	-35440	-	-	7	240	240	-50100	Specimen buckled
			+24100	-34100	+ 4.0[f]	+ 4.0					
EE8A	+21300	-35200	+21300	-35200	-	-	56	2413	2413	-50500	
			+20950	-34600	+ 1.7[f]	+ 3.5					
					69,000 psi COMPRESSIVE PRESTRESS						
E6	+27470	-27040	+27650	-27200	- 0.6[g]	- 0.6[a]	-	9	5473[a]	-68500	
E7	+30520	-30080	+30750	-30350	- 0.6[d]	- 0.6	-	0	582	-68500	
E8	+29470	-29030	+29600	-29150	- 0.3[d]	- 0.4	-	4588[k]	4588	-68200	

SUMMARY OF FATIGUE TEST RESULTS -- UNNOTCHED SPECIMENS OF ANNEALED ASTM -A7 Steel
69,000 PSI COMPRESSIVE PRESTRESS

Spec. No.	Nominal Stress Range max. + = tension - = compr.	min.	True Stress Range max. + = tension - = compr.	min.	Per Cent Change In Area For Computing True Range + = increase - = reduction	At Failure	No. of Cycles When Yielding Started 1000's	Stopped 1000's	No. of Cycles to Fail. 1000's	True Prestress psi	Remarks
F4	+32860	-32000	+33400	-32500	-1.4[d]	-2.7	-	44[k]	44	-68200	General Yielding Type of Failure
F5	+50500	0	+52500	0	-3.8[d]	-7.6	-	464[k]	464	-68600	Specimen accidentally scratched with micrometer
F6	+50350	+150	+52550	+160	-4.2[d]	-8.4	-	589[k]	589	-68500	General Yielding Type of Failure
F7	+50000	0	+51400	0	-2.6[d]	-5.4	-	11766[k]	11766	-68700	
F8	+50730	-870	+54500	-930	-6.8[d]	-13.7	-	173[k]	173	-68400	General Yielding Type of Failure
G4	+11600	-56000	+11170	-53900	+3.9[d]	+7.8	-	21[k]	21	-68200	Specimen buckled
G5	+12600	-53000	+12020	-50600	+4.7[d]	-	-	208[k]	208	-67800	Specimen buckled
G6	+13800	-52800	+13220	-50600	+4.3[d]	-	-	125[k]	125	-68900	Specimen buckled
G7	+14870	-50730	+13920	-47550	+6.8[d]	-	-	274[k]	274	-68900	Specimen buckled
G8	+16330	-48670	+16330	-48670	-	-	52	891	891	-68800	Specimen buckled
			+15860	-47300	+3.0[f]	+5.8					
H4	+15160	-48520	+15160	-48520	-	-	90	431	431	-68600	Specimen buckled
			+14880	-47600	+1.8[f]	+3.5					
H5	+15100	-47500	+15100	-47500	-	-	297	1086	1086	-69100	Specimen buckled
			+14880	-46800	+1.5[f]	+2.8					
H6	+16310	-45290	+16310	-45290	-	-	650	1925	1925	-68400	Specimen buckled
			+16130	-44800	+1.2[f]	+2.2					
H8	+17240	-45360	+17240	-45360	-	-	263	1029	1029	-69000	
			+17000	-44600	+1.6[f]	+3.2					
I4	+21240	-45460	+21240	-45460	-	-	31	342	342	-68800	
			+20630	-44050	+3.1[f]	+6.0					

SUMMARY OF FATIGUE TEST RESULTS -- UNNOTCHED SPECIMENS OF ANNEALED ASTM -A7 STEEL
ZERO PRESTRESS

Spec. No.	Nominal Stress Range max. + = tension - = compr.		True Stress Range max. + = tension - = compr.		Per Cent Change In Area For Computing True Range + = increase - = reduction	At Failure	No. of Cycles When Yielding Started 1000's	Stopped 1000's	No. of Cycles to Fail. 1000's	True Prestress psi	Remarks
M1A	+24440	-35960	+23150	-33950	+ 5.7[d]	+11.4	-	36[k]	36	-	Specimen buckled
Q1A	+17860	-38140	+17200	-36400	+ 5.0[d]	+ 9.8	-	375[k]	375	-	Specimen buckled
Q1B	+52090	+44510	+63950	+54600	-18.5[g]	-18.5[a]	-	2178	15074[a]	-	
K1A	+52520	+44680	+60600	+51600	-13.3[d]	-19.1	-	2502	2502[a]	-	
K1B	+29500	-35500	+27850	-34600	+ 2.5[b]	+ 2.5	-	5[k]	5	-	Specimen buckled
O1A	+20620	-35380	+19600	-33650	+ 5.1[d]	+ 8.2	-	195[k]	195	-	Specimen buckled
O1B	+19020	-35480	+17830	-33250	+ 6.6[e]	+ 7.1	-	907[k]	907	-	Specimen buckled
M1B	+54500	+54500	+67200	+67200	-18.9[h]	-18.9	-	0	0	-	Preload limit switch reached before starting test
S1A	+52850	+44750	+64500	+54600	-17.8[h]	-17.8	-	40[k]	40[a]	-	Preload limit switch reached a 40,000 cycles
					50,000 psi COMPRESSIVE PRESTRESS						
K8A	+17300	-40700	+16320	-38400	+ 6.0[e]	+ 6.4	-	1033[k]	1033	-50300	
Q3A	+19500	-35600	+18870	-34400	+ 3.3[g]	+ 3.3	-	198	3246	-50500	
T8A	+19550	-35550	+18890	-34350	+ 3.4[g]	+ 3.4[a]	-	940	12827[a]	-49800	
Z5A	+21380	-35220	+21380	-35220	-	-	38	1842	1842	-50200	Specimen buckled
			+20870	-34450	+ 2.2[f]	+ 4.3					
CC3A	+25060	-35440	+25060	-35440	-	-	7	240	240	-50100	Specimen buckled
			+24100	-34100	+ 4.0[f]	+ 4.0					
EE8A	+21300	-35200	+21300	-35200	-	-	56	2413	2413	-50500	
			+20950	-34600	+ 1.7[f]	+ 3.5					
					69,000 psi COMPRESSIVE PRESTRESS						
E6	+27470	-27040	+27650	-27200	- 0.6[g]	- 0.6[a]	-	9	5473[a]	-68500	
E7	+30520	-30080	+30750	-30350	- 0.6[d]	- 0.6	-	0	582	-68500	
E8	+29470	-29030	+29600	-29150	- 0.3[d]	- 0.4	-	4588[k]	4588	-68200	

TABLE 4 (CONT'D)

SUMMARY OF FATIGUE TEST RESULTS -- UNNOTCHED SPECIMENS OF ANNEALED ASTM -A7 Steel
69,000 PSI COMPRESSIVE PRESTRESS

Spec. No.	Nominal Stress Range max. + = tension - = compr.		True Stress Range max. + = tension - = compr.		Per Cent Change In Area For Computing True Range + = increase - = reduction	At Failure	No. of Cycles When Yielding Started 1000's	Stopped 1000's	No. of Cycles to Fail. 1000's	True Prestress psi	Remarks
F4	+32860	-32860	+32860	-32860	-1.4[d]	-2.7	-	44[k]	44	-68200	General Yielding Type of Failure
F5	+50500	0	+52500	0	-3.8[d]	-7.6	-	464[k]	464	-68600	Specimen accidentally scratched with micrometer
F6	+50350	+150	+52550	+160	-4.2[d]	-8.4	-	589[k]	589	-68500	General Yielding Type of Failure
F7	+50000	0	+51400	0	-2.6[d]	-5.4	-	11766[k]	11766	-68700	
F8	+50730	-870	+54500	-930	-6.8[d]	-13.7	-	173[k]	173	-68400	General Yielding Type of Failure
G4	+11600	-56000	+11170	-53900	+3.9[d]	+7.8	-	21[k]	21	-68200	Specimen buckled
G5	+12600	-53000	+12020	-50600	+4.7[d]	-	-	208[k]	208	-67800	Specimen buckled
G6	+13800	-52800	+13220	-50600	+4.3[d]	-	-	125[k]	125	-68900	Specimen buckled
G7	+14870	-50730	+13920	-47550	+6.8[d]	-	-	274[k]	274	-68900	Specimen buckled
G8	+16330	-48670	+16330	-48670	-	-	52	891	891	-68800	Specimen buckled
			+15860	-47300	+3.0[f]	+5.8					
H4	+15160	-48520	+15160	-48520	-	-	90	431	431	-68600	Specimen buckled
			+14880	-47600	+1.8[f]	+3.5					
H5	+15100	-47500	+15100	-47500	-	-	297	1086	1086	-69100	Specimen buckled
			+14880	-46800	+1.5[f]	+2.8					
H6	+16310	-45290	+16310	-45290	-	-	650	1925	1925	-68400	Specimen buckled
			+16130	-44800	+1.2[f]	+2.2					
H8	+17240	-45360	+17240	-45360	-	-	263	1029	1029	-69000	
			+17000	-44600	+1.6[f]	+3.2					
I4	+21240	-45460	+21240	-45460	-	-	31	342	342	-68800	
			+20630	-44050	+3.1[f]	+6.0					

SUMMARY OF FATIGUE TEST RESULTS -- UNNOTCHED SPECIMENS OF ANNEALED ASTM -A7 STEEL

86,000 psi COMPRESSIVE PRESTRESS

Spec. No.	Nominal Stress Range max. + = tension - = compr.	True Stress Range max. + = tension - = compr.	Per Cent Change In Area For Computing True Range + = increase - = reduction	At Failure	No. of Cycles When Yielding Started 1000's	Stopped 1000's	No. of Cycles to Fail. 1000's	True Prestress psi	Remarks
M4	+10350 -60250	+10350 -60250	0	0	-	0	3184	-84500	
P4	+11750 -60850	+11750 -60850	-	-	1461	11053[k]	11053	-87100	
		+11610 -60100	+1.2[f]	+2.4					
T2	+18050 -60650	+18050 -60650	-	-	38	95	95	-84500	Specimen buckled
		+17500 -58900	+3.1[f]	+5.8					
Y6	+13900 -60800	+13900 -60800	-	-	330	3580	3580	-86400	
		+13770 -60200	+0.9[f]	+1.8					
BB4	+15250 -60550	+15250 -60550	-	-	666	2086	2086	-86200	
		+15100 -60000	+1.0[f]	+2.0					
			97,000 psi COMPRESSIVE PRESTRESS						
B5	+15370 -45430	+15370 -45430	0	0	-	0	6830[a]	-97000	
B8	+ 9900 -60800	+ 9900 -60800	0	0	-	0	5021[a]	-97300	
C3	+ 3950 -76050	+ 3940 -75800	+0.3	-	647	2533	2533	-97300	
		+ 3910 -75300	+1.0	+2.1					
N1	+10450 -75450	+10450 -75450	-	-	190	507	507	-92100	
		+ 9950 -74600	+1.0[f]	+2.0					
P6	+ 9350 -75550	+ 9350 -75550	-	-	122	402	402	-91900	
		+ 9320 -75300	+0.5[f]	+0.9					
T4	+ 7250 -75650	+ 7250 -75650	-	-	272	2434	2434	-91700	Specimen buckled
		+ 7110 -74200	+1.9[f]	+3.7					
Y8	+11250 -75650	+11250 -75650	-	-	282	786	786	-93200	Specimen buckled
		+11080 -74500	+1.6[f]	+2.9					
			60,000 psi TENSILE PRESTRESS						
M3	+54950 +14650	+54950 -14650	0	0	-	0	7085[a]	+59100	

TABLE 4 (CONT'D)

SUMMARY OF FATIGUE TEST RESULTS -- UNNOTCHED SPECIMENS OF ANNEALED ASTM -A7 STEEL

60,000 psi TENSILE PRESTRESS

Spec. No.	Nominal Stress Range max. + = tension - = compr.	min.	True Stress Range max. + = tension - = compr.	min.	Per Cent Change In Area For Computing True Range + = increase - = reduction	At Failure	No. of Cycles When Yielding Started 1000's	Stopped 1000's	No. of Cycles to Fail. 1000's	True Prestress psi	Remarks
N3	+70200	+29800	+80500	+34200	-12.8[d]	-25.8	-	5	5	+59800	General Yielding Type of Failure
Q5	+64880	+29520	+75650	+34500	-14.2[d]	-28.4	-	8	8	+58600	General Yielding Type of Failure
S4	+61970	+29630	+72400	+34650	-14.4[d]	-29.0	-	26	26	+59600	General Yielding Type of Failure
W1	+60080	+29720	+60080	+29720	0	0	-	0	4561[a]	+59500	
Z3	+60970	+29630	+61050	+29750	- 0.3[b]	- 0.3[a]	-	12	2892[a]	+59700	
					74,000 TENSILE PRESTRESS						
M5	+74970	+44630	+85900	+51200	-12.7[d]	-25.4	-	4	4	+73600	General Yielding Type of Failure
N7	+73630	+44370	+85300	+51400	-13.7[d]	-27.3	-	6	6	+74200	General Yielding Type of Failure
P8	+73280	+44520	+88100	+53600	-16.8[d]	-33.7	-	6	6	+73300	General Yielding Type of Failure
S6	+72670	+44430	+85050	+52000	-14.6[d]	-29.2	-	4	4	+71900	General Yielding Type of Failure
W7	+70720	+44480	+79600	+50000	-11.2[d]	-22.4	-	13	13	+70500	General Yielding Type of Failure
Y4	+69000	+44800	+69000	+44800	0	0	-	0	4464[a]	+74900	
AA7	+70180	+44420	+70180	+44420	0	0	-	0	4705[a]	+73800	

[a] No failure

[b] Based on initial area start of dynamic test

[c] Based on final area

[d] Based on average of initial and final areas during dynamic test

[e] Based on average of areas where preload essentially stabilized and at failure

[f] Based on average of areas where yielding began and at failure

[g] Based on area where yielding appeared to stop

[h] Based on area where preload limit switch was reached

[j] True stress range before yielding began

[k] Yielding occurred throughout the test

SUMMARY OF FATIGUE TEST RESULTS -- NOTCHED SPECIMENS OF ANNEALED ASTM-A7 STEEL --
THEORETICAL STRESS CONCENTRATION FACTOR = 2.0

Spec. No.	Nominal Stress Range max. (+ = tension, - = compr.)	Nominal Stress Range min. (+ = tension, - = compr.)	True Stress Range max. (+ = tension, - = compr.)	True Stress Range min. (+ = tension, - = compr.)	Per Cent Change In Net Area For Computing True Range (+ = increase, - = reduction)	At Failure (+ = increase, - = reduction)	No. of Cycles Where Yielding Stopped 1000's	No. of Cycles to Fail. 1000's	Remarks
									(All reference to no. of cycles is in 1000's.)
AA2A	+19000	-19000	+19000	-19000	0	0	0	2110	
AA2B	+24760	- 8540	+24760	- 8540	0	0	0	7342[a]	
Z8A	+25740	-10660	+25800	-10690	-0.4[d]	- 0.7	3099[e]	3099	
Z8B	+37950	- 450	+38200	- 450	-0.7[d]	- 1.4	540[e]	540	
L1A	+41460	- 460	+41460	- 460	0	- 0.3	0	313	
L7A	+20480	-20920	+20480	-20920	0	0	0	867	
L7B	+36910	- 450	+36910	- 450	0	- 1.6	0	623	
M2A	+19320	-35180	+19320	-35180	0	0	0	130	
M4A	+16020	-35520	+16020	-35520	0	0	0	239	
M4B	+13930	-35570	+13930	-35570	0	0	0	366	
M8A	+11080	-35320	+11080	-35320	0	0	0	624	
M8B	+24250	-24250	+24250	-24250	0	0	0	321	
N2A	+32480	-10420	+32480	-10420	0	- 1.6	0	388	
N6B	+ 8380	-35520	+ 8320	-35230	+0.7[c]	+ 0.7	617[e]	617	
N6A	+44880	- 620	+45800	- 630	-2.0[d]	- 4.1	100[e]	100	
O5A	+38000	-10500	+38350	-10600	-0.9[d]	- 1.8	91[e]	91	
P3A	+34680	- 720	+34680	- 720	0	- 1.0	0	1507	
P7A	+55980	+14480	+59100	+15300	-5.9[c]	- 5.9	11	165	
P7B	+49500	+14200	+52100	+14960	-5.0[c]	- 5.0	14	382	
Q4A	+46580	+14220	+48850	+14900	-4.5[c]	- 4.5	18	529	
S5A	+ 5200	-55100	+ 4995	-52950	+4.2[c]	+ 4.2	97[e]	97	
T3A	+66650	+29250	+79000	+34700	-15.7[c]	-15.7	121[e]	121	
T1A	- 5650	-55650	- 5450	-53700	+3.7[c]	+ 3.7	26	131	131 cycles to first crack 707 cycles without fracture or serious propagation
T1B	-12200	-55500	-11810	-53700	+3.2[c]	+ 3.2	12	2394	2394 cycles to first crack 6361 cycles without fracture or serious propagation

TABLE 5 (CONT'D)

SUMMARY OF FATIGUE TEST RESULTS -- NOTCHED SPECIMENS OF ANNEALED ASTM-A7 STEEL -- THEORETICAL STRESS CONCENTRATION FACTOR = 2.0

Spec. No.	Nominal Stress Range max. (+ = tension, - = compr.)	Nominal Stress Range min. (+ = tension, - = compr.)	True Stress Range max. (+ = tension, - = compr.)	True Stress Range min. (+ = tension, - = compr.)	Per Cent Change In Net Area For Computing True Range (+ = increase, - = reduction)	Per Cent Change In Net Area At Failure (+ = increase, - = reduction)	No. of Cycles Where Yielding Stopped 1000's	No. of Cycles to Fail. 1000's	Remarks
T3B	+61580	+29320	+67900	+32230	-9.2[c]	-9.2	405[e]	405	
T5A	+59570	+29230	+64500	+31620	-7.7[c]	-7.7	30	656	
W2A	- 5700	-70300	- 5250	-64700	+8.5[c]	+8.5	18[e]	18	18 cycles to first crack and buckling of specimen 300 cycles without fracture or serious propagation
W2B	-17650	-70750	-16600	-66500	+6.4[c]	+6.4	18	223	233 cycles to first crack 447 cycles without fracture or serious propagation
W4A	-24730	-70670	-23000	-65800	+7.5[c]	+7.5	12	837	12 cycles to buckling of specimen. 837 cycles to first crack. 1783 cycles without fracture or serious propagation
Y5A	+26120	-26540	+26120	-26540	0	0	0	126	126 cycles to first crack 166 cycles to fracture
Z2A	+ 5300	-35100	+ 5270	-34950	+0.4[d]	+0.7	0	1766	1766 cycles to first crack 2409 cycles to essential fracture
Z6a	+44050	+15050	+44050	+15050	0	-3.2	0	1041	
AA6A	+57020	+29780	+59400	+31000	-4.0[d]	-8.0	18	2145	

[a] No failure

[b] Based on initial net area

[c] Based on final net area since majority of yielding occurred very early in the test.

[d] Based on average of initial and final net areas during dynamic test

[e] Yielding occurred throughout the test

RESULTS OF S-N INTERPOLATION TO ESTABLISH NUMBER OF CYCLE CONTOURS

UNNOTCHED SPECIMENS

ZERO PRESTRESS

No. of Cycles 1000's	Nominal Stresses max. psi	Nominal Stresses min. psi	True Stresses max. psi	True Stresses min. psi
100	+53750	+45000	+65400	+55000
500	+53100	+45000	+64700	+55000
2000	+52850	+45000	+64550	+55000
100	+53600	+15000	+65700	+18000
500	+52100	+15000	+63000	+18000
2000	+51400	+15000	+60800	+18000
100	+36500	-12000	+44000	-12000
500	+33300	-12000	+34700	-12000
2000	+31400	-12000	+31400	-12000
50,000 psi Compressive Prestress				
100	+27000	-35000	+24650	-35000
500	+24250	-35000	+22000	-35000
2000	+21850	-35000	+19700	-35000
86,000 psi Compressive Prestress				
100	[a] +21750	-60000	[a] +21200	-60000
500	+18600	-60000	+18800	-60000
2000	+15870	-60000	+15170	-60000

[a] Long extrapolation below 2×10^6 cycles

No. of Cycles 1000's	Nominal Stresses max. psi	Nominal Stresses min. psi	True Stresses max. psi	True Stresses min. psi
100	+54100	+30000	+68200	+38000
500	+53100	+30000	+67100	+38000
2000	+52200	+30000	+66200	+38000
100	+46850	0	+63500	0
500	+44400	0	+50600	0
2000	+44050	0	+47700	0
100	+30350	-30350	+30350	-30350
500	+24500	-24500	+24500	-24500
2000	+23900	-23900	+23900	-23900
69,000 psi Compressive Prestress				
100	+27700	-45000	+24250	-45000
500	+19950	-45000	+18350	-45000
2000	+16700	-45000	+16000	-45000
97,000 psi Compressive Prestress				
100	[b] +15500	-75000	[b] +14250	-75000
500	+10300	-75000	+ 9250	-75000
2000	+ 5800	-75000	+ 5000	-75000

[b] Too few valid points to be accurate

RESULTS OF S-N INTERPOLATION TO ESTABLISH NUMBER OF CYCLE CONTOURS

NOTCHED SPECIMENS

No. of Cycles 1000's	Nominal Stresses max. psi	min. psi	True Stresses max. psi	min. psi
100	+68300	+30000	+78200	+32000
500	+61400	+30000	+66200	+32000
2000	+57300	+30000	+60600	+32000
100	+46450	0	+46450	0
500	+38750	0	+38750	0
2000	+35100	0	+35100	0
100	+27950	-27950	+27950	-27950
500	+22300	-22300	+22300	-22300
2000	+19100	-19100	+19100	-19100
100	+ 3500	-55000	+ 2800	-53000
500	- 9700	-55000	- 9000	-53000
2000	-11500	-55000	-10800	-53000

No. of Cycles 1000's	Nominal Stresses max. psi	min. psi	True Stresses max. psi	min. psi
100	+60650	+15000	+63400	+15000
500	+48100	+15000	+49700	+15000
2000	+43150	+15000	+40500	+15000
100	+37200	-11000	+37600	-11000
500	+30900	-11000	+31100	-11000
2000	+26300	-11000	+26400	-11000
100	+20700	-35000	+20700	-35000
500	+12800	-35000	+12800	-35000
2000	+ 4500	-35000	+ 4500	-35000

TABLE 7

MAXIMUM ERRORS BETWEEN DERIVED AND EXPERIMENTAL RESULTS

Material	Number of Cycles 1000's	Error in	Theoretical Stress Concentration 1.0	1.5	2.0	4.0	5.0
			Maximum Error in Per Cent				
Annealed ASTM A7 Steel	100	Slope	-44.8	-	+ 1.3	-	-
		Intercept	+45.2	-	+ 1.3	-	-
	500	Slope	-46.0	-	+ 6.0	-	-
		Intercept	+59.3	-	+ 3.4	-	-
	2000	Slope	-33.4	-	+10.4	-	-
		Intercept	+41.4	-	+ 0.6	-	-
24S-T3 Aluminum Alloy	100	Slope	-10.2	-18.0	- 4.3	+ 7.7	-14.2
		Intercept	- 9.3	+ 2.7	0.0	-17.4	-25.1
	500	Slope	+22.6	- 7.6	+11.2	+ 5.1	+ 4.9
		Intercept	+ 2.7	+10.5	+ 9.3	-13.9	-14.0
	2000	Slope	+71.0	+ 6.9	+15.6	+ 4.7	+13.3
		Intercept	+ 1.6	+ 3.1	+ 2.3	-19.0	-13.6
75S-T6 Aluminum Alloy	100	Slope	-27.8	-46.2	-38.2	-24.3	- 7.9
		Intercept	- 5.3	+16.1	+14.9	-12.2	- 9.0
	500	Slope	+38.0	-30.2	-21.0	-15.4	- 2.1
		Intercept	- 1.1	+13.3	+ 9.6	-15.4	-12.7
	2000	Slope	+ 0.4	-17.4	-14.2	- 0.8	+ 8.3
		Intercept	- 5.8	- 3.4	- 6.7	-21.8	- 8.7
Normalized 4130 Steel	100	Slope	-38.6	+20.0	+35.2	-26.8	-40.5
		Intercept	+ 4.0	+ 9.6	- 3.2	+17.7	- 9.3
	500	Slope	-18.2	+19.3	+31.6	- 6.9	- 1.3
		Intercept	+ 5.3	+14.6	+ 7.2	- 7.9	- 0.4
	2000	Slope	- 6.4	+ 8.3	+32.8	+36.2	+17.7
		Intercept	+ 2.6	+11.3	+ 4.5	-11.6	- 2.7

COMPARISON OF DERIVED FATIGUE INTERCEPT AND AVERAGE FATIGUE STRESS FOR FAILURE UNDER ZERO TO TENSION AXIAL LOADS AS GIVEN BY BARON AND LARSON

Theoretical Stress Concentration Factor = 2.32 In All Cases

Designation (Baron and Larson)	Ultimate Strength psi	Yield Strength psi	Reduction of Area Per Cent	Elongation in 2" Per Cent	Number of Cycles 1000's	Maximum Fatigue Stress (psi) Derived	Maximum Fatigue Stress (psi) Test	Error Per Cent
High Strength Low Alloy Steel (ASTM A242-50T)								
A	79500	55000	59.3	50.0	398	29200	31500	- 7.3
					642	27600	27000	+ 2.2
					2059*	24200	25000	- 3.2
B	65200	44400	61.2	55.0	440	23200	35000	-33.8
					683	22100	31500	-29.8
					1510	20200	27000	-25.2
C	82600	47800	60.5	47.8	292	42500	35000	+21.4
					532	39600	31500	+25.8
					2170*	33700	27000	+24.8
D	74400	57000	60.1	50.0	330	23600	35000	-32.6
					385	23200	31500	-26.4
					891	21000	27000	-22.2
E	77900	48200	61.5	50.2	418	35200	35000	+ 0.6
					1166	31300	31500	- 0.6
					3058*	28000	27000	+ 3.7
F	78800	49500	60.8	50.0	489	33800	35000	- 6.3
					899	31600	31500	+ 0.3
					2063*	28700	27000	+ 6.3
G	73600	51200	60.6	51.0	175	30200	40000	-23.0
					298	28400	37500	-23.7
					1230	24000	35000	-31.4
					2013*	22600	31500	-28.2

COMPARISON OF DERIVED FATIGUE INTERCEPT AND AVERAGE FATIGUE STRESS FOR FAILURE UNDER ZERO TO TENSION AXIAL LOADS AS GIVEN BY BARON AND LARSON

Theoretical Stress Concentration Factor = 2.32 In All Cases

Designation (Baron and Larson)	Ultimate Strength psi	Yield Strength psi	Reduction of Area Per Cent	Elongation in 2" Per Cent	Number of Cycles 1000's	Maximum Fatigue Stress (psi) Derived	Test	Error Per Cent
				Rimmed Steel				
H	52700	31100	63.8	57.5	111	28200	31500	-10.5
					438	24000	27000	-11.1
				Carbon Steel (ASTM A7)				
					264	33600	31500	+ 6.7
I	70000	36600	53.3	50.5	651	30500	27000	+11.3
					1460	27800	25000	+11.2
					136	31900	31500	+ 1.3
					408	27200	27000	+ 0.7
J	62100	34400	57.2	53.0	943	25500	23000	+10.9
					178	29600	31500	- 6.0
					382	27200	30000	- 9.3
K	60000	35400	60.5	54.2	863	24700	27000	- 8.5
					996	24300	25000	- 2.8
					1428	23200	23000	+ 0.9
				Silicon Steel (ASTM A94)				
					328	38200	35000	+ 9.1
L	90000	51800	44.2	40.5	1681	31700	31500	+ 0.6
					2009	31000	27000	+14.8
					300	43200	35000	+23.4
					528(?)	40500	31500	+28.6
M	88800	48400	50.4	43.5	437(?)	41500	30000	+38.4
					1559	35600	27000	+31.8

TABLE 5 (Cont'd)

COMPARISON OF DERIVED FATIGUE INTERCEPT AND AVERAGE FATIGUE STRESS FOR FAILURE UNDER ZERO TO TENSION AXIAL LOADS AS GIVEN BY BARON AND LARSON

Theoretical Stress Concentration Factor = 2.32 In All Cases

Designation (Baron and Larson)	Ultimate Strength psi	Yield Strength psi	Reduction of Area Per Cent	Elongation in 2" Per Cent	Number of Cycles 1000's	Maximum Fatigue Stress (psi) Derived	Maximum Fatigue Stress (psi) Test	Error Per Cent
Silicon Steel (ASTM A94) Cont'd								
N	90800	51500	46.9	40.5	287	41900	37500	+11.7
					498	39400	35000	+12.6
					754	37400	33000	+13.3
					2649*	32400	31500	+ 2.9
O	83600	46500	58.6	49.2	123	46500	37500	+24.0
					321	41500	35000	+18.6
					927	36900	33000	+11.8
					2165	33400	31500	+ 6.0

* No Failure

TABLE 9

SUMMARY OF RESULTS FROM CALIBRATION OF SONNTAG MACHINE

Weigh Bar No.	Eccentric Constant lb/unit	Preload Constant lb/div.	Max. Drift in Preload During Dynamic Run lb	Average Backlash in Preload lb	Preload Zero Determined From Calibration Curves div.	Date of Calibration	Remarks
C-1	1.01	20.8(T)[a] 21.8(T) 21.3(C) 20.6(C)	+ 18 - 50	50(T) 48(C)	1002(T) 1001(T) 1004(C) 1002(C)	4-29-53	All strains recorded by oscillograph.
[b]C-2	1.09	23.3(T) 23.1(T) 24.2(C) 24.0(C)	+156 - 0	60(T) 95(C)	1001(T) 996(T) 1001(C) 998(C)	4-30-53	All strains recorded by oscillograph. Machine not warmed up prior to calibration.
[c]C-3	1.01	22.0(T) 21.9(T) 23.6(C) -	+204 -110	85(T) -	1002(T) 997(T) 994(C) -	5-4-53	All strains recorded by oscillograph.
C-1	-	21.0(T) 21.0(T) 21.3(C) 20.9(C)	- -	40(T) 35(C)	1000(T) 998(T) 1001(C) 1000(C)	6-15-53	All strains measured by strain indicator.
C-2	-	21.6(T) 21.4(T) 21.8(C) 21.8(C)	- -	50(T) 63(C)	1003(T) 1000(T) 1003(C) 998(C)	6-15-53	

TABLE 9 (CONT'D)

SUMMARY OF RESULTS FROM CALIBRATION OF SONNTAG MACHINE

Weigh Bar No.	Eccentric Constant lb/unit	Preload Constant lb/div.	Max. Drift in Preload During Dynamic Run lb	Average Backlash in Preload lb	Preload Zero Determined From Calibration Curves div.	Date of Calibration	Remarks
C-1	-	21.6(T) 21.4(T) 21.2(C) 21.2(C)	- -	40(T) 30(C)	1002(T) 1001(T) 1003(C) 1001(C)	8-11-53	All strains measured by strain indicator.
C-2	-	21.5(T) 21.3(T) 21.7(C) 21.8(C)	- -	58(T) 55(C)	1005(T) 1002(T) 1007(C) 1003(C)	8-11-53	Avg. load applied per cycle of automatic preload = 22 lb as determined on weigh bar C2 and is constant for full range of preload. (No fatigue tests conducted from 9-30-53 to 1-12-54)
C-1	-	21.5(T) 21.4(T) 21.4(C) 21.8(C)	- -	10(T) 20(C)	1001(T) 1000(T) 1001(C) 1000(C)	1-12-54	All strains recorded by strain indicator. Machine not warmed up prior to calibration of weigh bar C-2.
[b]C-2	-	22.2(T) 22.2(T) 22.6(C) 22.4(C)	- -	0(T) 45(C)	998(T) 998(T) 998(C) 997(C)	1-12-54	
C-1	-	21.3(T) 21.3(T) 21.0(C) 21.0(C)	- -	28(T) 40(C)	1001(T) 1002(T) 1002(C) 1001(C)	4-8-54	
C-2	-	22.0(T) 21.9(T) 22.0(C) 22.2(C)	- -	35(T) 75(C)	1002(T) 1000(T) 1003(C) 998(C)	4-8-54	All strains measured by strain indicator.

TABLE 9 (CONT'D)

SUMMARY OF RESULTS FROM CALIBRATION OF SONNTAG MACHINE

Weigh Bar No.	Eccentric Constant lb/unit	Preload Constant lb/div.	Max. Drift in Preload During Dynamic Run lb	Average Backlash in Preload lb	Preload Zero Determined From Calibration Curves div.	Date of Calibration	Remarks
[b] C-1	-	21.6(T) 21.6(T) 21.6(C) 21.5(C)	- -	30(T) 22(C)	1000(T) 1001(T) 1001(C) 1000(C)	4-10-54	All strains measured by strain indicator. Machine not warmed up prior to calibration of either weigh bar.
[b] C-2	-	22.3(T) 22.3(T) 22.5(C) 22.4(C)	- -	25(T) 65(C)	1000(T) 998(T) 999(C) 996(C)	4-10-54	
Av.	1.01	21.5(T) 21.6(C)	+111 - 80	44(T) 46(C)	1001(T) 1001(C)		

[a] (T) = Tension; (C) = Compression.

[b] These calibrations not included in average since machine was not warmed up prior to calibration.

[c] Calibration range for this weigh bar only covers the entire range of the machine using both the eccentric and preload mechanism in loading.

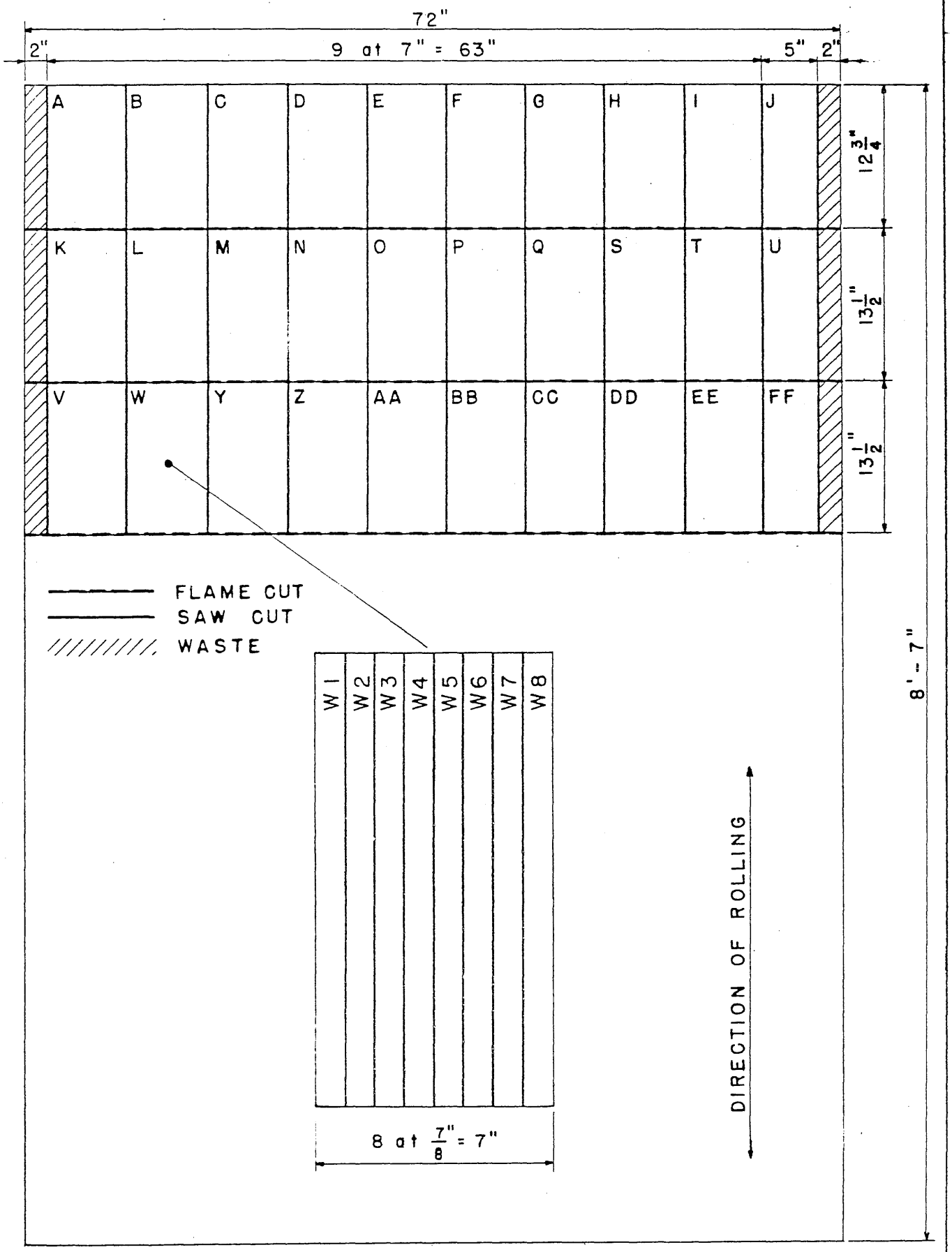

FIG. 1 PARENT PLATE SHOWING LOCATION OF SPECIMEN STOCK AND THE NUMBERING SYSTEM EMPLOYED

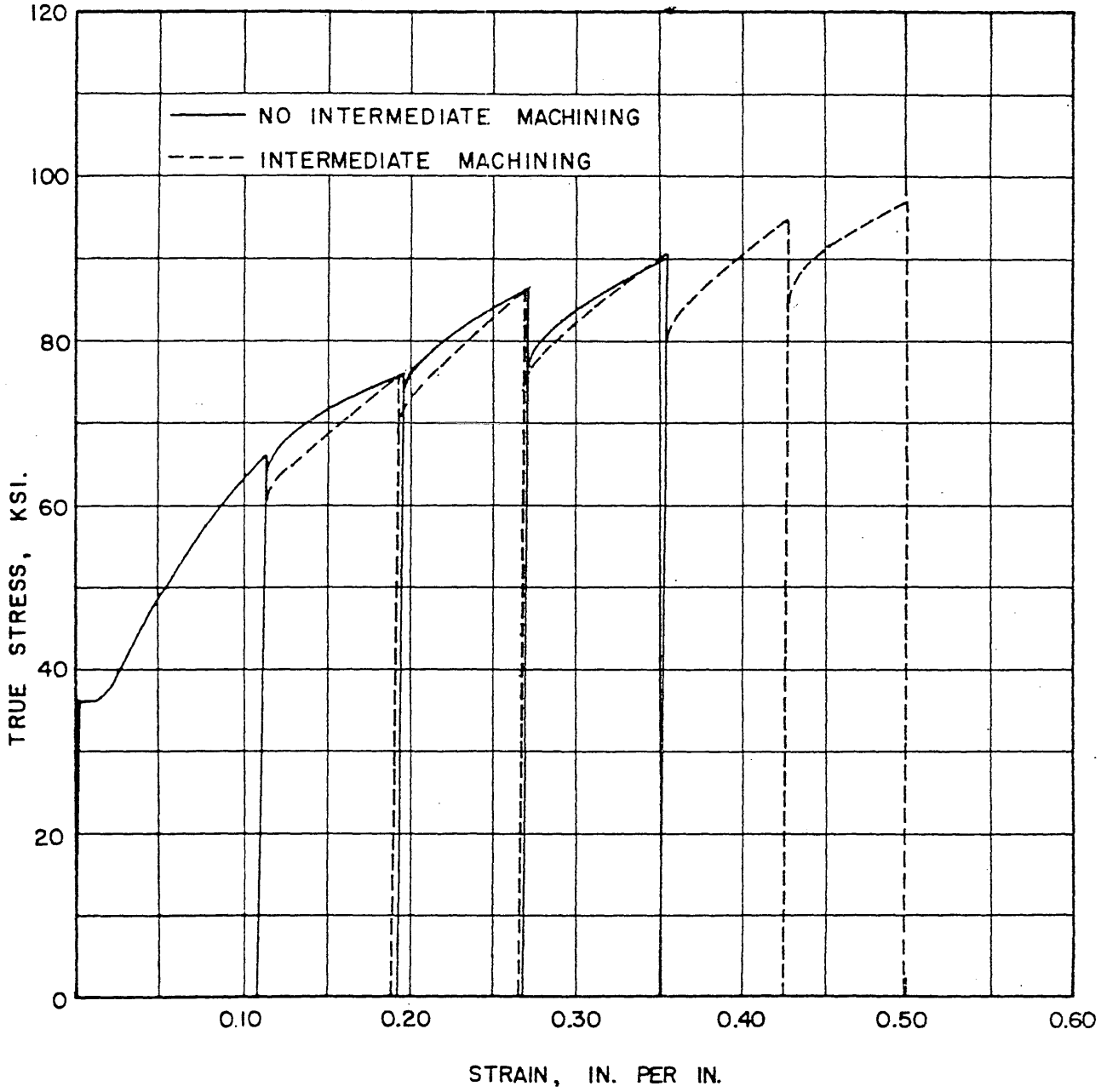

FIG. 2 STRESS-STRAIN DIAGRAM ILLUSTRATING THE STATIC COMPRESSIVE PRESTRESSING PROCESS

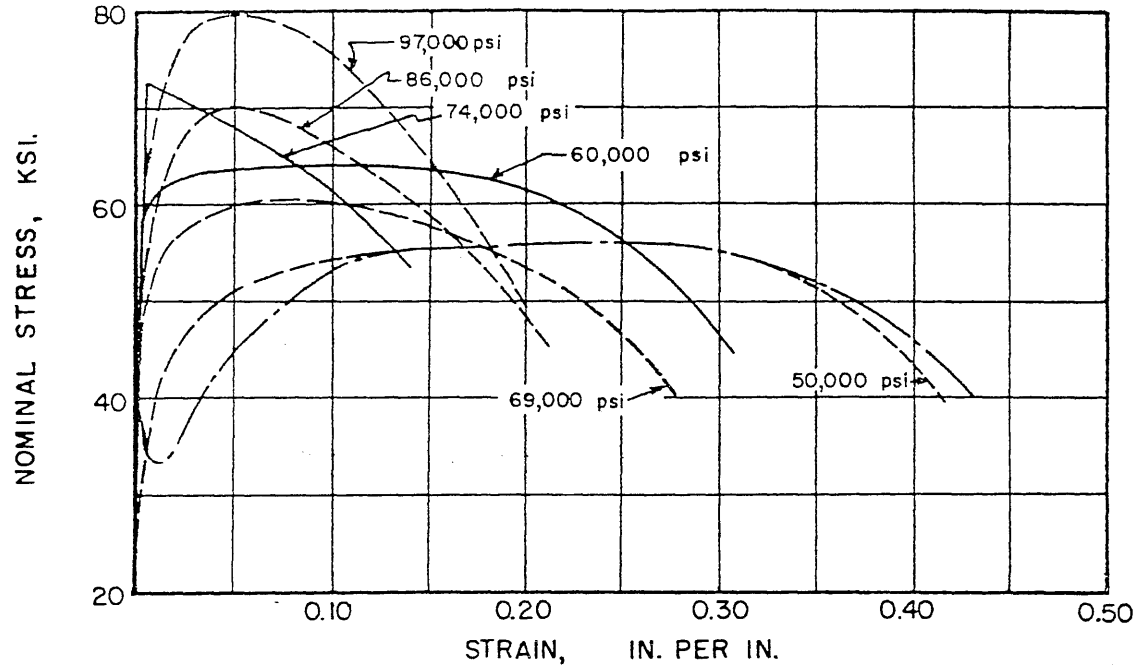

a. NOMINAL STRESSES

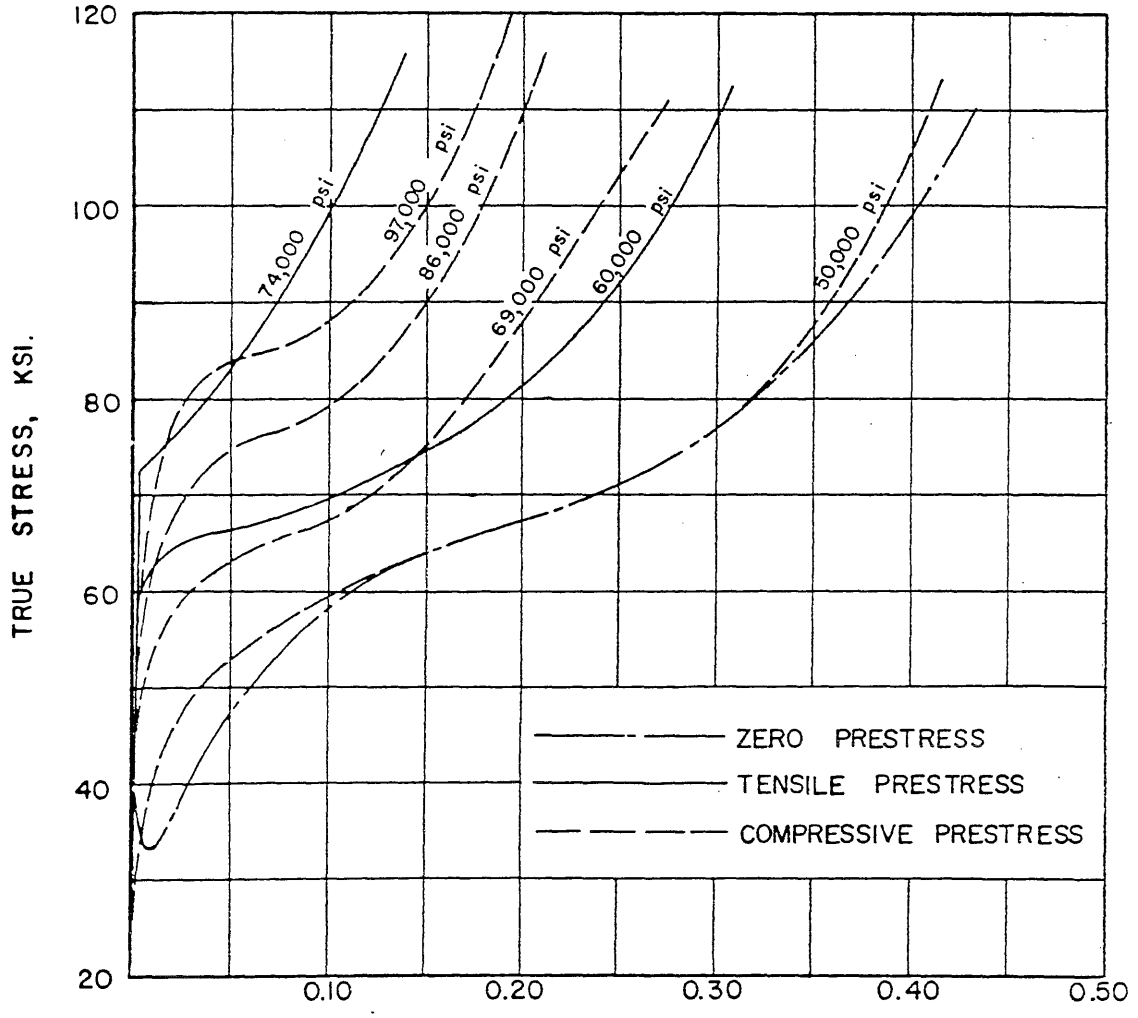

b. TRUE STRESSES

FIG. 3 COMPARISON OF STATIC TENSILE PROPERTIES OF STRAIN HARDENED ANNEALED ASTM-A7 STEEL

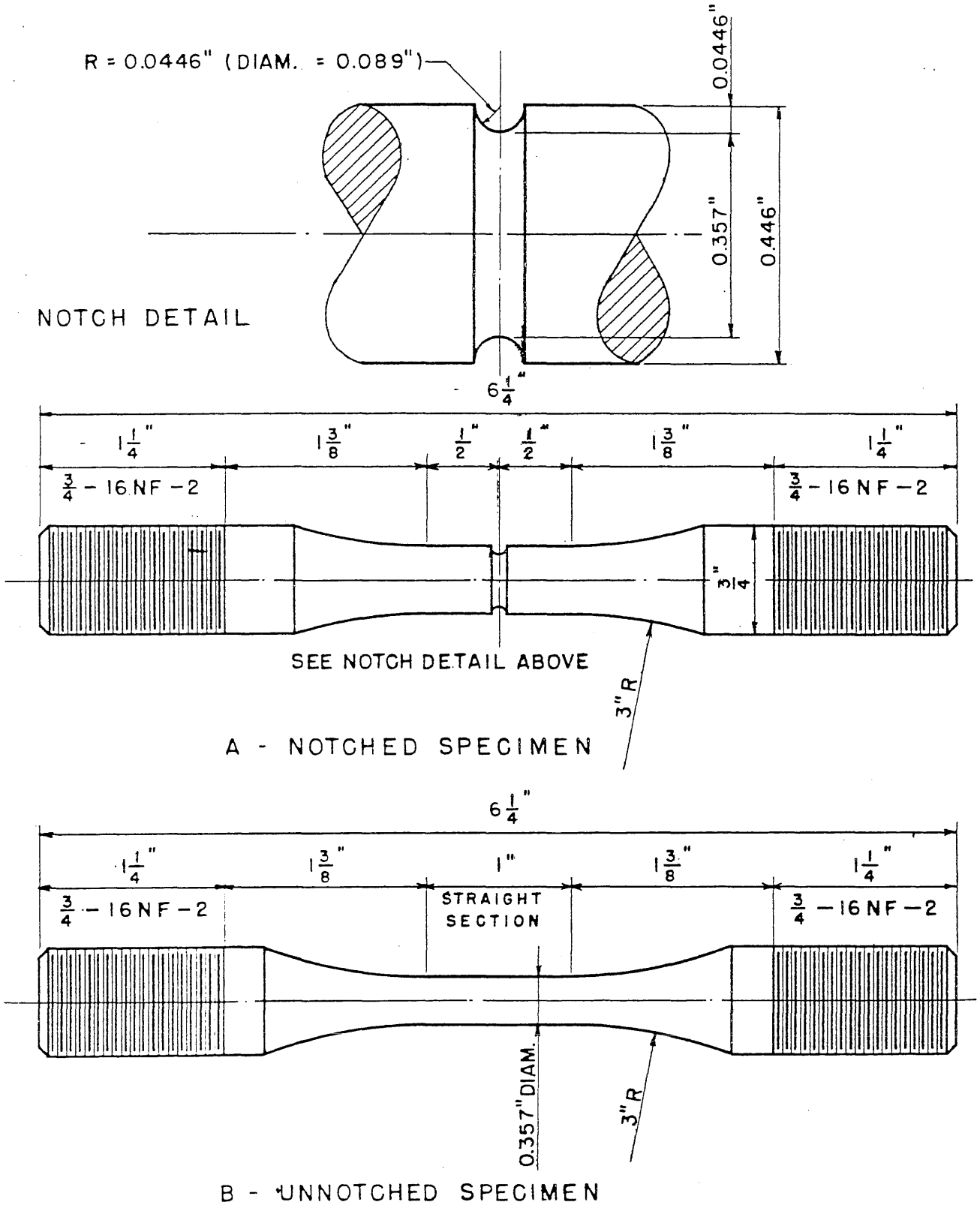

FIG. 4 DETAILS OF SONNTAG AXIAL FATIGUE SPECIMENS

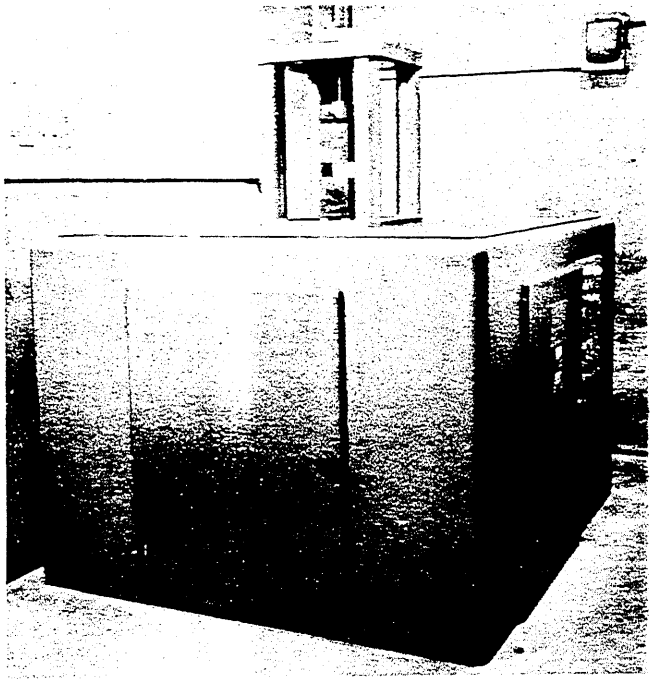

FIG. 5 GENERAL VIEW OF SONNTAG MACHINE

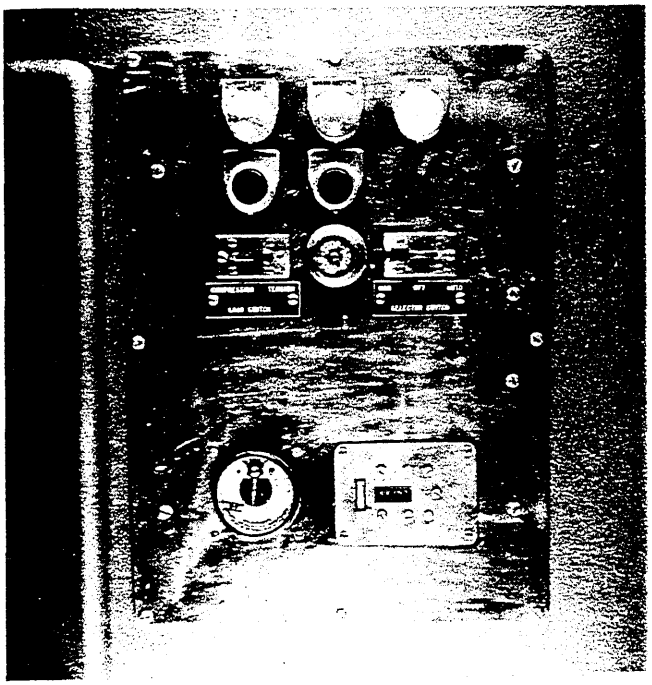

FIG. 6 VIEW OF THE CONTROL PANEL FOR THE SONNTAG MACHINE

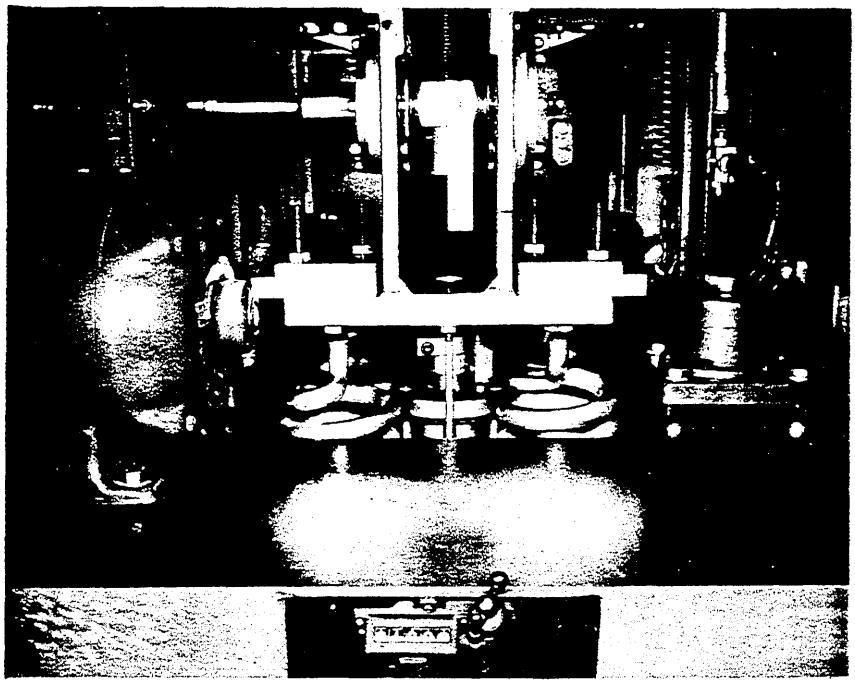

FIG. 7 INTERIOR VIEW OF THE SONNTAG MACHINE SHOWING THE OSCILLATOR, ITS SUPPORTING MECHANISM AND THE PRELOAD COUNTER

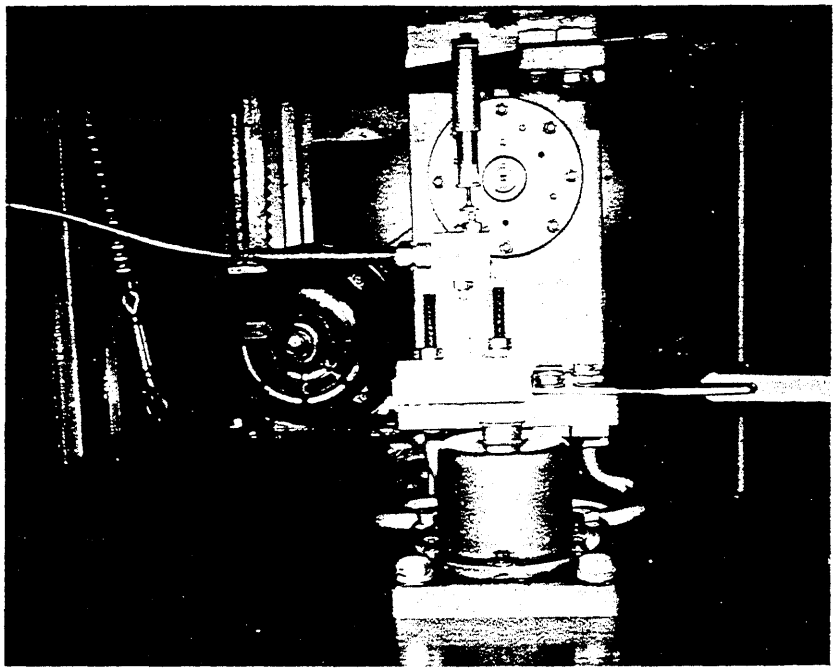

FIG. 8 INTERIOR VIEW OF THE SONNTAG MACHINE SHOWING THE OSCILLATOR AND THE ADDED LIMIT SWITCH

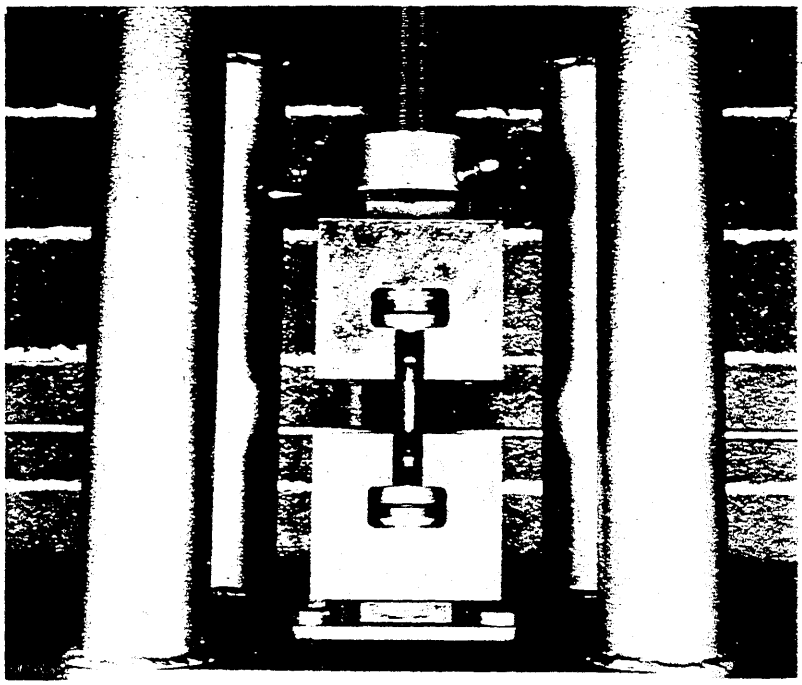

FIG. 9 SIDE VIEW OF THE SONNTAG TENSION-COMPRESSION APPARATUS

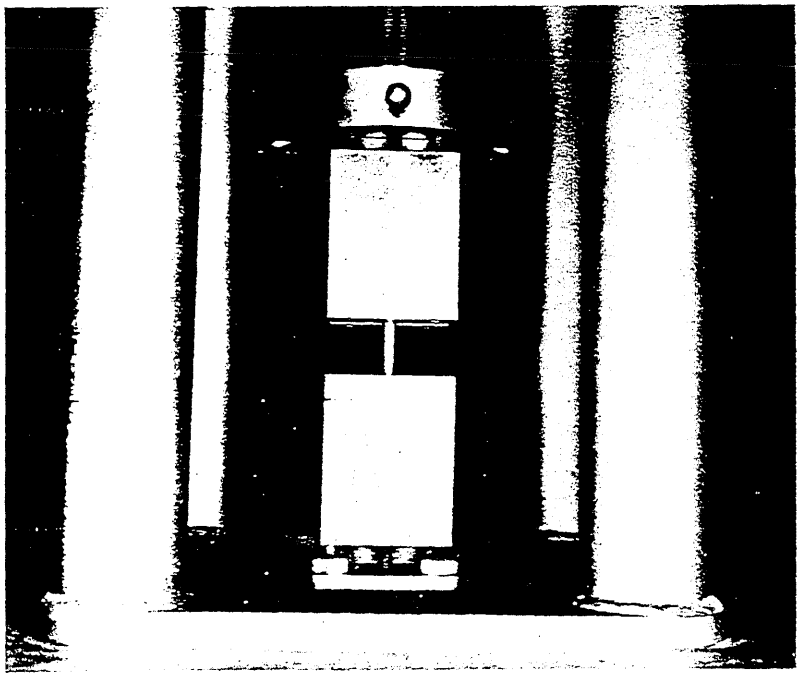

FIG. 10 END VIEW OF THE SONNTAG TENSION-COMPRESSION APPARATUS

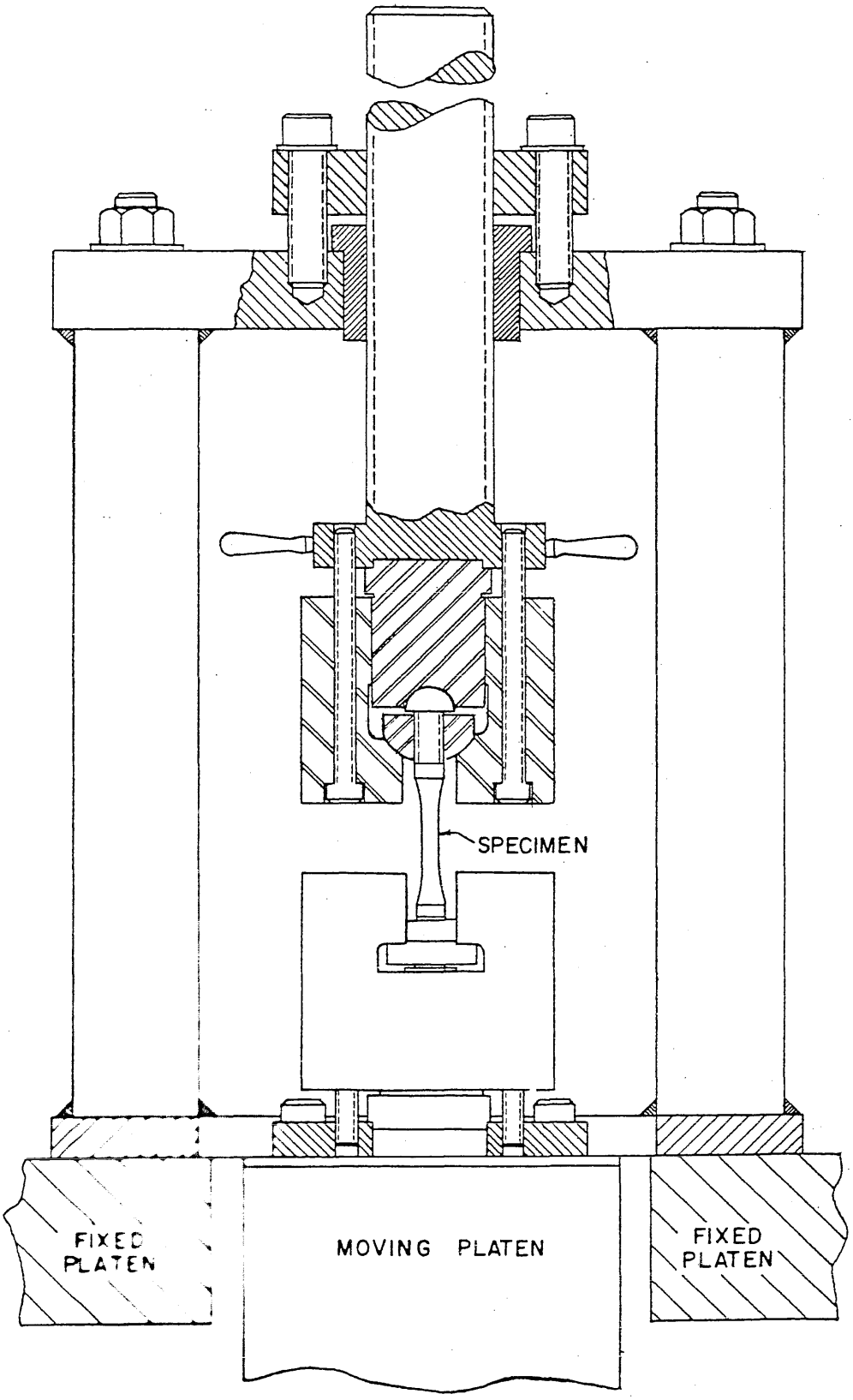

IG.II SECTION DRAWING OF THE SONNTAG TENSION-COMPRESSION APPARATUS

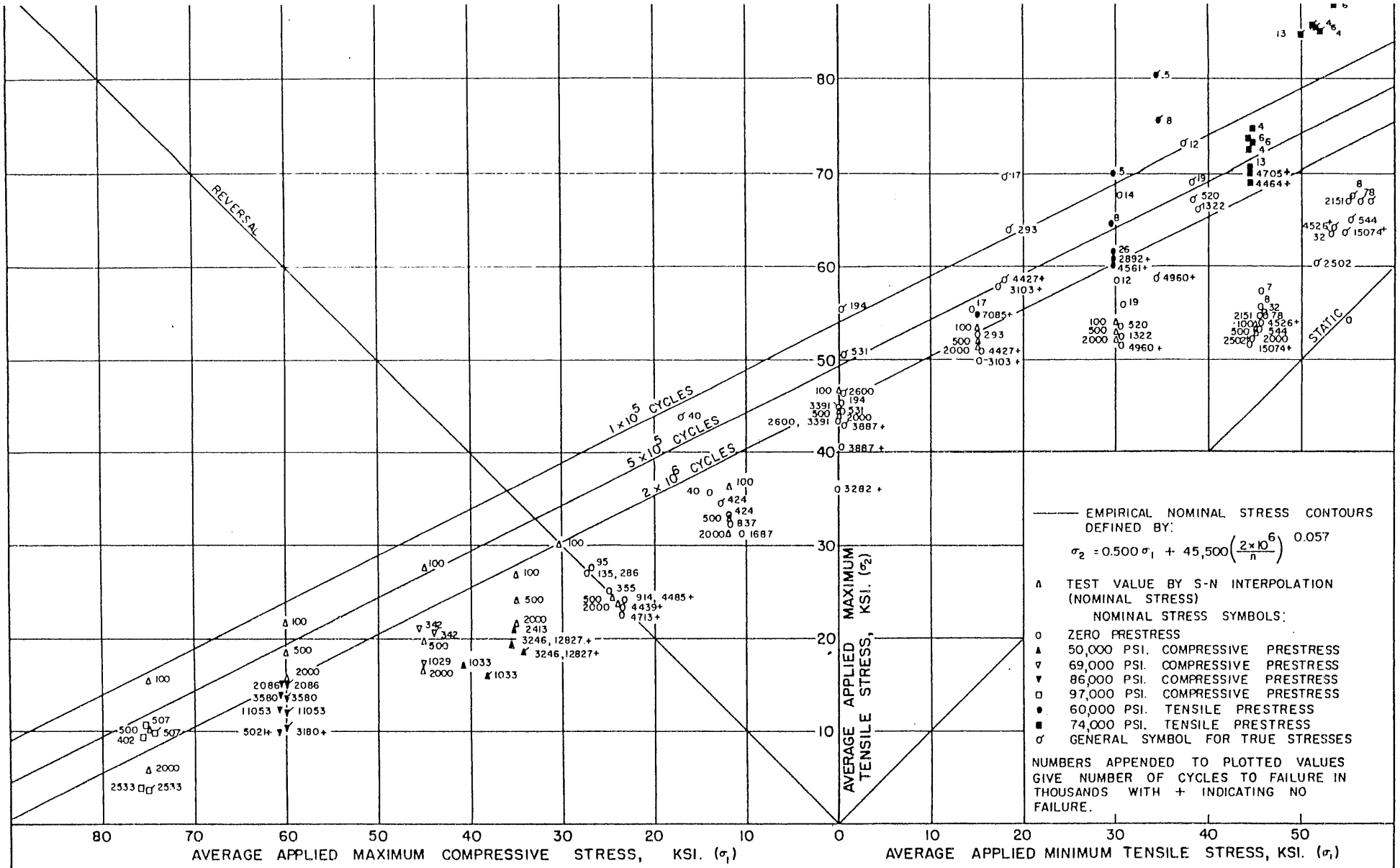

FIG. 12 EMPIRICAL CYCLE CONTOURS FOR UNNOTCHED ANNEALED ASTM-A7 KILLED STEEL COMPARED TO INTERPOLATED TEST VALUES

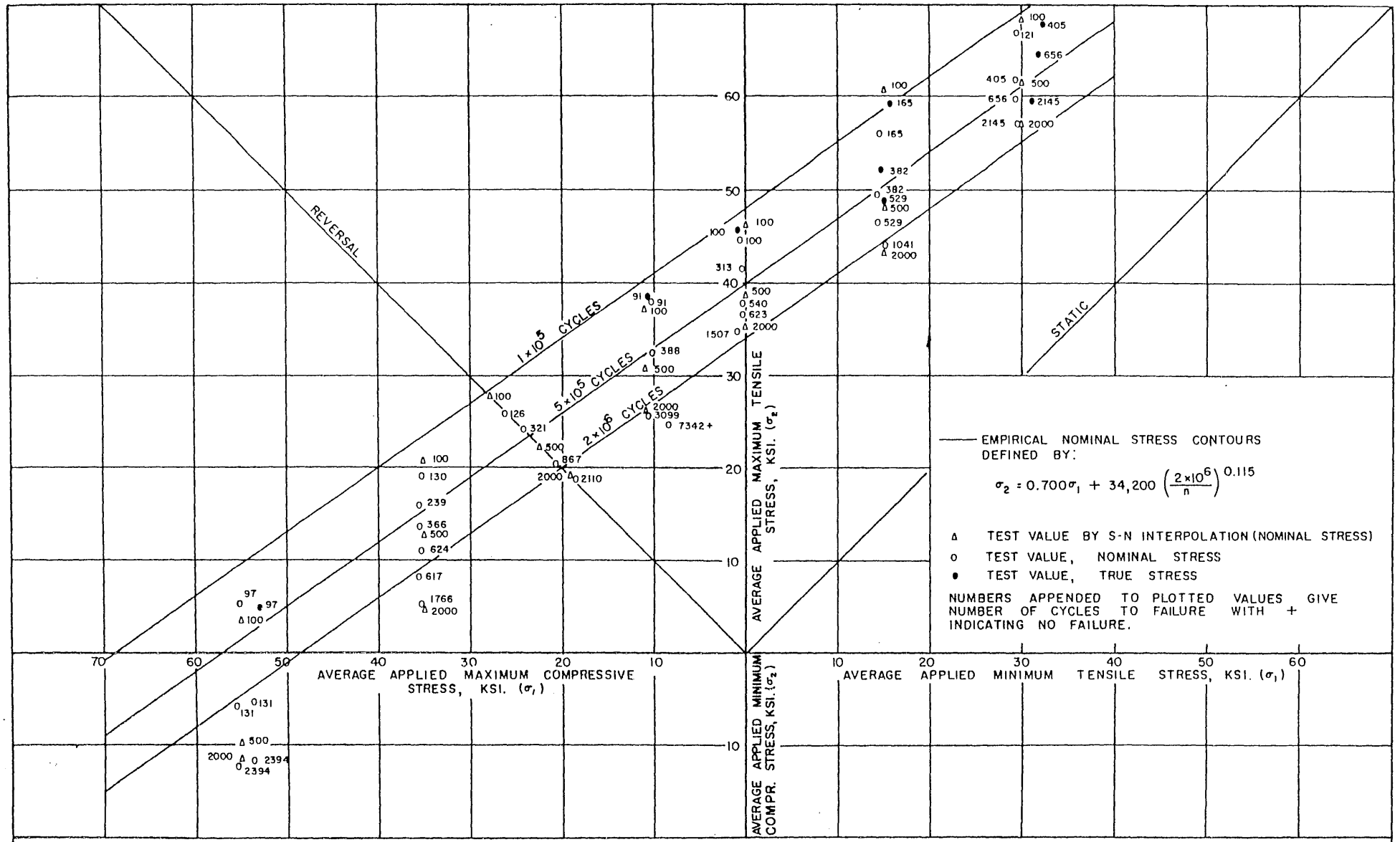

FIG. 13 EMPIRICAL CYCLE CONTOURS FOR NOTCHED ANNEALED ASTM-A7 KILLED STEEL WITH A THEORETICAL STRESS CONCENTRATION FACTOR OF 2.0 COMPARED TO INTERPOLATED TEST VALUES

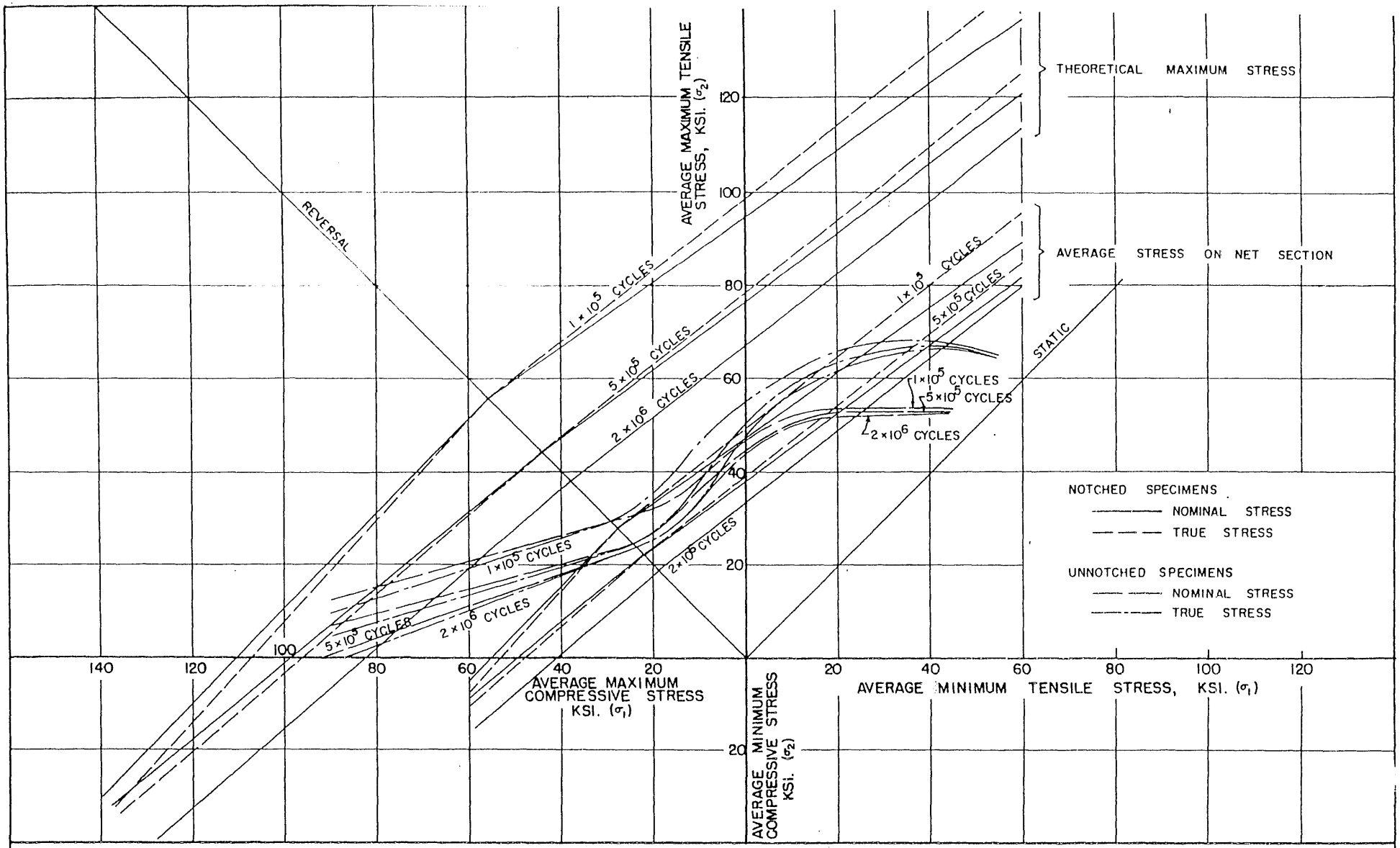

FIG. 14 COMPARISON OF INTERPOLATED CYCLE CONTOURS FOR STRESSES IN UNNOTCHED SPECIMENS WITH THOSE FOR THE AVERAGE STRESSES AND THE STRESSES AT THE ROOT OF THE NOTCH IN NOTCHED SPECIMENS

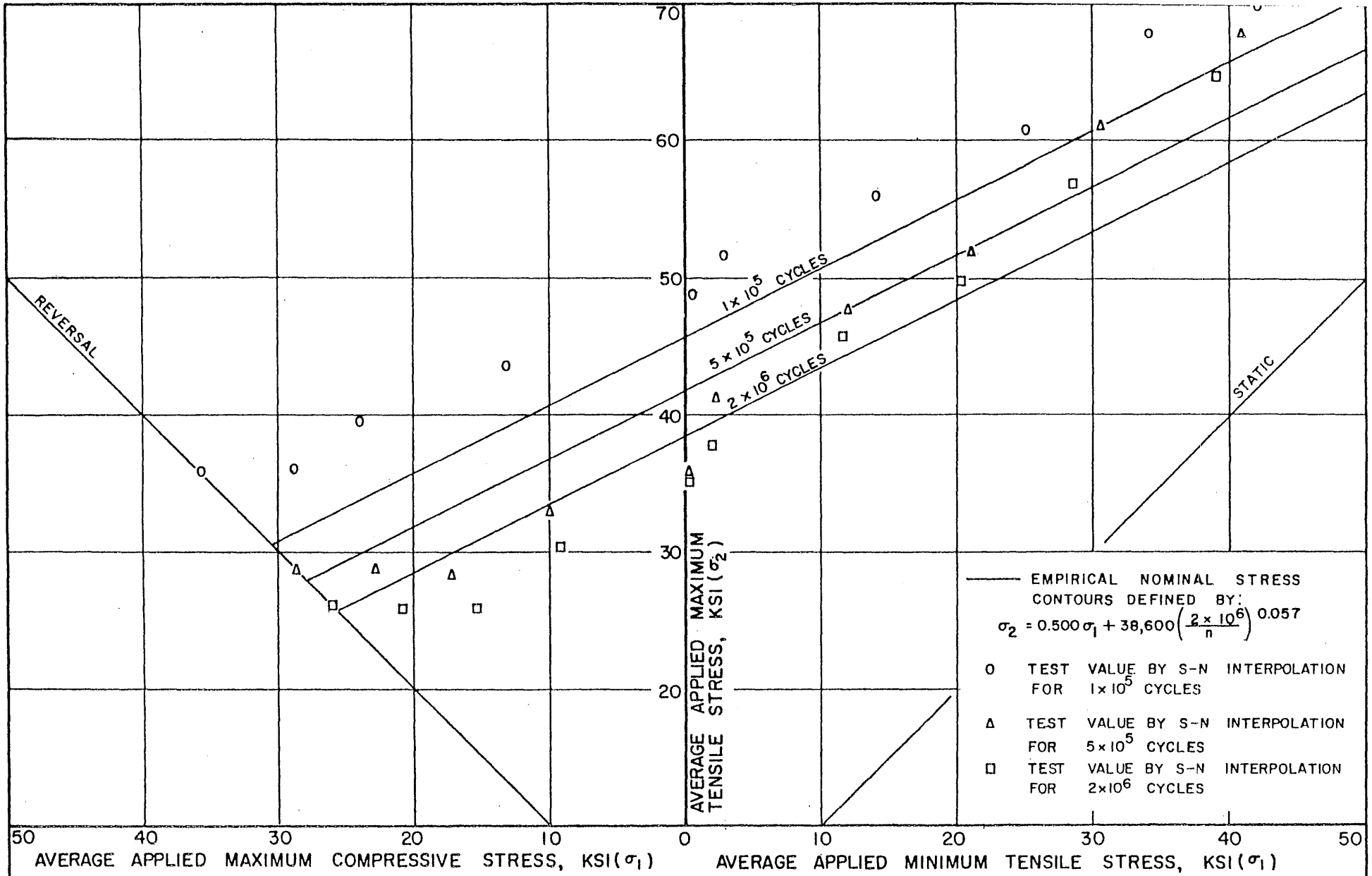

FIG. 15 EMPIRICAL CYCLE CONTOURS FOR UNNOTCHED 24S-T3 ALUMINUM ALLOY COMPARED TO INTERPOLATED TEST VALUES

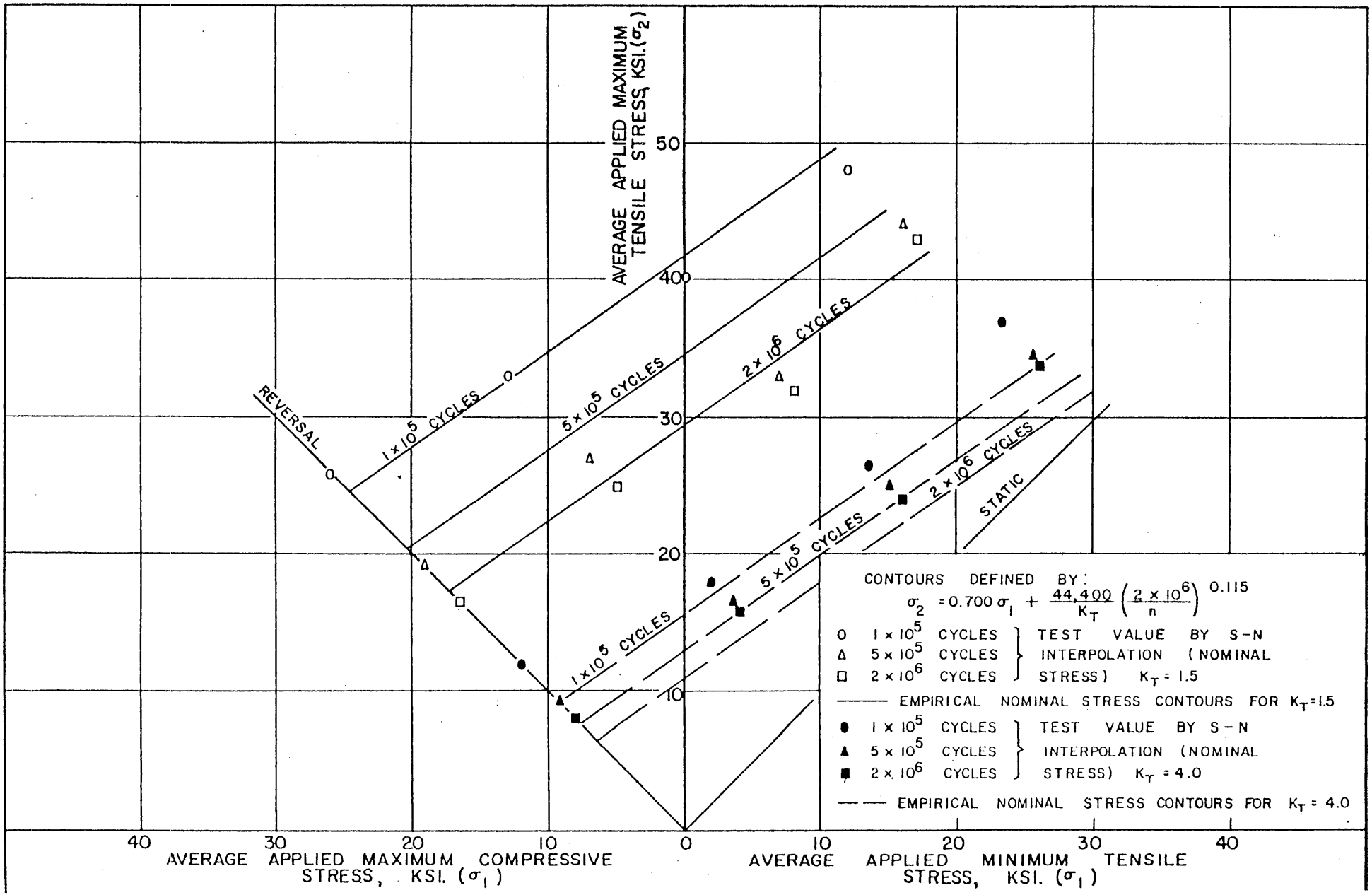
AVERAGE APPLIED MAXIMUM TENSILE STRESS, KSI.(σ_2)
50
40
30
20
10
0
REVERSAL
1 x 10^5 CYCLES
5 x 10^5 CYCLES
2 x 10^6 CYCLES
STATIC
CONTOURS DEFINED BY:
$\sigma_2 = 0.700\,\sigma_1 + \frac{44,400}{K_T}\left(\frac{2 \times 10^6}{n}\right)^{0.115}$
1 x 10^5 CYCLES
5 x 10^5 CYCLES
2 x 10^6 CYCLES
TEST VALUE BY S-N INTERPOLATION (NOMINAL STRESS) K_T = 1.5
EMPIRICAL NOMINAL STRESS CONTOURS FOR K_T=1.5
1 x 10^5 CYCLES
5 x 10^5 CYCLES
2 x 10^6 CYCLES
TEST VALUE BY S-N INTERPOLATION (NOMINAL STRESS) K_T = 4.0
EMPIRICAL NOMINAL STRESS CONTOURS FOR K_T = 4.0
40
30
20
10
0
10
20
30
40
AVERAGE APPLIED MAXIMUM COMPRESSIVE STRESS, KSI. (σ_1)
AVERAGE APPLIED MINIMUM TENSILE STRESS, KSI. (σ_1)

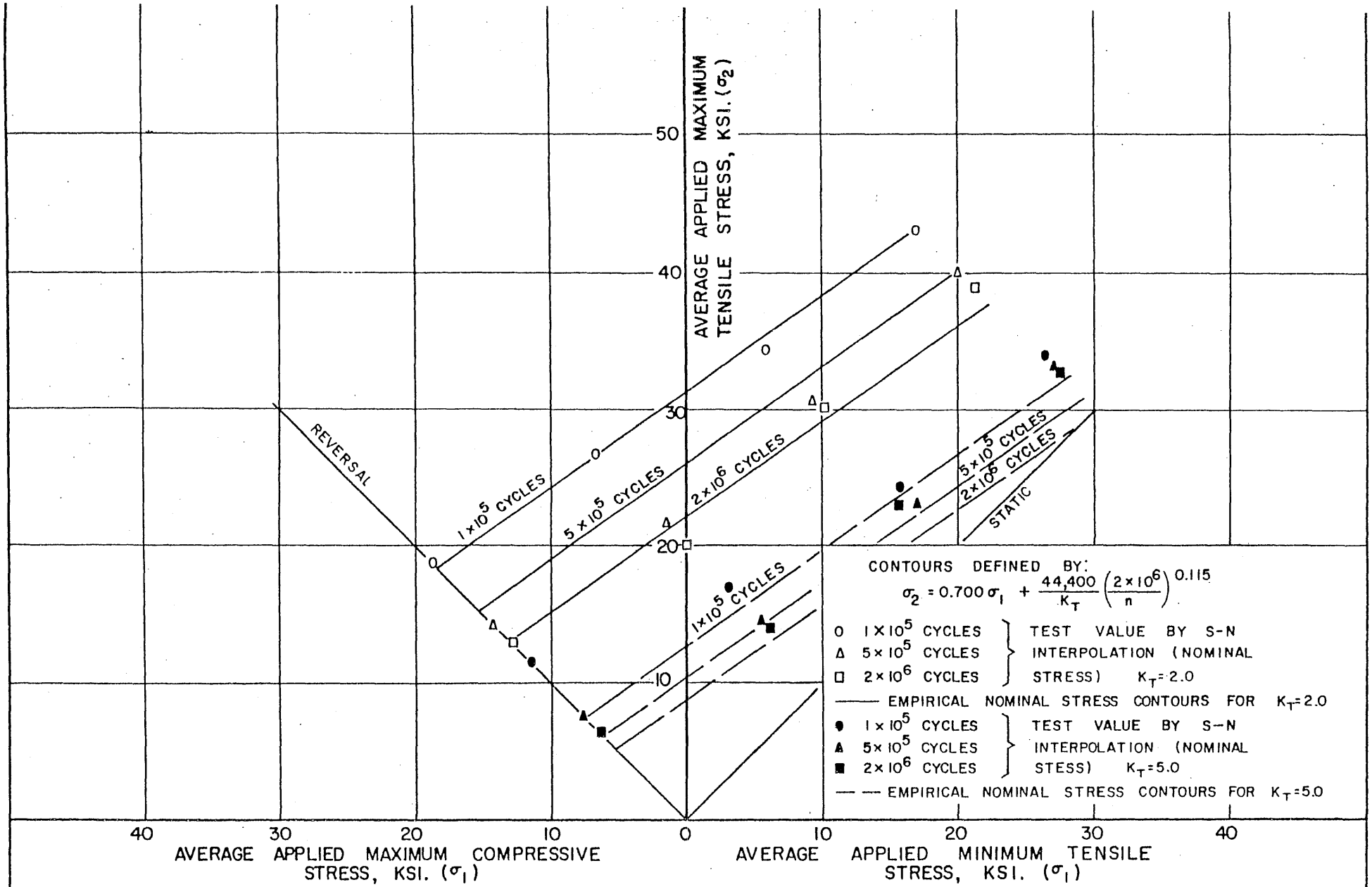

FIG. 17 EMPIRICAL CYCLE CONTOURS FOR NOTCHED 24S-T3 ALUMINUM ALLOY WITH THEORETICAL STRESS CONCENTRATION FACTORS OF 2.0 AND 5.0 COMPARED TO INTERPOLATED TEST VALUES

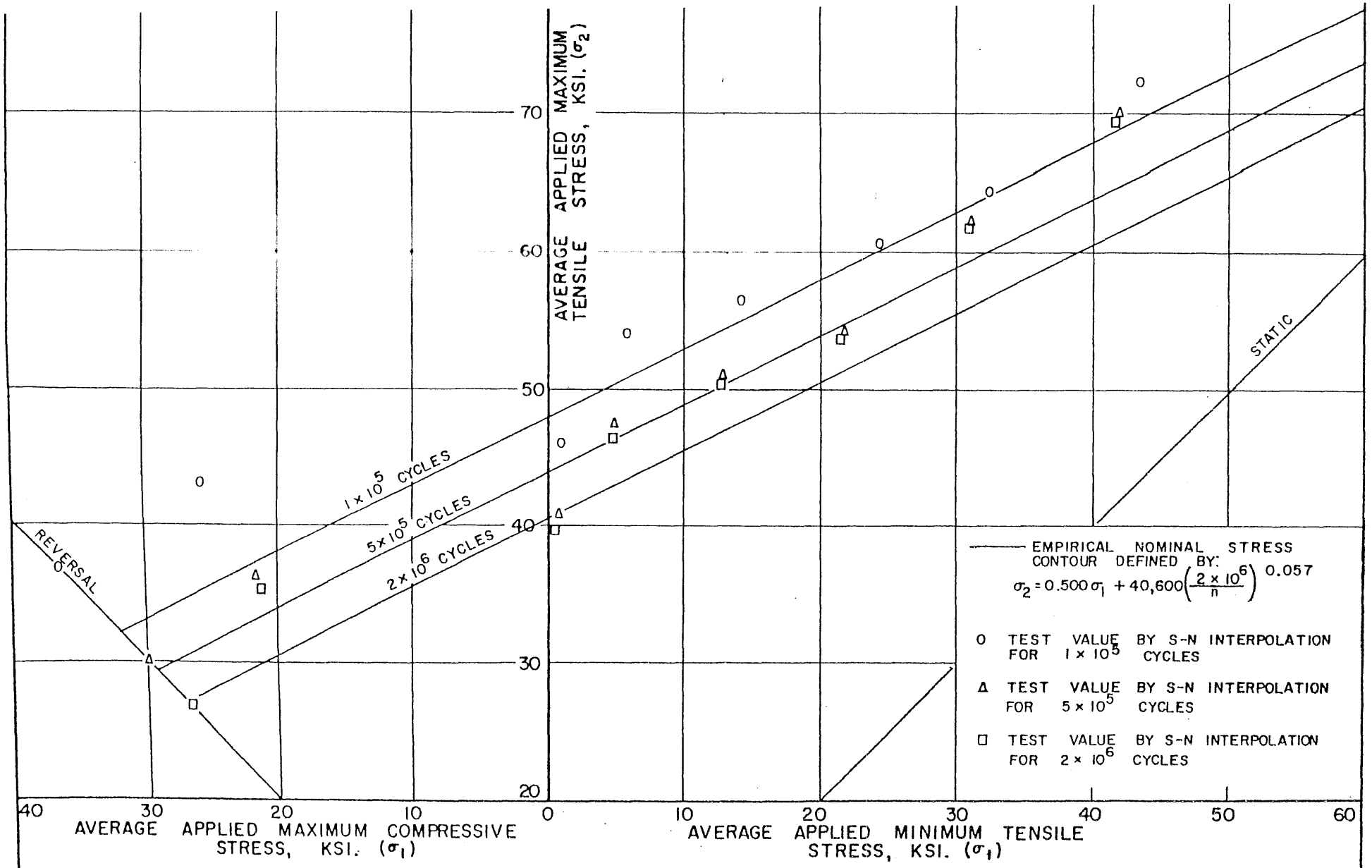

FIG.18 EMPIRICAL CYCLE CONTOURS FOR UNNOTCHED 75S-T6 ALUMINUM ALLOY COMPARED TO INTERPOLATED TEST VALUES

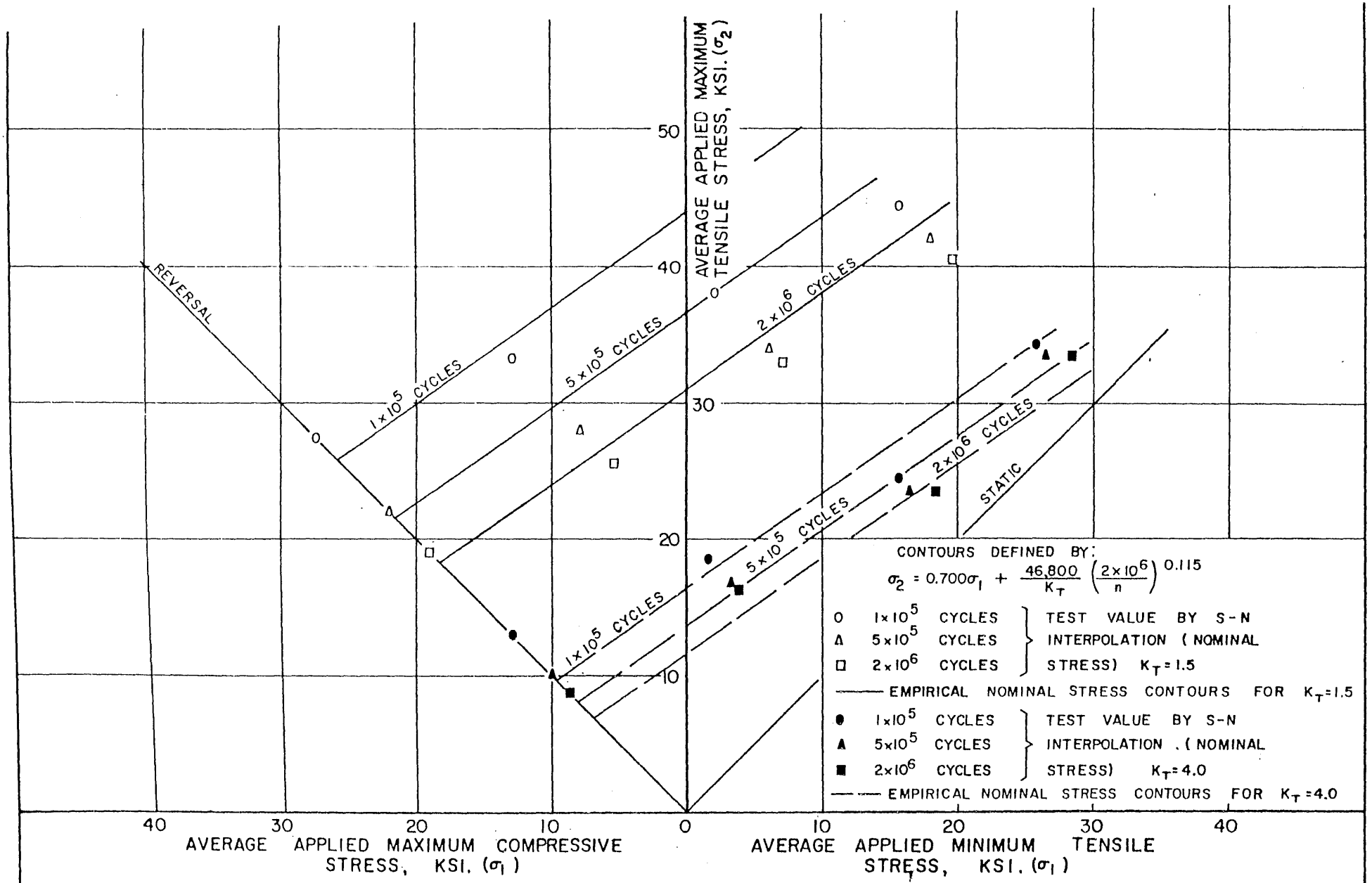

FIG. 19 EMPIRICAL CYCLE CONTOURS FOR NOTCHED 75S-T6 ALUMINUM ALLOY WITH THEORETICAL STRESS CONCENTRATION FACTORS OF 1.5 AND 4.0 COMPARED TO INTERPOLATED TEST VALUES

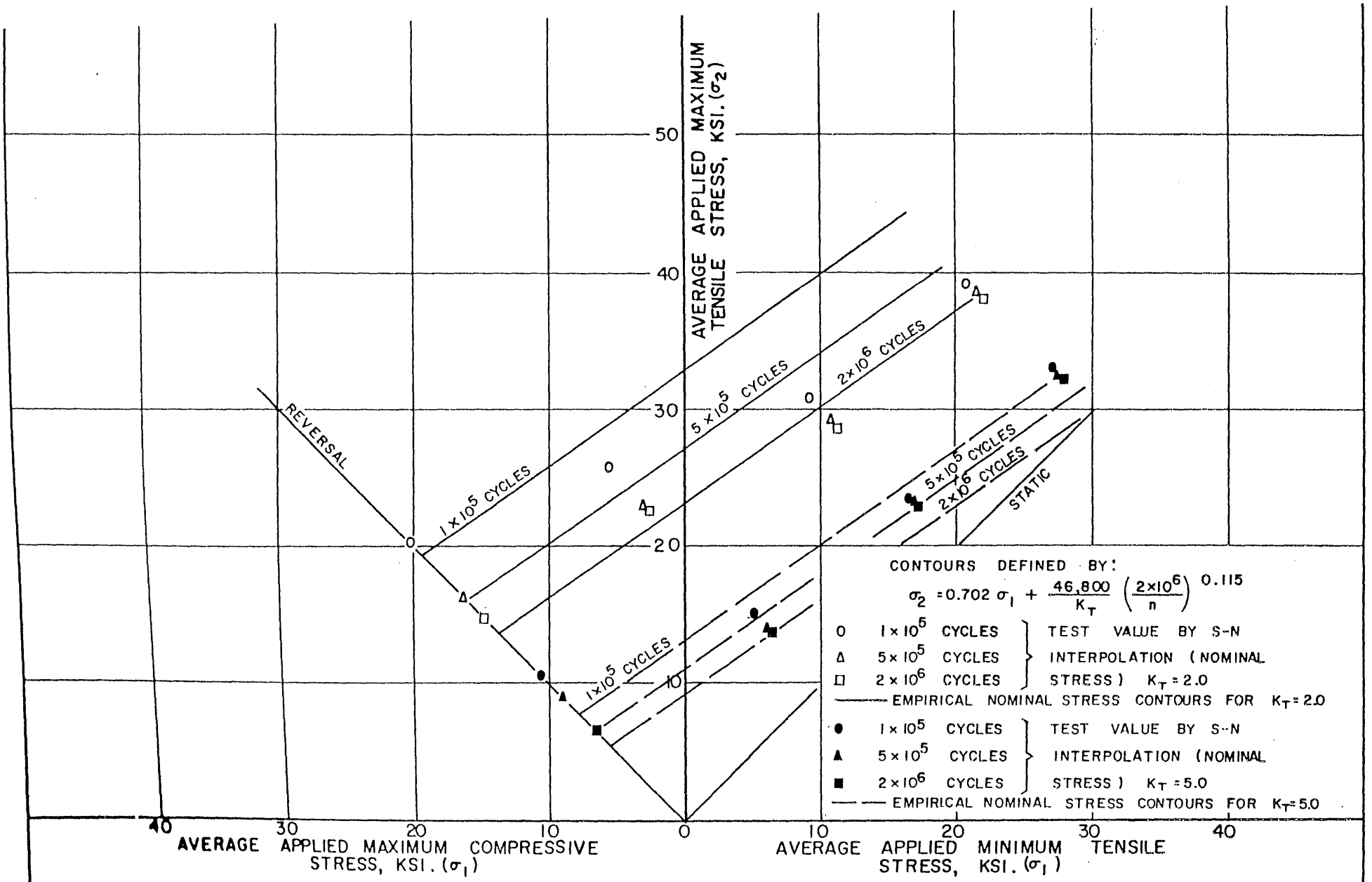

FIG. 20 **EMPIRICAL** CYCLE CONTOURS FOR NOTCHED 75S-T6 ALUMINUM ALLOY WITH THEORETICAL **STRESS** CONCENTRATION FACTORS OF 2.0 AND 5.0 COMPARED TO INTERPOLATED TEST VALUES

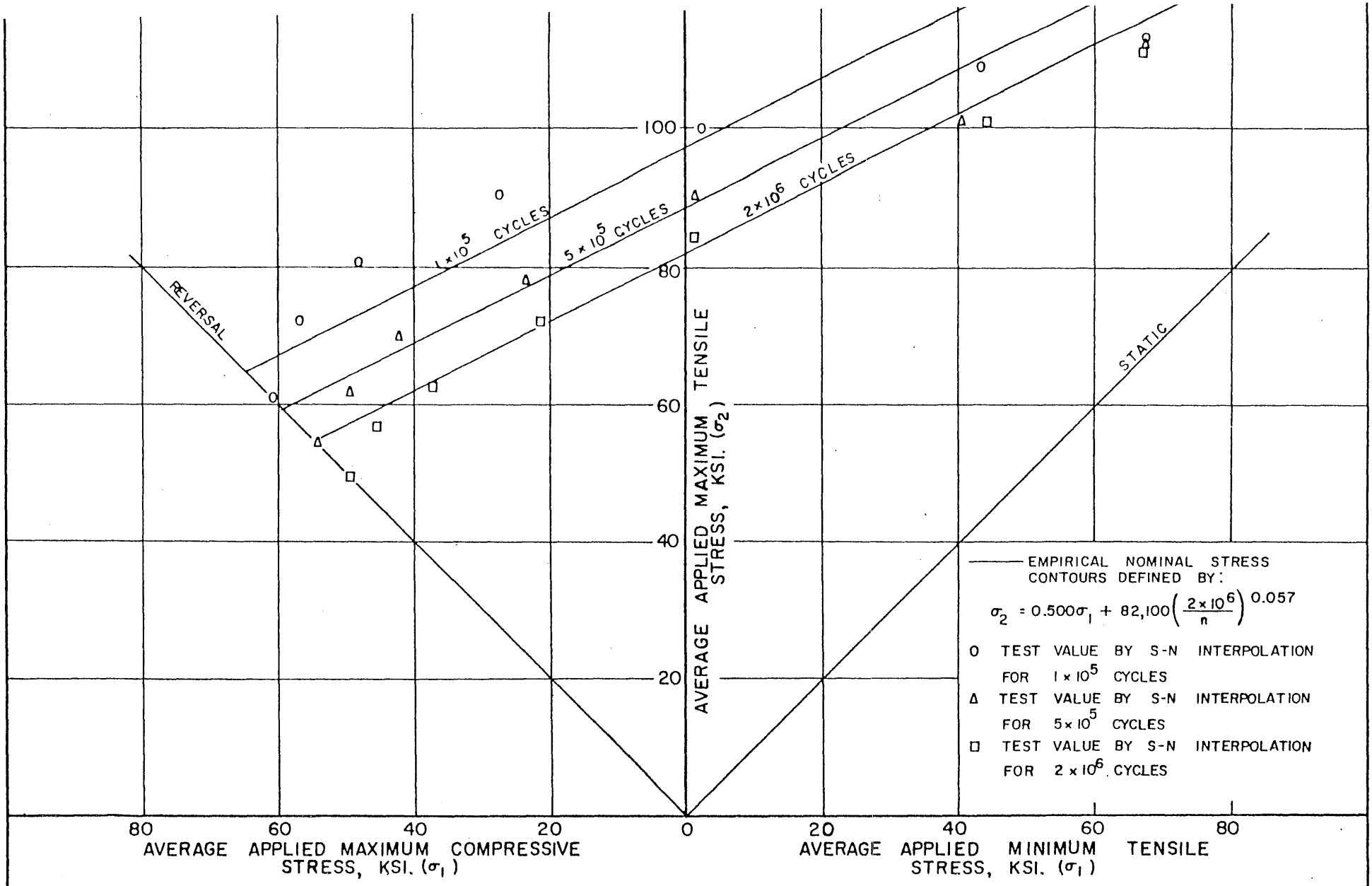

FIG. 21 EMPIRICAL CYCLE CONTOURS FOR UNNOTCHED NORMALIZED 4130 STEEL COMPARED TO INTERPOLATED TEST VALUES

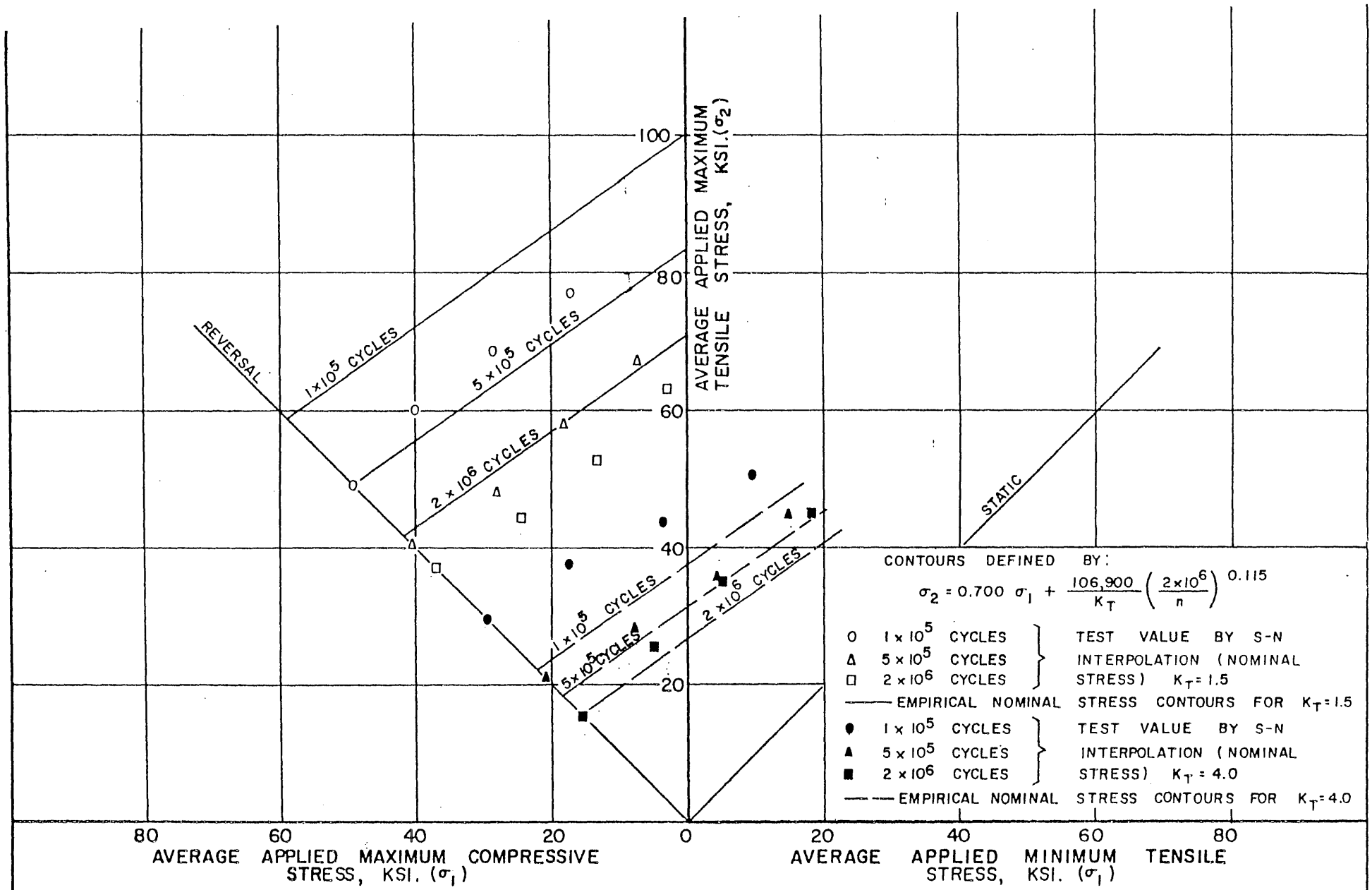

FIG. 22 EMPIRICAL CYCLE CONTOURS FOR NOTCHED NORMALIZED 4130 STEEL WITH THEORETICAL STRESS CONCENTRATION FACTORS OF 1.5 AND 4.0 COMPARED TO INTERPOLATED TEST VALUES

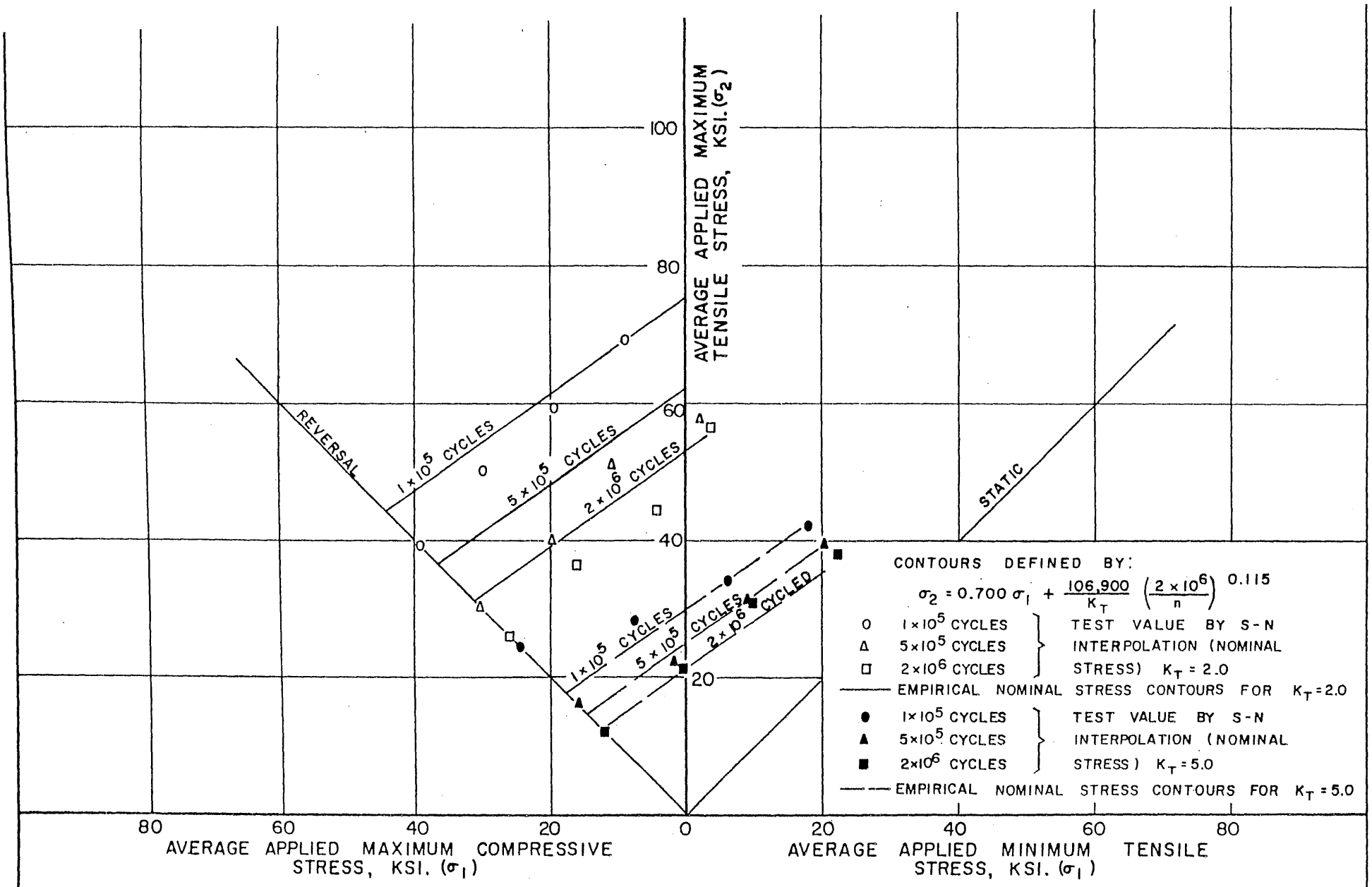

FIG. 23 EMPIRICAL CYCLE CONTOURS FOR NOTCHED NORMALIZED 4130 STEEL WITH THEORETICAL STRESS CONCENTRATION FACTORS OF 1.5 AND 4.0 COMPARED TO INTERPOLATED TEST VALUES

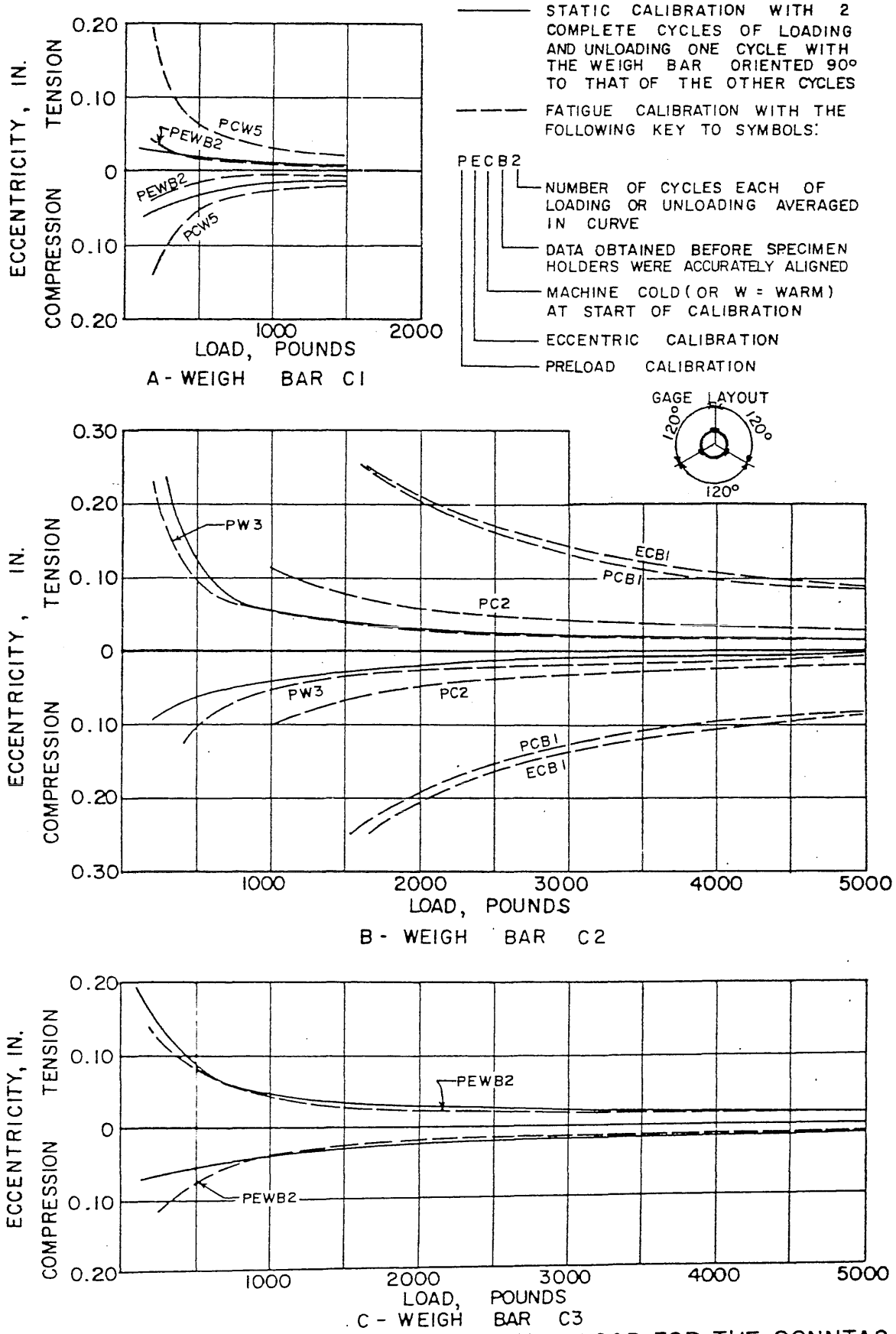

FIG. 24 VARIATION OF ECCENTRICITY OF APPLIED AXIAL LOAD FOR THE SONNTAG MACHINE INCLUDING A COMPARISON OF SIMILAR ECCENTRICITIES RESULTING FROM STATIC LOADING IN THE BALDWIN MACHINE.

DISTRIBUTION LIST

Technical Reports

Contract N6ori-71, Task Order V. Project NR-031-182

Chief of Naval Research
Department of the Navy
Washington 25, D. C.
Attn: Code 438 (2)

Director
Office of Naval Research
Branch Office
346 Broadway
New York 13, New York (1)

Director
Office of Naval Research
Branch Office
1000 Geary Street
San Francisco 9, California (1)

Director
Office of Naval Research
Branch Office
1030 E. Green Street
Pasadena, California (1)

Officer in Charge
Office of Naval Research
Branch Office, London
Navy 100
FPO, New York, New York (1)

Director
Naval Research Laboratory
Washington 25, D. C.
Attn: Technical Information Officer (6)

Director
Naval Research Laboratory
Washington 25, D. C.
Attn: Code 2020, Technical Library (1)

Director
Naval Research Laboratory
Washington 25, D. C.
Attn: Code 3500
Metallurgy Div. (1)

Office of Naval Research
The John Crerar Library Bldg.
10th Floor, 86 E. Randolph St.
Chicago 1, Illinois (1)

Bureau of Aeronautics
Department of the Navy
Washington 25, D. C.
Attn: N. E. Promisel, AE-41 (3)

Bureau of Aeronautics
Department of the Navy
Washington 25, D. C.
Attn: Technical Library, TD-41 (1)

Bureau of Ships
Department of the Navy
Washington 25, D. C.
Attn: Code 337L, Tech. Library (1)

Bureau of Ships
Department of the Navy
Washington 25, D. C.
Attn: Code 343 (3)

Bureau of Yards and Docks
Department of the Navy
Washington 25, D. C.
Attn: Research and Standards Division (1)

Bureau of Ordnance
Department of the Navy
Washington 25, D. C.
Attn: Tech. Library, Ad3 (1)

DISTRIBUTION LIST (CONT'D)

Bureau of Ordnance
Department of the Navy
Washington 25, D. C.
Attn: Rex (3)

Commanding Officer
U. S. Naval Ordnance Laboratory
White Oaks, Maryland (1)

Commanding Officer
U. S. Naval Ordnance Test Station
Inyokern, California (1)

Director
Materials Laboratory
Building 291
New York Naval Shipyard
Brooklyn 1, New York
Attn: Code 907 (1)

Commanding Officer
Naval Air Materiel Center
Naval Base Station
Philadelphia, Pennsylvania
Attn: Aeronautical Materials
Laboratory (1)

Superintendent
Naval Gun Factory
Washington 25, D. C.
Attn: Metallurgical Laboratory
DE713 (1)

Director
David Taylor Model Basin
Washington 7, D. C. (1)

U. S. Naval Engineering
Experiment Station
Annapolis, Maryland
Attn: Metals Laboratory (1)

Post Graduate School
U. S. Naval Academy
Annapolis, Maryland
Attn: Dept. of Metallurgy (1)

Mr. Fred C. Bailey
Research Coordinator
Committee on Ship Construction
2101 Constitution Avenue
Washington 25, D. C. (1)

Mr. F. X. Finnigan
Resident Representative
Office of Naval Research
1209 West Illinois Street
Urbana, Illinois (1)

Office of the Chief of Engineers
Department of the Army
Washington 25, D. C.
Attn: Research and Development
Branch (1)

Chief of Staff, U. S. Army
The Pentagon
Washington 25, D. C.
Attn: Director of Research
and Development (1)

Office of Chief of Ordnance
Research and Development Service
Department of the Army
The Pentagon
Washington 25, D. C.
Attn: ORDTB, E. L. Hollady (2)

Office of Ordnance Research
Duke University
2127 Myrtle Drive
Durham, North Carolina
Attn: Dr. A. G. Guy (1)

Argonne National Laboratory
P. O. Box 5207
Chicago 80, Illinois
Attn: Dr. Hoylande D. Young (1)

Commanding Officer
Frankford Arsenal
Frankford, Pennsylvania
Attn: Laboratory Division (1)

Commanding Officer
Watertown Arsenal
Watertown, Massachusetts
Attn: Laboratory Division (1)

Commanding General
U. S. Air Forces
The Pentagon
Washington 25, D. C.
Attn: Research and Development
Division (1)

DISTRIBUTION LIST (CONT'D)

Wright Air Development Center
Wright-Patterson Air Force Base
Dayton, Ohio
Attn: Materials Laboratory (1)

Wright Air Development Center
Wright-Patterson Air Force Base
Dayton, Ohio
Attn: Flight Research Laboratory (1)

National Advisory Committee for Aeronautics
1512 H Street, N. W.
Washington 25, D. C. (1)

U. S. Atomic Energy Commission
1901 Constitution Avenue, N. W.
Washington 25, D. C.
Attn: B. M. Fry (2)

U. S. Atomic Energy Commission
New York Operations Office
P. O. Box 30, Ansonia Station
New York 23, New York
Attn: Div. of Techn. Info. and Declassification Service (1)

U. S. Atomic Energy Commission
Library Branch, Technical Information Office, ORE
P. O. Box E
Oak Ridge, Tennessee (1)

Mound Laboratory
U. S. Atomic Energy Commission
P. O. Box 32
Mianisburg, Ohio
Attn: Dr. M. M. Haring (1)

Knolls Atomic Power Laboratory
P. O. Box 1072
Schenectady, New York
Attn: Document Librarian (1)

Los Alamos Scientific Laboratory
P. O. Box 1663
Los Alamos, New Mexico
Attn: Document Custodian (1)

Oak Ridge National Laboratory
P. O. Box P
Oak Ridge, Tennessee
Attn: Central Files (1)

University of California
Radiation Laboratory
Information Division
Room 128, Building 50
Berkeley, California
Attn: Dr. R. K. Wakerling (1)

Sandia Corporation
Sandia Base
Classified Document Division
Albuquerque, New Mexico
Attn: Mr. Dale M. Evans (1)

Westinghouse Electric Corporation
Atomic Power Division
P. O. Box 1468
Pittsburgh 30, Pennsylvania
Attn: Librarian (1)

Chief
Exchange and Gift Division
Library of Congress
Washington 25, D. C. (2)

General Electric Company
Technical Services Division
Technical Information Group
P. O. Box 100
Richland, Washington
Attn: Miss M. G. Freidank (1)

Carbide and Carbon Chemicals Div.
Central Reports and Information Office (Y-12)
P. O. Box P
Oak Ridge, Tennessee (1)

Carbide and Carbon Chemicals Div.
Plant Records Department, Central Files (K-25)
P. O. Box P
Oak Ridge, Tennessee (1)

DISTRIBUTION LIST (CONT'D)

Battelle Memorial Institute
505 King Avenue
Columbus, Ohio
Attn: H. C. Cross (1)

Armour Research Foundation
Metals Research Laboratory
35 West Thirty-Third Street
Chicago, Illinois
Attn: W. E. Mahin (1)

University of Utah
Salt Lake City, Utah
Attn: Dean H. Eyring (1)

Iowa State College
P. O. Box 14a, Station A
Ames, Iowa
Attn: Dr. F. H. Spedding (1)

Armed Services Technical
Information Agency
Documents Service Center
Knott Building
Dayton 2, Ohio (1)

Office of Technical Services
Department of Commerce
Washington 25, D. C. (1)

Rand Corporation
Nuclear Energy Division
1700 Main Street
Santa Monica, California
Attn: Mr. Marc Peter Jr. (1)

Brookhaven National Laboratory
Technical Information Division
Upton, Long Island, New York
Attn: Research Library (1)

Contract Administrator, SE Area
Room 13, Staughton Hall
c/o George Washington University
707 - 22nd Street, N. W.
Washington 6, D. C.
Attn: Mr. R. F. Lynch (1)

Dr. W. Baldwin
Metals Research Laboratory
Case Institute of Technology
Cleveland, Ohio (1)

Mr. J. L. Bates
Managing Director
Technical Department
Maritime Commission
Washington, D. C. (1)

Professor Lynn Beedle
Fritz Engineering Laboratory
Lehigh University
Bethlehem, Pennsylvania (1)

Dean L. M. Boelter
University of California
Los Angeles, California (1)

Dr. J. E. Dorn
University of California
Berkeley, California (1)

Dr. J. E. Duberg
Structures Research Division
NACA
Langley Field, Virginia (1)

Mr. Samuel Epstein
Research Engineer
Bethlehem, Pennsylvania (1)

Professor A. M. Freudenthal
Columbia University
New York, New York (1)

Professor M. Gensamer
Department of Metallurgy
Columbia University
New York, New York (1)

Dr. N. J. Hoff, Head
Department of Aeronautical
Engineering and Applied Mech.
Polytechnic Institute of Brooklyn
99 Livingston Street
Brooklyn 2, New York (1)

DISTRIBUTION LIST (CONT'D)

Professor L. S. Jacobsen
Stanford University
Stanford, California (1)

Dr. Bruce Johnston
301 W. Engineering Building
University of Michigan
Ann Arbor, Michigan (1)

Professor B. J. Lazan
Department of Mechanics
University of Minnesota
Minneapolis 14, Minnesota (1)

Dr. C. W. MacGregor
Massachusetts Institute
of Technology
Cambridge, Massachusetts (1)

Professor R. F. Mehl
Metals Research Laboratory
Carnegie Institute of Technology
Pittsburgh, Pennsylvania (1)

Mr. R. E. Peterson
ASTM Committee E-9 on Fatigue
Westinghouse Research Laboratory
East Pittsburgh, Pennsylvania (1)

Mr. J. T. Ranson
Engineering Research Laboratory
Experimental Station
E. I. DuPont de Nemours
Wilmington, Delaware (1)

Dr. C. S. Smith
Institute for Study of Metals
University of Chicago
Chicago, Illinois (1)

General Electric Research
Laboratories
1 River Road
Schenectady, New York
Attn: Mr. J. H. Holloman (1)

Dr. C. A. Zapffe
6410 Murray Hill Road
Baltimore, Maryland (1)

University of Illinois

Professor N. M. Newmark
Department of Civil Engineering (2)

Dean W. L. Everitt
College of Engineering (1)

Dean O. Tippo
Graduate College (1)

Professor W. C. Huntington, Head
Department of Civil Engineering (1)

Professor T. J. Dolan
Department of Theoretical and
Applied Mechanics (1)

Project Staff: W. H. Munse
G. K. Sinnamon
R. J. Mosborg
H. C. Roberts
J. E. Stallmeyer
W. J. Hall
W. J. Austin
J. L. Merritt (8)

Files (5)

Extra Copies (10)